1996

# Tool condition monitoring using laser diffraction for rotating cutters.

Koushik. Ray
*University of Windsor*

# TOOL CONDITION MONITORING USING LASER DIFFRACTION FOR ROTATING CUTTERS

by

Koushik Ray

A Thesis
Submitted to the Faculty of Graduate Studies and Research
through the Department of Industrial and Manufacturing Systems Engineering
in Partial Fulfilment of the Requirements for
the Degree of Master of Applied Science at the
University of Windsor

Windsor, Ontario, Canada

1996

ISBN 0-612-11024-9

# ABSTRACT


With the increasing use of Computer Numerical Control (CNC), there is a growing need for reliable on-line tool condition monitoring systems that are capable of sensing worn or broken tools. A tool condition monitoring system not only prevents losses owing to spoilt jobs but also minimizes premature tool replacement. In the long run, it helps to reduce manufacturing costs, increase machine tool utilization, optimize cutting conditions and build a reliable and intelligent manufacturing system.

This thesis presents a new method of tool condition monitoring for machining processes that employ rotating cutters, such as milling and drilling. It focusses on end-milling cutters but it can be extended to other types of rotating cutters as well.

The method used for tool wear measurement is based on laser diffraction. As a coherent laser light source passes through a slit, which is formed between a reference edge and the cutting edge of the cutter, a characteristic diffraction pattern is obtained. The luminous pattern of light consists of a number of fringes. The image can be captured by a CCD camera and various image processing techniques are employed to determine the fringe spacing. The fringe spacing is mathematically correlated to the width of the slit and accordingly, can be used to calculate the tool wear.

A prototype measurement system was designed and fabricated. Experiments were conducted and good results were obtained. Comparing the mechanical and optical measurements methods, the maximum error was only 16%. This method proved to be a reliable tool wear measurement method even for low values of the tool wear.

# DEDICATION

To my parents, sister and brother.

# ACKNOWLEDGEMENTS

I wish to express my sincere appreciation to Dr. R. Du, who supervised my thesis work, for his guidance, support and encouragement throughout the study. Some of his suggestions were crucial to the success of the project. I would also like to express my gratitude to Dr. W. P. North and Dr. W. H. El-Maraghy, for their valuable advice, ideas, comments and important criticisms, most of which have been taken care of in the thesis. I specially thank Dr. North for providing me with a computer with a frame grabber board and a He-Ne laser source which were a vital part of the setup.

I thank Mr. Tom Williams for helping me with the electronic hardware, Dieter Liebsch for making the facilities of the Technical Support Centre available for fabrication and experimentation. I also thank Ms. Jacquie Mummery, secretary, for her assistance and friendship. I thank Mr. Rajat Debgupta for his dedicated help and support in performing the experiments.

I would like to thank Sensor Adaptive Machines Incorporated for making their laboratories available to me in the initial stage.

Finally, I convey my thanks to all those who have helped me in various ways and regret the fact that space and time do not allow me to mention their names.

# TABLE OF CONTENTS

# LIST OF TABLES

# LIST OF FIGURES

# NOMENCLATURE

| | | |
|---|---|---|
| A | : | Constant |
| $D_o$ | : | Interfringe Distance without wear |
| $D_\omega$ | : | Interfringe Distance with wear |
| R | : | Tool Nose Radius |
| e | : | Tool Tip Difference |
| VB | : | Flank Wear |
| WB | : | Tool Wear |
| $\alpha$ | : | Angle of Incidence |
| $\beta$ | : | Clearance Angle |
| $\lambda$ | : | Wavelength of Light |

# LIST OF ABBREVIATIONS

| | | |
|---|---|---|
| ACO | : | Adaptive Control Optimization |
| CAD | : | Computer Aided Design |
| CAM | : | Computer Aided Manufacture |
| CAPP | : | Computer Aided Process Planning |
| CCD | : | Charge Coupled Device |
| CIM | : | Computer Integrated Manufacturing |
| CNC | : | Computer Numerical Control |
| EDM | : | Electro Discharge Machining |
| HSS | : | High Speed Steel |
| KB | : | Kilo Byte |
| RPM | : | Revolutions Per Minute |
| RSM | : | Response Surface Methodology |
| TCM | : | Tool Condition Monitoring |
| VGA | : | Video Graphics Array |

# CHAPTER 1

## I. INTRODUCTION

### 1.1 Background

In the past few decades, there has been a constant growth of awareness in the machining industry to fabricate parts with higher precision and surface finish. Parts with higher accuracy and better surface finish are desirable since they often lead to longer life due to reduced wear, tear, friction and so forth. To obtain these parts, tool condition monitoring is the key. It improves surface finish, dimensional accuracy, productivity and reduces costs in unattended manufacturing systems, by timely tool replacement and other control measures.

A large number of studies have been carried out in the search for different types and methods of tool condition monitoring [Cook 1973]. However, a reliable tool condition monitoring system is still a goal of research. A relatively reliable prototype has been designed and fabricated at Sensor Adaptive Machines Inc. (SAMI), which measures tool wear for single point cutting tools. This sensor is an off-line and direct approach type sensor that senses the tool tip wear using a small video camera. The SAMI Tool tip sensor has been found to perform well, especially in dry cutting. The current work focusses on monitoring the condition of rotating cutters used in processes such as drilling and milling.

Tool condition monitoring has many advantages. It improves productivity by reducing unnecessary and premature tool replacement. It improves the quality of the finished product by preventing jobs from being spoilt due to the use of worn out tools. This also prolongs the life of the machine tool as well as eliminates undesirable chatter and vibration in the machine. Noise and chatter are detrimental to the life of the machine considering its capital intensiveness. It is very important to preserve and prolong the life of the machine tool. In order to achieve a system which is unmanned, it is necessary to incorporate different kinds of sensors which can monitor the machining process from different perspectives. Hence, there are many physical quantities which one has to keep track of.

Modern manufacturing equipment has to be very flexible and automatic [Tonshoff *et al.*, 1988]. There is an economic reason why tool condition monitoring is desirable. The machine tools have to work free of error in order to ensure economic usage of the machine tool. This results in reduced costs by replacing the tool at the correct time, reduction in the number of spoilt parts during machining and better utilization of the machine tool itself in terms of time.

Since the age of rapid industrialization, things have continued to change even at the present day. Automation has brought about an increase in productivity, decrease in manufacturing cost and the reduction of manual labour. Previously, in the first phase, hard labour was replaced by the engine or motor driven machines. The foot operated lathe became engine driven. In the next phase, came the numerically controlled machines or NC machines. This invention did away with the manually operated slides and tool carriages. The Computer Numerical Control (CNC) brought about drastic changes which almost eliminated the machine operators. In addition, this promoted precision and accuracy of the machined parts besides boosting productivity. The next generation of machines will definitely have an added dimension like built-in tool wear sensors and intelligent control of the machine tool. Already some complex machining centres have adaptive control systems built in. This would be a brief picture from the time perspective.

**Tool Condition Sensing**

The next generation of machines will first need different sensors incorporated into the machine itself. These sensors will primarily be engaged in sensing machining conditions, performance indices and tool condition monitoring. The tool condition monitoring will consist of various components, of which the first one is the sensor itself. The acquired data has to be treated in various ways and carefully analyzed. The data processing demands a large amount of computation and comparison. After the data processing is over, the output signal can be used for decision making.

Sensor based monitoring and diagnostic systems have become very useful in improving the efficiency of manufacturing systems [Tonshoff *et al.*, 1988]. The efficiency of a manufacturing system is affected by tool failure and hence many diagnostic systems are being developed to monitor the tool failure. Hence tool wear monitoring and estimation is essential for improving the productivity of an unmanned automatic manufacturing system [Ravindra *et al.*, 1994].

The sensor output signal can be sent to a learning system or an intelligent controller which will generate the necessary commands to follow or actions to take. This indeed makes the manufacturing system more and more sophisticated with less and less human intervention.

Optical measurement is considered to be the primary standard in measuring length. Using laser diffraction one can measure apertures of a very small size. In the present study this aperture is formed by the gap between the reference edge and the flute of the end-mill cutter. This aperture width varies as the tool wears out.

## Motivation

Tool Condition Monitoring is the only way by which a stand-alone manufacturing system can detect whether the cutting tool is worn out or not. Thus it is an essential part of such a system. Opto-electronic systems for in situ monitoring or the flank wear has been found to work [Jeon and Kim 1988]. For the control to be performed successfully, the in situ measurement of tool wear is of crucial importance.

Tool wear monitoring is one of the key problems that could not be solved completely even today [Giusti *et al.*, 1987]. This will be essential in setting up a modern unmanned factory and would be a part of the control system.

Problems faced using the tool wear sensor for turning are mainly the repeatability error and the coolant problem. Experimental results for end-milling processes using laser diffraction show a good repeatability [Fan and Du, 1994].

Other different tool condition sensors have been tried by various authors with limited success. Only some of these have been implemented in an industrial environment. Numerous sensors have been tested in the laboratory to determine the suitability in the industrial environment [Lister and Barrow, 1986; Dan and Matthew, 1990]. The limited success has been due to the complexity of the process involved [Ulsoy and Koren, 1993].

There has been a great deal of work carried out on different methods of tool condition monitoring. Unfortunately they mostly deal with single point cutting tools and processes like turning.

Timely replacement of the worn out cutter is possible if the condition of the tool is monitored. This can be mechanised and automated. Hence introducing tool condition monitoring will help in the achievement of better surface finish, better dimensional accuracy, fewer spoilt jobs, less premature tool replacement and so on. All the advantages of tool condition monitoring help in reducing overall manufacturing costs.

Rotating cutters are very commonly used in the metal cutting. Hence there exists a potential for developing a system that can measure the tool wear for rotating cutters.

This leaves one with room to explore the various aspects of tool wear monitoring and control.

## 1.2 Objectives

This research involves developing a reliable method for tool wear monitoring for rotating cutters using laser diffraction.

The objectives of the research can be stated as follows:

1. To develop a method of measurement of tool wear for rotating cutters. In this case, end-milling cutters are used for milling operations.

2. To fabricate a prototype rotating tool condition monitoring system including the hardware and software aspects.

3. To determine the performance characteristics of this tool condition monitoring system.

Some of the experiments were carried out at Sensor Adaptive Machines, Inc. (SAMI), Windsor, Ontario using their optical sensors and other supporting hardware for data acquisition and signal processing. Further investigations were carried out in the laboratories at the University of Windsor.

A greater part of the experiments were carried out at the Technical Support Centre at the University of Windsor using their machine tools. All fabrication work related to the experimental setup was carried out by the author. Later, experiments were carried out according to the plan. The software, PROFILEX, has been coded to meet the requirements of the sensor system.

**Thesis Organization**

This thesis is organized as follows. The literature survey on tool life, application of diffraction using laser as a light source and tool condition monitoring is presented in Chapter 2. In Chapter 3, the theoretical aspects are introduced and explained. The working principle of the Optical Sensor system is developed and the methodology is laid out. The details of the experimental setup that deal with the design and fabrication work are given in Chatper 4. The experimentation is outlined in Chapter 5, which is followed by the results obtained. Finally Chapter 6 deals with the conclusions and recommendations and further outlines the future scope of this project.

# CHAPTER 2

## II. LITERATURE REVIEW

### 2.1 Tool Life and Measurement

There is an internationally recognized criteria for defining tool life. The wear zones are flank wear and crater wear as shown in Figure 2-1. This illustration is for turning inserts but it is equally applicable for other kinds of cutters.

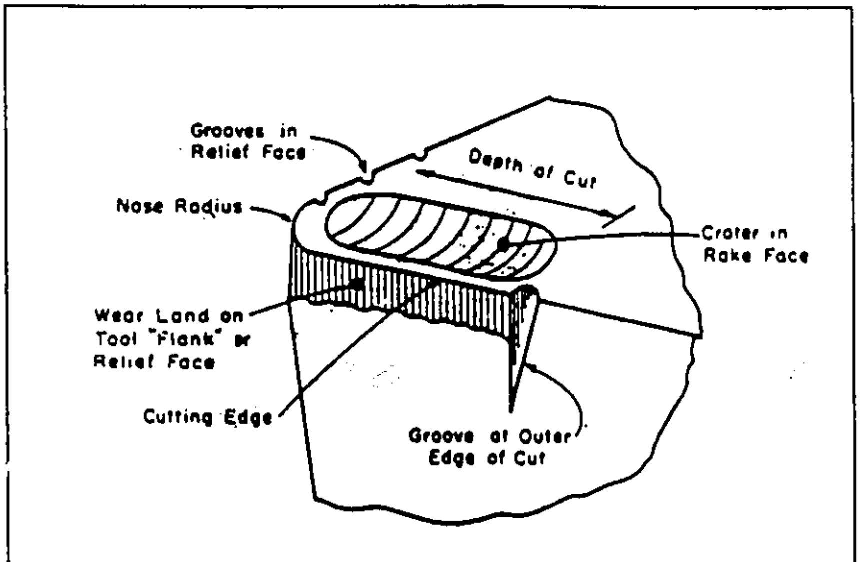


**Figure 2-1** : Geometry of Tool Wear.

The International Standards Organization defines the tool wear based on the profile of the leading edge of the groove as shown in Figure 2-2. If the profile is uniform, the average value of VB of the wear land length is measured and a tool can be used unless VB is greater than 0.3 mm. If the wear is uneven, the maximum peak land length of the groove $VB_{max}$ is less or equal to 0.6 mm.

Tool life measurement and testing was carried out by Wu (1964) by using response surface methodology, which is a statistical approach. This reduces the number of experimental tests to be carried out in order to develop a reliable tool life predicting equation. It involves postulation of a mathematical model, design of the experiment, choice of cutting conditions, experimentation, estimation of the parameters, adequacy check and estimation of confidence intervals. In the current work, there are a few factors, like Repeatability and other physical influences that affect the measurement of tool wear. A comprehensive design of the experiment is necessary to evaluate these different aspects.

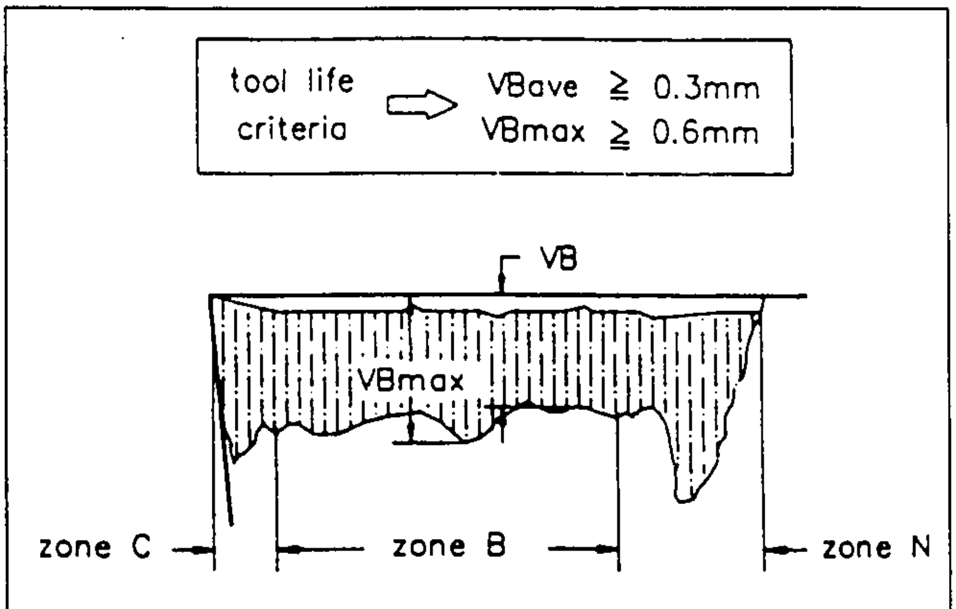


**Figure 2-2 :** Typical Tool Life Criteria and Profile of Flank Wear.

In the study carried out by Cook (1973), various features of tool wear have been revealed. The tool wear at high speed and temperature have been emphasised. Microstructure studies have demonstrated the mechanism of such tool wear. Tool life and wear rate have different implications to different people. The exact form of tool wear vary for different machining operations. Most of the investigations have been carried out on turning tests and a great deal of data is available on this. Tool wear can be characterised by different wear land and crater wear. For example, in the turning operation, physical characteristics are tool conditions such as tool failure, accelerated wear and tool softening. Figure 2-3 shows the typical tool life curve for constant cutting conditions.

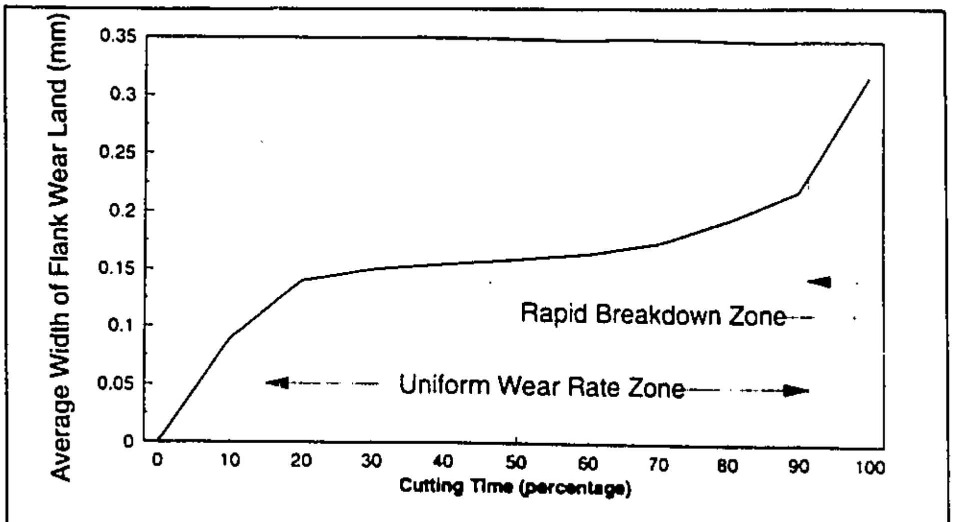


**Figure 2-3** : Typical Tool Life Curve for Constant Cutting Conditions.

## 2.2 Tool Condition Monitoring Methods

The necessity of tool condition monitoring for appropriate tool wear control becomes more important especially in the modern manufacturing systems in which many numerically controlled (NC) and computer numerically controlled (CNC) machines are operated in a more flexible and unmanned way [Jeon and Kim 1988]. The performance of the cutting tool is the most critical element in automated machining [Lee *et al.*, 1992, Lee *et al.*, 1986] Machining with a blunt tool or a broken tool can cause workpiece quality to deteriorate and possibly damage the capital intensive machine tools.

Tool wear and breakage might require the attention of the operator of the machine tool as often as every 3 minutes [Luggen 1991]. Tool Condition Monitoring and Sensing systems substitute for the skilled operator's eyes and ears and the signal to replace the tool can be generated. The simplest tool monitoring system is not a true tool monitoring system. It simply records the actual cutting time of each tool and compares that with pre-programmed limits for the tool's life.

There are two basic methods of tool condition monitoring: direct methods and indirect methods. The direct methods are based on the direct measurement of the worn area of the tool by optical methods, CCD camera, pneumatic probes, etc. [Jeon and Kim]. These methods required high measuring accuracy but are difficult to implement because the tool and the workpiece are interrupted by chips and coolant. Direct methods usually involve some actual measurements of the wear or failure [Lister and Barrow, 1986].

There is another way of classifying tool condition sensors. They may be classified as on-line sensors and off-line sensors. The on-line sensors can detect the signal, process it and take the necessary action while the actual machining is going on. Off-line sensors will require the tool to return to a particular resting position and measurements are carried out between cuts or passes.

Different tool condition sensing techniques are broadly studied under the following headings. They are 1) Direct Methods and 2) Indirect Methods. Again some of these methods are on-line and some are off-line. Cook (1980) has researched different types of tool condition monitoring both on-line and off-line. As the need for Tool Wear Sensor grows, there is great opportunity for invention.

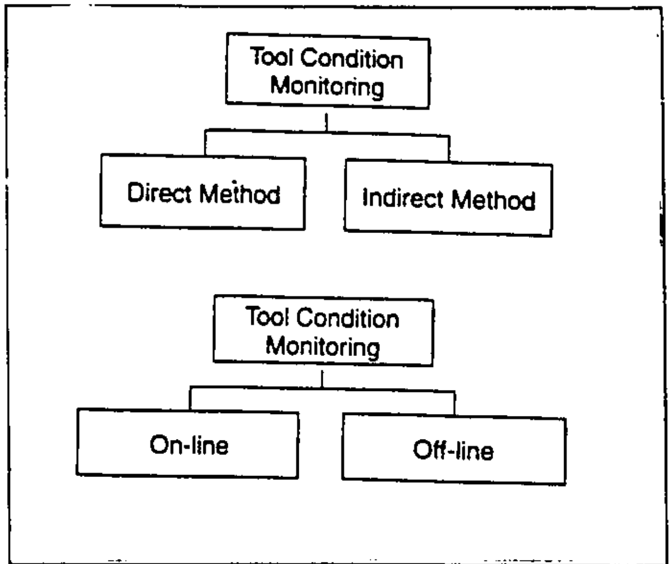

**Figure 2-4:** Classification of Tool Condition Monitoring.

Discontinuous direct or off-line sensors and continuous-indirect or on-line sensors are two classes of tool wear sensors [Arsovski 1983].

### Direct Methods

Direct Methods can be further classified into the following subgroups and a brief description is outlined.

1. Tool Geometry Measurement: As a tool wears out there are distinct changes that take place in the tool geometry. This can be measured by direct mechanical gauging, ultrasonic method, profile tracing, optical and pneumatic methods.

2. Optical Scanning: Optical Scanning usually involves a CCD camera that takes a picture of the tool tip between cuts. Alternatively, a laser can be used to generate diffraction patterns. This pattern can be captured by a CCD camera [Cook 1980].

3. Workpiece Size: Change of work piece size is a clear indication of tool wear. This is the most important quantity that relates to the quality of the job and as well as tool wear.

4. Distance Measurement: In a typical turning operation the work surface progresses towards the tool as the tool wears out. There are inherent causes of error due to force, temperature and vibration. Some methods of measurement that may be useful are length measurement, ultrasonics and air gages.

5. Electrical techniques: Measurement of contact resistance between the tool and the work piece can be useful in tool wear measurement. They can be achieved by applying film resistors to the tool flank or a resistive follower. This resistive follower is equipped with a resistive pad which wears out as the tool does.

6. Radioactivity: Most of the radioactive methods are not very safe off-line methods. A radioactive tool is used and the activity transferred on to the chips is monitored. The micro-isotopes that are used have extremely small quantities of activity. Cook (1980) has studied this method in detail and used micro-isotope for sensing tool wear, but it has been found that this method is neither practical nor reliable [Cook 1980].

7. Analysis of wear particles: The chips can be analyzed in other ways than radiation measurement, such as chemical analysis or electron micro-probe analysis. The chemical properties of the chip vary as the tool wears out.

**Indirect Methods**

Indirect Methods can also be classified into the following subgroups. They are usually on-line methods.

1. Force Measurement: Increase in the torque of the spindle is one good indication of a worn tool for a lathe. A great deal of work has been done in this area. In most cases (not all), force increases with the progress of tool wear. But the rise in the spindle torque could be due to other factors as well, such as variation of work piece hardness, depth of cut and cutting speed. The ratio of the forces will, however, indicate tool wear or failure [Leskovar 1982].

In learn-mode systems, the cutting force in the feed axis can be measured for assessing the condition of the tool [Luggen 1991]. If there is a predetermined increase of the feed force, a tool change signal is generated.

Typically the force on the ball-screw drives in the machine tool may increase whenever a worn tool is used for operations. Tool change signals can be initiated based on the fluctuations in these signals.

2. Mechanical Vibration: Acoustic emissions and mechanical vibrations are very useful signals that carry different types of information. With the progression of tool wear, there is a change in the spectrum of the signal. Acoustic emissions increase up to five times the normal value near the end of the tool life [Luggen 1991]. Vibrations can be measured by placing an accelerometer on the tool holder. The drawback to this method is that it is not possible to generalize the characteristics of a worn out tool in terms of signature analysis. Every setup will have a characteristic normal signature and one that characterizes a worn out tool.

3. Power Input: As tools wear, forces rise and hence there is an increase in the

power input [Luggen 1991]. The power input technique is less sensitive than force measurement but is easier to implement. A spectral distribution of power has also been studied which is a direct reflection of cutting forces.

4. Temperature: Tool tip temperature or the chip temperature will rise due to tool wear. Numerous investigations lead to the conclusion that tool wear rate is strongly related to the temperature of the tip [Solaja 1958]. But again it cannot define the end of the tool life. Geometric inspection of tool tip gives better results.

## Other Related Work

An intelligent supervisory controller has been proposed by Kendall and Bauoumi (1988). The essential process information is defined when the APT (Automatic Programmed Tools) program is written by the programmer. The tool life estimates used to establish the cutting speed and feed are one of the most important pieces of information.

Manufacturing processes like EDM (Electrical Discharge Machining) that require on-line monitoring of the spark gap, may be supervised by a neural network [Konishi *et al.*, 1992]. Neural networks that have a high ability of pattern recognition are useful in such cases. This helps in monitoring as well as diagnosis of manufacturing processes.

One of the most complex problems in the development of Adaptive Control Optimization (ACO) systems is that of making a correct choice of the wear sensor [Arsovski 1983]. The sensor must have high accuracy and reliability and be economically viable at the same time. A machinability database and its related software support is necessary to come up with an ACO system [Balakrishnan and DeVries, 1985].

One major requirement for Process Condition Monitoring is that there must be means of acquiring data, signal processing and mathematical modelling strategies [Brandon and Binglin, 1992].

The selection of economically optimal machining rate variables i.e. cutting speed and feed rate is one of the most important decisions to be made [Petropoulos 1973]. A geometric programming technique has been used to solve this nonlinear problem to optimize the constrained unit cost model. This technique is easy to apply and has been proved successful.

Surface finish, dimensional accuracy and condition of surface layer are the principal goals in finish turning [Solaja 1958]. A mathematical relationship was found that related the length of the grooves and the width of the wear-land on the clearance face with the value of maximum roughness on the surface generated. A model was developed that relates tool material, feed, cutting speed, depth of cut, rake and clearance angles of tools.

Another mathematical model for surface finish prediction have been suggested in terms of cutting speed, feed and axial depth of cut for milling processes [Alauddin *et al.*, 1993]. The effect of those parameters on surface roughness can be investigated using response surface methodology (RSM) which is a mathematical tool.

Hasegawa *et al.*, (1976) has developed a surface roughness model for turning using RSM methodology. The results obtained determined a relationship between surface roughness and machining parameters like speed, feed, depth of cut and tool nose radius.

In the study carried out by Leskovar and Peklenik (1982), it was found that the surface properties depend mostly on the machining process and condition under which it takes place. For establishing the surface integrity, one has to know the right order of machining processes and their influences on the development of residual stresses on the work piece material.

Finish machining is characterized by small depth of cut and feed. The major interests are dimensional accuracy, surface finish and tool life [Shaw and Crowell, 1965]. In this work, by Shaw and Crowell, a study was carried out which includes the contributions to surface roughness due to sub-surface fracture, built-up edges, vibration, geometry of the tool nose, plastic side flow at tool tip and the concentrated tool wear that occurs on the secondary cutting edge. The ultimate objective was to minimize the cost of machining.

Cook (1973) found that when a tool is reground, economic considerations may suggest its removal even before other criteria apply. This criterion is the estimate of average cost per cutting edge over the life of the tool.

The economic advantage of incorporating TCM is that the machine tools have a greater utilization in terms of machine time usage. A study carried out by Tonshoff (1988), shows that out of the total available machining time, only 10 percent is useful if there is no monitoring. Most of this is due to 8 hours per shift restriction. If a factory could run round the clock, by incorporating tool condition monitoring, as much as 65 percent machine time utilization is possible as illustrated in Figure 2-5.

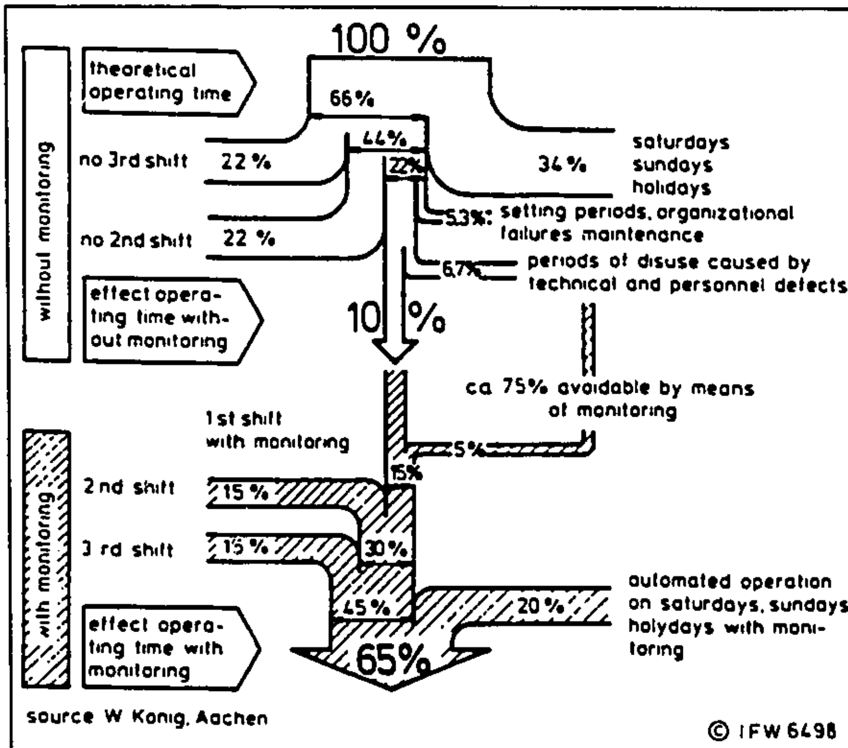


**Figure 2-5** : Economic Importance of Monitoring in Manufacturing Processes. [Tonshoff 1988]

## 2.3 Optical Methods

There have been numerous attempts made to make a prototype tool condition monitoring system. The tool condition sensor is the key element of such a system. After the sensor collects the signals, the second stage is signal processing. The subsequent stage is the analysis and decision making whether a tool should be replaced or not. It has been emphasized by many researchers that optical sensors describe the tool condition characteristics very closely. Laser diffraction techniques also have been developed [Fan and Du 1994]. A well designed experiment could substantially reduce the number of experiments to be carried out [Alauddin *et al.*, 1993].

## Related Work

Some of the relevant results that provide a benchmark to the current experiments have been presented here.

A prototype tool condition monitoring system for turning cutters has been developed at Sensor Adaptive Machines Inc., (SAMI). The importance of on-line tool condition monitoring has been emphasized in many recent publications. A very reliable system under various cutting conditions has been first attempted at SAMI (Du *et al.*, 1993).

The heart of this system is the tool tip sensor. It consists of an arrangement as illustrated in Figure 2-6. The optical sensor for the single point cutter is an optical device coupled with a CCD camera. It is housed in a steel enclosure measuring about 9 inches wide, 4 inches in height and 2 inches in thickness. It is mountable on a lathe turret in various ways and is configurable depending on the cutter to be monitored. It has a pneumatic self cleaning mechanism which drives away the chips and coolant around it.

The lower branch of this sensor has a white source of light which shines on the tool tip from below at an angle of 45 degrees. The CCD camera is present just above the tool on the upper branch of this horse shoe shaped sensor. There is a focussing arrangement controlled by the software running the sensor. The image of the shadow of the tool tip is formed onto the CCD camera which is then carried to the frame grabber board in the IBM compatible PC. This board comes with a few manufacturer supplied subroutines which the software uses to access the image from the frame grabber. The software runs under the environment of Microsoft Windows. The frame grabber captures the image in an array of 240 pixels by 430 pixels with 256 grey levels.

After the image is captured by the frame grabber, various image processing operations are carried out. It is filtered and then finally an edge detection algorithm finds the tool tip profile by differentiation.

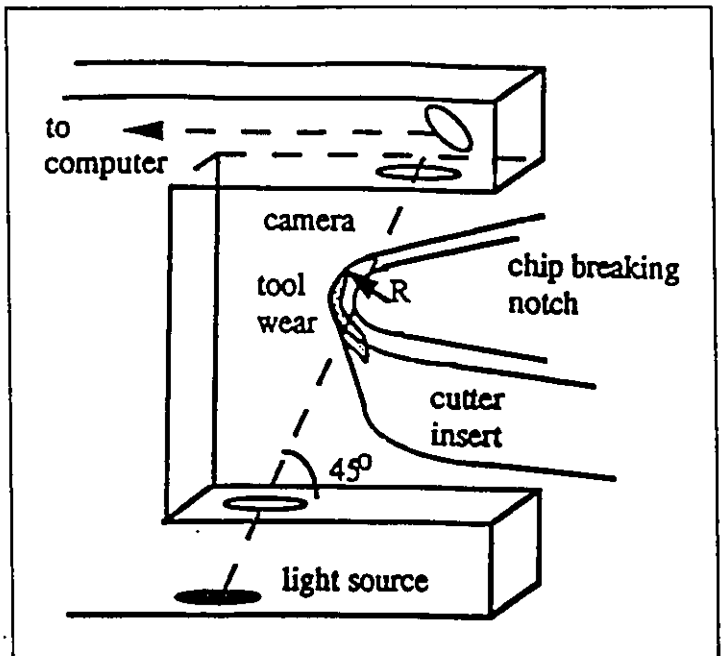


**Figure 2-6** : Illustration of a Typical Optical Tool Condition Sensor.

At the beginning, one set of observations is made and stored in the memory of the computer. All subsequent measurements that are carried out are processed using the same method and are finally compared with the master profile. In other words, the tool wear is calculated based on the difference between the current profile and the master profile at any given time.

The software has the option of saving the intermediate results and images which could be studied later on. It can directly give the user information about tool wear, rate of wear, tool compensation to be applied and so on. Figure 2-6 shows a schematic diagram of the tool condition sensor and how it works. The angle $\alpha$ as shown is approximately 45 degrees at which the light source is incident. R is the insert nose radius. Figure 2-7 shows the different tool condition indices and their physical descriptions. The top part shows the master tool profile and the current tool profiles. The flank wear, VB, of the tool insert is also shown.

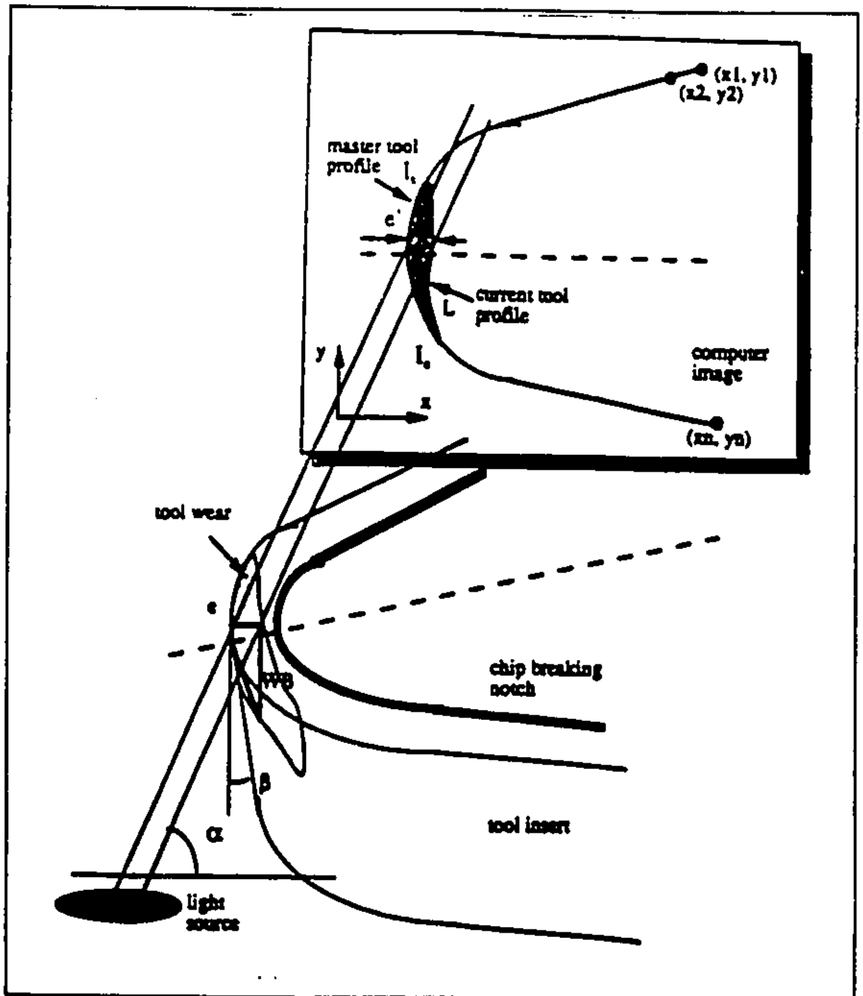


**Figure 2-7 :** Different Tool Condition Indices for Tool Tip Sensor.

The experiments were designed carefully by the Taguchi experiment design method. By this it was possible to carry out a relatively low number of runs yet come up with the variation of many parameters. Cutting speed, depth of cut, feed and the tool wear are the controllable factors here. Before starting the experiment, the master tool edge profile is stored in the computer. After every cut is taken the current tool edge profile is stored. The tool wear, WB, and other parameters are calculated based on the master profile and the current profile. Subsequently, coolant was used while cuts were taken, to study the effects of coolant on the performance of the sensor.

Other data such as the surface finish of the workpiece $R_a$, was measured by a stylus. The tool flank wear, VB was measured by a microscope after every cut.

The results of analysis have been carefully reviewed. By using various cutting conditions it was possible to obtain relationships between tool wear and other input parameters. The optical tool condition sensor can effectively describe the characteristic features of the insert during wear. The average tool wear which is found by computation can be used in determining whether a tool should be replaced or not. Again the amount of wear can also be used for tool compensation thereby allowing the tool to be used longer.

To summarize, the most important tool wear characteristic features are average tool wear WB and the tool tip wear e. The surface finish can be predicted based on prediction models using the cutting conditions as inputs. The whole experiment redefines the tool life based on the surface finish of the workpiece under allowable cutting conditions. These data can be used to maximize the material removal rate under required surface finish. Hence this information is also useful for the selection of cutting conditions as well.

With reference to the tool tip sensor developed in SAMI, the tip difference e with the number of cuts is plotted in Figure 2-8. This shows the nature of the tool tip difference, e, as tool wear progresses. This tip difference is calculated based on the difference between the master tool profile and the current tool profile. The experimental values as obtained show some degree of scatter, but largely indicates when the tool is worn out and needs replacement.

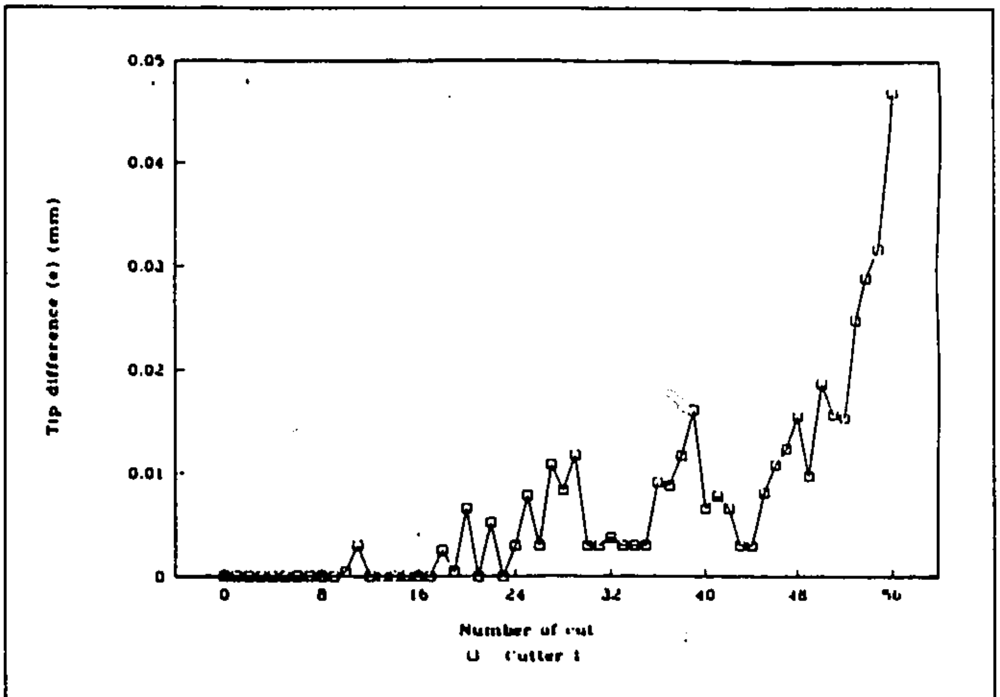


**Figure 2-8 :** Tool Tip Wear Pattern using Tool Tip Sensor for Turning.

## Fan's Work

A laser diffraction technique which could be used for tools like milling cutters was one done by Fan and Du (1994). With the advent of optics and computer vision technologies, it is possible to construct a measurement system which employs diffraction of laser. It is not only technically feasible, but also economically viable and advantageous. A prototype sensor could hence be made that employs this technique.

Some of the results obtain by Du and Fan (1994) have been presented here to show what one can expect from this sensor. Experiments were carried out using end-mill cutters and the tool wear was measured using 2D imaging. The cutters tested were HSS 4-flute end-mills with a diameter of 25.4 mm, a relief angle of 8 degrees and a helix angle of 30 degrees. During the cutting tests, a water soluble cutting fluid was used. A number of slot milling of steel plates were carried out with various cutting conditions. Table C-1 shows the summary of results obtained from the experiments conducted. The cutter conditions A through F represent the new tool until the tool is damaged with increasing degrees of wear which eventually lead to breakage.

The results of this investigation can be summarised in the following way. This method provides means for very high resolution required by tool condition monitoring. The calculations are rather simple and straight forward. The only information required for measuring tool wear is the fringe spacing and how it varies. This can be done at a very high speed which is ideal for on-line tool condition monitoring. Also, this method is not found to be sensitive to the cutting conditions and the environment. Experimental tests carried out using cutting fluids only show that this method is accurate, reliable and robust. Hence this method is expected to find many industrial applications.

The diffraction method as compared to the conventional method of tool wear measurement have also been studied. The results are encouraging so far. Figure 2-9 shows the comparison between tool wear measurement by diffraction method and that by microscope readings. There were three tests carried out in all.

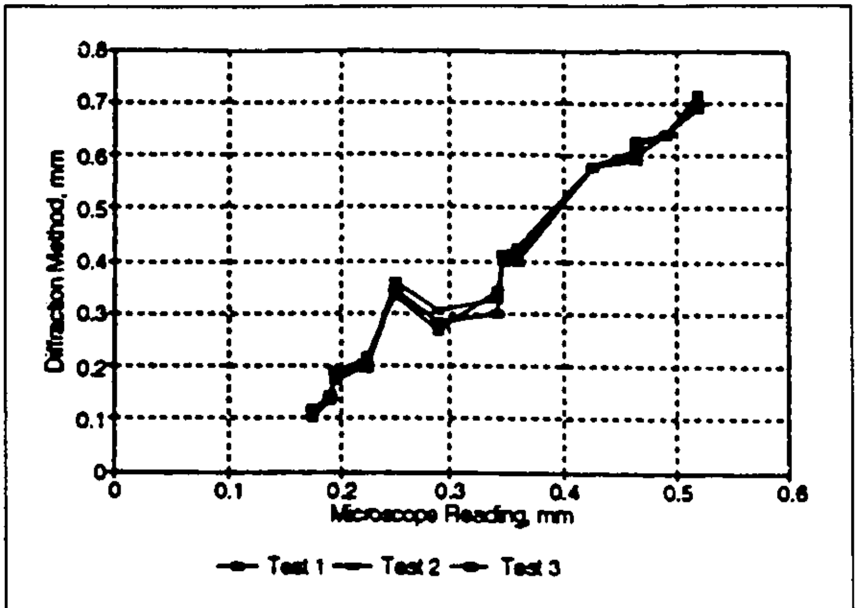


**Figure 2-9** : Comparison between Estimated Tool Wear and Measured Tool Wear

## 2.4 Scope of Work

From the literature survey, it is clear that there is a need for tool condition monitoring. Incorporation of TCM will improve tool utilization, higher accuracy, better surface finish, lesser wear and tear on machine tool due to vibration and chatter. On the other hand, it is an additional investment on the machine tool and will be economically feasible if the costs at least offset the benefits.

TCM for turning cutters have been done by researchers but there has been no sensor built for rotating cutters. There are a number of reasons for this. They are:

(i) It is a practical challenge to solve this problem.

(ii) Rotating Cutters are difficult to position and measure automatically.

Optical diffraction of laser light has applications in the area of small distance measurement. Optical measurement of distance is one of the primary standards of measuring length. Hence there lies a potential for this method to be used in the system. It has been tested on an optical bench by Fan and Du (1994) and it gave promising results.

TCM using laser diffraction apparently has a potential for the future machining industry and needs to be investigated further on how it can be implemented. The main steps involved will be methodology definition, fabrication of setup, experimentation and analysis.

TCM using laser diffraction for rotating cutters is challenging and has not been attempted before. Sufficient background information is available and the necessary literature has been explored. The things which can be done include design and fabrication of a new setup, calibration of the same, experimentation, determination of its performance and, finally, proving that this system works reliably.

# CHAPTER 3

## III. THEORETICAL BACKGROUND

### 3.1 Optical Sensors

In this age of automation, computer vision is one of the developing fields applied in manufacturing. It provides a very reliable means of grabbing the field of view and performing various kinds of analysis. Computer vision has applications starting from the daily needs of life to space exploration. Today, in the industrial sector, computer vision is extensively used for automated inspection systems, shape recognition and a host of other applications. It can be used not only for identifying objects and shapes, but also can be used in precise optical measurements.

In the industries, computer vision can be applied to various fields. It can be applied to inspection of manufactured parts, identification of different parts coming down on a conveyor belt, tool wear monitoring and many other applications, where the human elements could be eliminated. Computer vision is undoubtedly playing a key role in today's manufacturing. It can at times eliminate the need for human operators for just inspection and control. It can be integrated with the CIM (Computer Integrated Manufacturing) for automatic sensing and data acquisition for decision making. Thus, computer vision is now an essential component of industrial automation just like transfer lines and robots.

It is possible to do two dimensional and even three dimensional imaging using computer vision. An example of the one dimensional computer vision pertaining to daily life is that of bar code readers. Light point sensors are used in burglar alarms and security systems. Two and three dimensional imaging are used for object identification, remote sensing, surveying, exploration and other scientific areas.

Optical sensors are of different types. In terms of dimension, they can be zero, one or two dimensional sensors. The most common type of two dimensional sensor is a Charge Couple Device (CCD) Camera. This has a two-dimensional array of pixels where the intensity of light can be sensed. Usually this intensity results in an output 0 to 255 in the form of one byte. A monochromatic camera would thus be able to sense the illumination level at the particular pixel of consideration and report 256 different gray levels. For video cameras, however the output signal is available in the form of composite video which is analogue in nature. This signal has to be digitized by either a video digitizer or a frame grabber board. Such hardware is usually mounted on the mother board of a personal computer (PC). Software support is also required to integrate and control the board with the PC.

A color camera would produce three such intensity levels based on the three primary colors red, green and blue. However such a camera is not required if the only objective is measurement of length.

Another alternative to luminous intensity measurement is a travelling photo-diode detector. It is possible to track the intensity of light without dividing the light pattern into an array of pixels. The disadvantage, however, is that a complicated mechanical arrangement is required and such a device has low speed. The advantage of a photo-diode arrangement is that there is no need of a screen where the light pattern is produced on.

The photo-diode is capable of directly measuring the laser intensity.

Computer vision is more of a system. The optical sensor is the physical entity that allows us to convert the luminous intensity information into a corresponding electrical form. But, computer vision has various distinct stages or parts that can be broadly classified into the following: a) Scanning, b) Image Acquisition, c) Preprocessing, and finally d) Image Classification. In subsequent sections they will be individually dealt with and discussed in more detail.

### 3.2 Theoretical Background

Fan and Du (1994) has outlined a new method of monitoring multiple teeth cutters. A laser beam passes through the gap between the edge of the tooth and a reference edge held parallel and close to it. But this experiment has been conducted on an optical bench and does not demonstrate whether it can be practically used as a sensor in a machine tool. The preliminary results as obtained are encouraging enough to go ahead in designing and fabricating a prototype sensor. Once this sensor is fabricated there lies a great deal of work to be carried out in terms of setting standards, calibration, developing software for control amongst other things.

The setup for such a sensor is illustrated in Figure 3-4. After each cut, the spindle stops and the tool is brought very close to the reference edge. It is however important that the cutter is properly oriented with respect to the reference edge. Now, as it stops, a beam of laser light is passed through this gap which is of the order of 0.001 inch. A screen behind captures the diffraction pattern. A CCD camera grabs this picture and processes the rest in the computer.

## Optical Diffraction

The single slit diffraction problem is first considered. In this problem the following assumptions are made. Figure 3-1 illustrates the basic single slit diffraction problem.

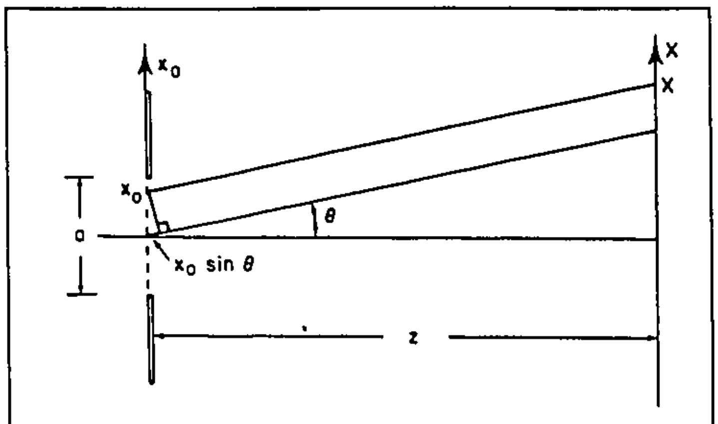


**Figure 3-1** : Principle of Diffraction of Light

(i) It is assumed that a monochromatic coherent beam of light passes through a long and narrow slit formed between the two sharp edges.

(ii) It is also assumed that the problem is one-dimensional.

(iii) The distance z to the observation plane as shown is so long that field at x can be regarded as a plane wave.

(iv) The width of the slit is a in the $x_0$ direction which is much smaller compared to the length of the slit along $y_0$ direction.

From the left on Figure 3-1, a plane wave of unit intensity falls onto the slit.

According to Huygen's principle, the contribution to the field at a point x from an arbitrary point $x_0$ inside the slit is equal to the field of a spherical wave with its centre at $x_0$. The expression for a plane wave, obliquely incident at an angle $\theta$ can be written as:

$$\Delta u(x) = \exp(i\ k\ x \sin\ \theta\ - i\phi) = e^{i\alpha x}\ e^{-i\phi} \qquad (3.1)$$

where $\alpha$ can be substituted as:

$$\alpha = k \sin\theta \approx k\ \frac{x}{z} = \frac{2\pi x}{\lambda z} \qquad (3.2)$$

The arbitrary phase constant $\phi$ is equal to zero for the wavelet originating from $x_0$=0. The relative phase from any point $x_0$ inside the slit then becomes:

$$\phi = k\ x_0 \sin\theta = \alpha\ x_0 \qquad (3.3)$$

To calculate the total field at the point x, the sum of the Huygen's wavelets are taken from all the points inside the slit. Therefore, on integration one has:

$$u(x) = e^{i\alpha x} \int_{-a/2}^{a/2} e^{-i\alpha x_0}\, dx = e^{i\alpha x}\ \frac{a \sin(\alpha a/2)}{\alpha a/2} \qquad (3.4)$$

Then the intensity becomes:

$$I(x) = |u(x)|^2 = a^2 \frac{\sin^2(\pi \frac{ax}{\lambda z})}{(\pi \frac{ax}{\lambda z})} \qquad (3.5)$$

In the derivation of equation (3.5), Fraunhofer approximation has been used. This is valid only if the observation plane is far away from the slit. On Figure 3-2, the relative luminous intensity of the diffraction pattern is shown as obtained from a single slit of width a. The relative intensity distribution is shown on figure 3-2. It consists of light and dark fringes with a maxima in the centre.

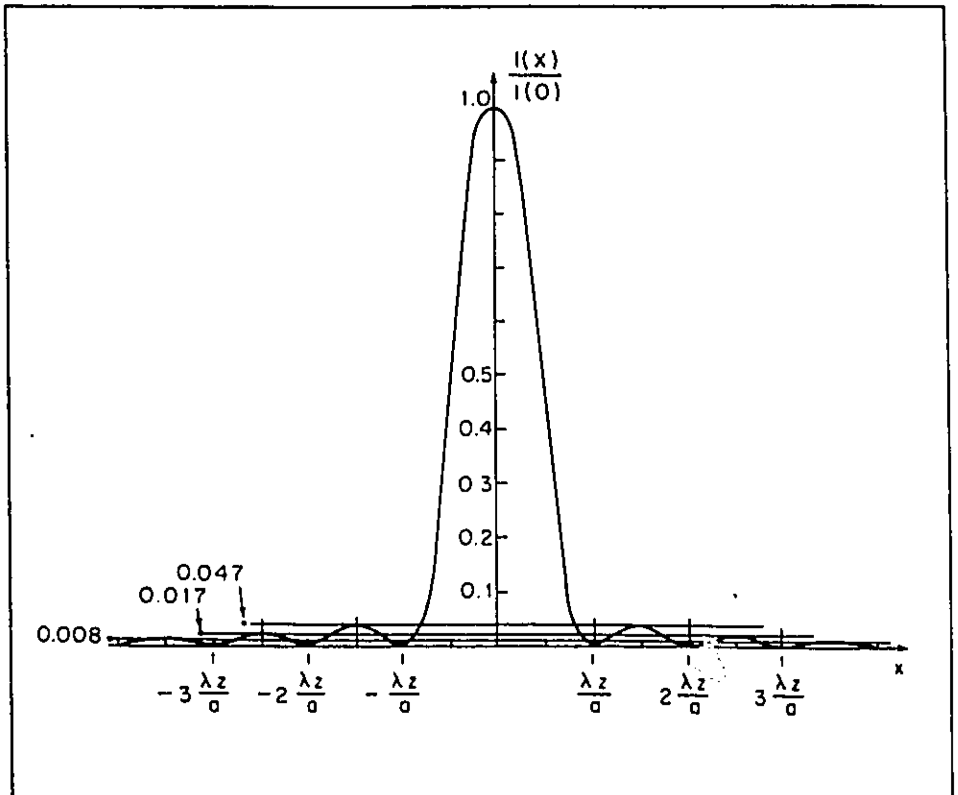


**Figure 3-2 :** Relative luminous intensity of a diffraction pattern from a slit of width a.

From equation (3.5) it is found that the fringe spacing between two consecutive minima on same side of the central maxima is given by:

$$\Delta x_n = \frac{\lambda z}{a} \qquad (3.6)$$

Figure 3-3 shows the diffraction pattern with how measurements are done. There are 7 bright spots on the pattern. The distance between the first minima is $d_1$. Similarly, the distances between the nth minima are $d_n$ where n is 1, 2, 3, and so on.

$X_n$ is the distance of the nth minima from the centre line. Hence $X_n$ is given by:

$$X_n = d_n/2$$

As shown on Figure 3-2, $X_1=\lambda z/a$ and $X_2=2\lambda z/a$. Hence, fringe spacing $\Delta X$ is given by:

$$\Delta X = X_2 - X_1 = \lambda z/a$$

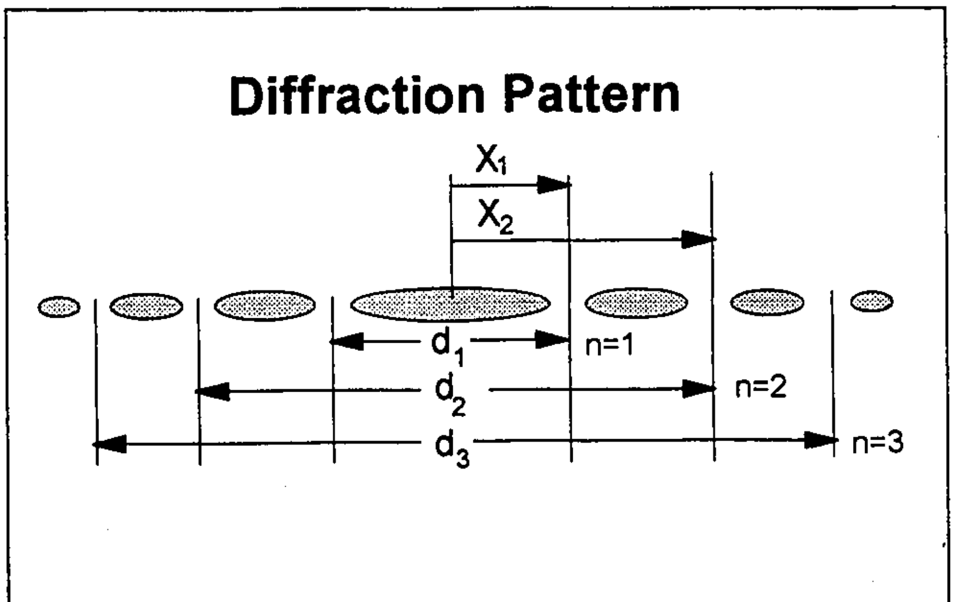


**Figure 3-3 :** Measurement of Fringe Spacing from the diffraction pattern.

From equation (3.6) if the fringe spacing $\Delta x$ is measured, the wavelength of light $\lambda$ and the distance of the screen z from the slit are known, the slit width, a, can be calculated.

$$a = \frac{\lambda z}{\Delta x} \tag{3.7}$$

It is further assumed in the problem that the lower end of the tool wears out while the upper end remains unaffected. If the width of the slit at the lower end is $a_\omega$ and that at the upper end is $a_0$. The difference in the widths will be a measure of the tool wear. Hence, ω will be given by:

$$\omega = a_\omega - a_0 \tag{3.8}$$

The wavelength and the distance are constants for the setup. Hence tool wear can be written incorporating a constant A which is the product of λ and z.

$$\omega = A\left(\frac{1}{\Delta x_\omega} - \frac{1}{\Delta x_0}\right) \tag{3.9}$$

where $A = \lambda z$

Therefore, ω can be worked out easily using the two different fringe spacing measurements. Figure 3-2 illustrates the intensity variation of the luminous pattern on the screen.

As shown in the figure, the intensity of light is not changing abruptly. Hence a great deal of image processing has to be carried out before measurements can be taken. The measurement of the value of Δx itself will involve many steps involving different image processing algorithms. Also, the first order diffraction fringe has the maximum intensity. The measurement of this is avoided as it is difficult to determine the edge.

### 3.3 Image Processing

The success of this sensor rests completely on image processing. The diffraction image captured by the camera is first digitized and stored onto a 2 dimensional array of bytes. Each pixel can assume a value between 0 and 255 and hence represents the captured image.

A series of techniques have to be applied to get rid of noise, ambient light and other troublesome factors. In case there is noise, frame averaging can be used to smoothen out the effects of noise. Alternatively one can also employ 3 by 3 filters.

Ambient light can be eliminated by subtracting the image without laser from the image obtained with laser. This will ensure that ambient light has no role to play in the subsequent operations and it is nullified. The other alternative is to conduct all measurements in a dark room.

**Image Pre-processing Techniques**

The image as it is scanned, also known as the raw image, has to be processed before it is possible to interpret the view field and its contents or carry out measurements. The different kinds of processing which can be done directly on the raw image are designated as preprocessing. One of the most popular primary steps is that of reducing the grey level image to a binary form. However, to locate the minima of the brightness profile, this method is not useful. The first thing to do is to choose a particular horizontal line on which measurements are going to be made on the brightness profile. One such profile is shown in the appendix in Figure 5-7.

As seen from the figure, the brightness profile is characterised by minima and plateaus. The plateaus are due to saturation of the CCD camera. The location of the minima is the greatest challenge since there could be local minima due to noise and other factors.

From observations it is found that noise levels have an amplitude of less than 10 grey levels whereas the brightness profile varies from 0 to 255 levels. Any local minima or maxima whose neighbouring opposite extrema is less than 10 levels is eliminated as noise. By this method, a greater part of the noise is eliminated.

If x(i) is the array representing the brightness profile, then all the minima are found using the condition:

$$x(i-1) \geq x(i) \leq x(i+1) \tag{3.10}$$

**Fringe Identification**

After performing the minima search on the brightness profile, the real and admissible minima are considered. They are subject to satisfying the following conditions thereof:

(i) The minima is at least 10 below the adjacent pixel values. Otherwise the minima is dismissed as a faulty minima or noise.

(ii) The minima is at least 50 below the adjacent maxima. Otherwise these are rejected.

The remaining minima which pass these criteria are the filtered minima that can be used for the fringe spacing calculations. The computer VGA card is extensively used for storing the image on the screen and performing all other operations. The selected fringe is painted on the screen with a different colour for further processing.

### Fringe Spacing Measurement

The desired fringe that was selected by highlighting with a different colour is now ready for measurement. The differences in the pixel values of the consecutive minima give the fringe spacing in pixels. All such values for a single brightness profile are obtained and the average is taken. Some of the fringe spacing values may be excessively away from the average. The values which are more than 10 percent away from the average are filtered out. The fringe spacing for the central bright fringe is actually double that of the rest of the fringe spacings. This gets eliminated in the process of filtering.

In this case a modified version of the omni operator was used to generate the edge detected image from the highlighted fringe. This operator was found to be fast and effective. This edge can be used to measure the fringe spacing at the top and the bottom of the image. Now the distance between two consecutive dark spots or minima gives the distance between two fringes termed as fringe spacing.

Measurement across the central maxima will give the best accuracy and in the current method all minima are considered which helps in achieving this.

## 3.4 Methodology and Analysis

The setup for the sensor is illustrated in Figure 3-4. There is a helium-neon gas laser source which provides the monochromatic and coherent light source. This beam passes through the gap between the flute of the end-milling cutter and the adjustable reference edge. This edge is held at the same helical angle as that of the flute. The diffraction pattern is obtained on the screen and this is captured by the CCD camera. The top part of the diffraction pattern refers to the unworn part of the tool. The bottom part corresponds to the worn part of the tool and hence the fringe spacing is smaller. It will be seen that as the tool gradually wears out, the shape of the pattern changes. It would assume a bell shaped nature when the tool wears starts to wear out. Now, if the space between two consecutive fringes in the diffraction pattern are taken, the one on the top will have a higher spacing than the one at the bottom. They are labelled $D_0$ and $D_\omega$ as shown in the Figure 3-4.

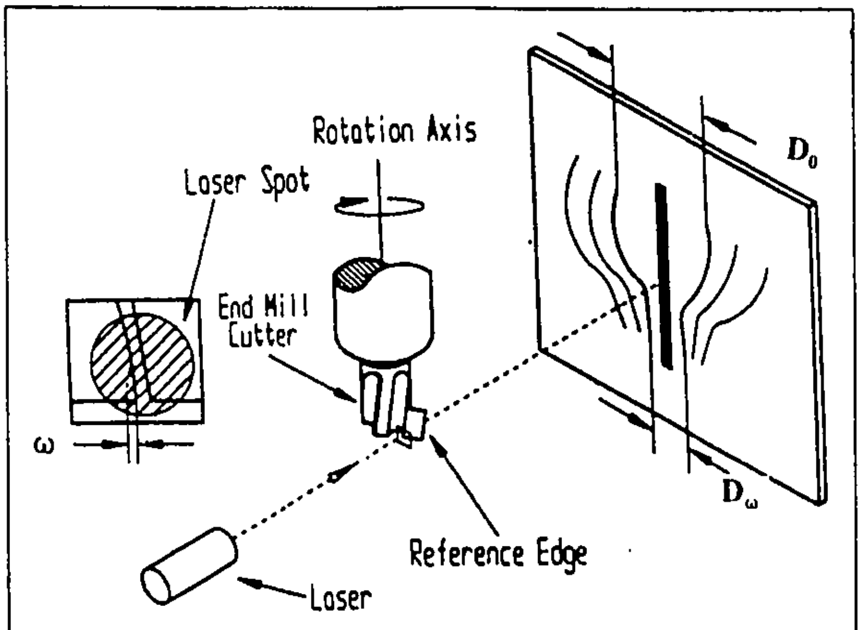


**Figure 3-4** : Setup for Tool Condition Sensor for Rotating Cutters

The tool wear VB can be found out from the value of ω and the clearance angle of the flute of the end mill cutter.

$$VB = \frac{\omega}{\sin(\beta)} \qquad (3.11)$$

where $\beta$ = clearance angle

Figure 3-5 illustrates a typical 2 flute end-mill cutter showing the side view and the axial view.

The analysis can be carried out after obtaining the measured tool wear. A comparison can be made between tool wear values obtained by conventional methods and the current work. Once this is established, the nature of tool wear, the tool life pattern and other things like how tool wear depends on various machining parameters can be studied.

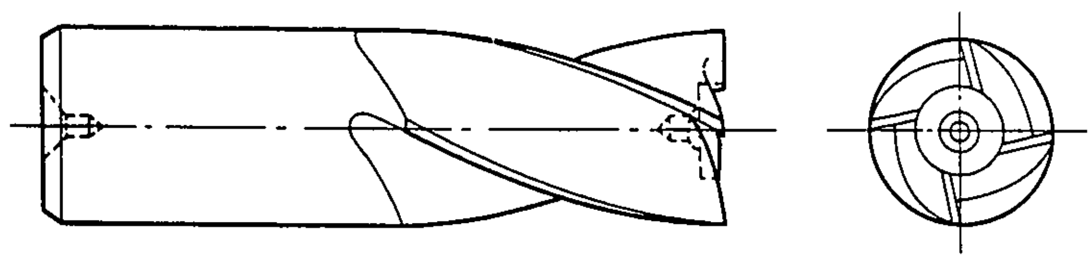

**Figure 3-5** : Standard End-Milling Cutter with Straight Shank

### 3.5 Criteria for Tool Radius Compensation or Replacement

There is an internationally recognized criteria for defining tool life. If the profile is uniform, the average value of VB of the wear land length is measured and a tool can be used unless VB is greater than 0.3 mm. Otherwise if the wear is uneven, the maximum peak land length of the groove $VB_{max}$ is less or equal to 0.6 mm. Now, if the clearance angle for the flute is 8 degrees which is typically the case, the allowable reduction in the radius of the cutter is given by:

$$WB = VB (\sin \beta)$$

where $\beta$ = clearance angle.

Given that:

Clearance Angle, $\beta$ = 8 degrees.

Flank Wear VB = 0.0118 (0.3 mm)

Then WB = 0.001644 inch (0.04175 mm)

Hence by this mode of tool wear the reduction in diameter of the rotating cutter is 0.003288 inch (20.8 microns).

It can be assumed that the tolerable value of tool wear WB is 0.001 inch from the dimensional measurement point of view.

For a rotating cutter such as an end milling cutter the criteria for correcting for the tool radius or replacement can be based on the radial wear on the flute. If the flank wears out such that the diameter of the cutter is reduced by 0.001 inch, then the cutter has to be either discarded or a tool radius compensation has to be employed. In other words, the cutter diameter database has to be updated with the new value of tool diameter for an end-mill. In the experiments discussed later, a 0.001 inch reduction in the cutter diameter will be used as the criterion to change the cutter or employ tool radius compensation. It is to be noted that the setup measures tool wear as radius whereas mechanical measurement involves tool diameter.

# CHAPTER 4

## IV. EXPERIMENTAL SETUP

### 4.1 Experimental Setup and Requirements

A brief description of the experimental setup is presented in this section. The different components and aspects of the system are classified and studied. This setup can

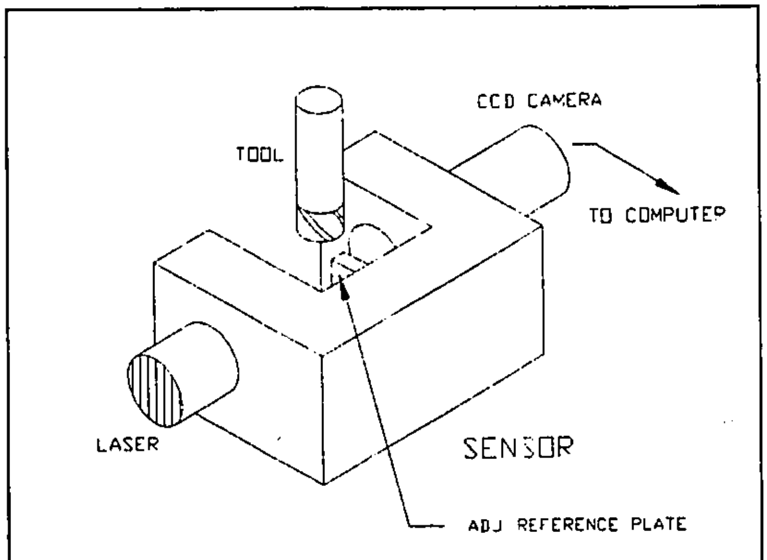


**Figure 4-1** : Conceptual Design of the Optical Sensor for Rotating Cutters.

be used in conjunction with a 3 axis NC machine with digital readout display. The experiments are conducted on such a machine in the Technical Support Centre of University of Windsor. The prototype sensor is presumed to be mounted onto the bed of the machine. The design of the prototype sensor is presented in Figure 4-1. It consists of a horse-shoe arrangement, where one end has the laser source and the other end has a screen and camera mounted. The cutter and the adjustable reference edge are mounted on the middle part of the sensor. The light source and the camera are controlled by the software running on an IBM compatible computer.

### 4.2 Design of the Experimental Setup

A brief description of the entire setup is presented in this section. The different components and aspects of the system are classified, studied and designed. This setup is used in conjunction with a 3 axis NC machine with digital readout display. A perspective view of the setup is given on Figure 4-4.

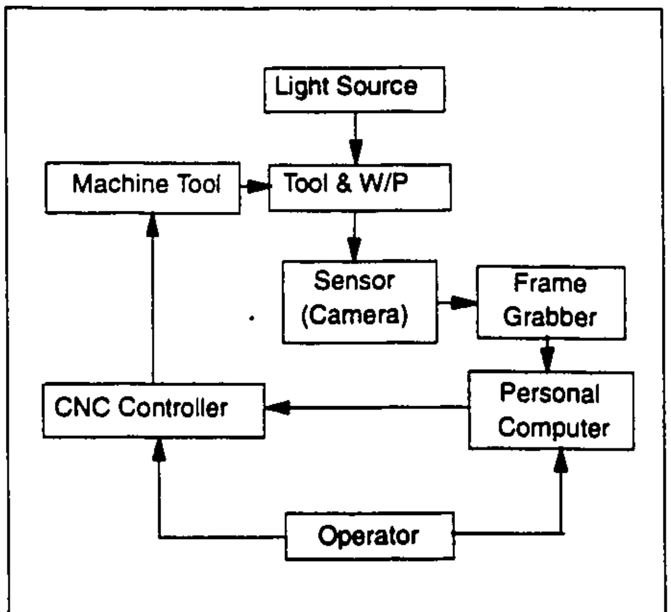


**Figure 4-2 :** Block Diagram of Tool Condition Monitoring using Optical Sensor.

The setup has been designed based on a few criteria. This prototype setup is capable of measuring tool wear for end-milling cutters with shank diameter up to 1 inch and cutter diameter up to 1-1/2 inch. The length of the tool could be between 3-1/2 inch to 4-1/2 inch. From the theoretical point of view, the cutters can have any number of flutes and any flute angle.

The whole setup has been designed in a way to provide maximum rigidity and strength. Most of the parts have been made out of aluminium and brass stock. The distance between the screen and the slit is kept quite low, only 6-1/2 inches, approximately.

A He-Ne laser source was readily available and was used as the light source. All parts like the laser source, the camera, the screen and the reference edge are movable in two axes to facilitate adjustments. The reference edge is mounted on a compound slide mechanism which moves the blade horizontally and vertically. It is also capable of tilting.

The cutter is held onto the baseplate using a V-Block. This provides means for a high degree of positioning accuracy.

### 4.3 Components of the Setup and Fabrication

The Tool Condition Monitoring System has a few components which may be classified as (a) Hardware and (b) Software.

### Hardware Used

The hardware used may be broadly classified into the following:

a) Laser source: The laser source is a He-Ne laser. It emits parallel light of wavelength 670 ± 10 nm with a beam diameter of 4 mm. It has random polarization.

b) Optical sensor: The optical sensor used here is a miniature CCD video camera which gives a composite video output. The camera is monochrome and is mounted directly onto a printed circuit board measuring 40 mm by 40 mm. It has a pre-focussed 4.3 mm lens.

c) Frame Grabber Board: The frame grabber board has a quad 512 by 512 pixel bit plane of which only one is necessary. It comes with the software subroutines for its operation along with the board. It has a composite video line in with an RCA connector. The composite video input is transformed into a 256 grey level image with 512 by 512 pixels.

d) Monitor: A monochrome monitor for pre-viewing the image grabbed by the camera. This is useful for setting up the equipment.

e) Personal Computer linkage: An IBM compatible personal computer is used as the main processor of information. It carries out all the operations related to the prototype sensor.

**Software Development**

The Software for this sensor must be capable of a few things. Firstly it has to communicate with the frame grabber board which is mounted on the computer bus. It must capture the image when signalled and turn the laser on while taking the snapshot. After acquiring the image, it has to do image pre-processing and processing until such an image is formed, which is ready for measurements. When the final processed image is brought over, the fringes can be identified and the distance between fringes can be measured.

Therefore, a menu driven interactive software, which controls the computer vision card and interfaces it with the mother board of the PC and also carries out all the computation, is necessary. The computer program is currently being developed in Pascal programming language. It captures the image from the CCD camera, and performs various operations on the image. It requires a 80486 based PC with a numeric co-processor and a video graphic adapter (VGA) of resolution of 640 by 480 pixels. The program calculates the tool wear automatically and displays it. It also gives the user certain statistical results obtained during the analysis of the image for further study. The software listing is presented in Appendix B of this text.

**Fabrication of the Setup**

All the parts of the setup have been designed and manufactured at the technical support Centre at the University of Windsor. Most parts needed an accuracy 0.001 inch to be able to fit each other and give the desired accuracies. Optical devices, especially ones measuring fractions of thousandths of an inch, require such precision. The micrometer slides have a resolution of 0.0001 inch.

### 4.4 Working of the System

The system has been designed to accommodate an end-milling cutter on the V-Block. The laser light passes through the slit formed between the reference edge and the flute of the cutter and forms a diffraction pattern on the frosted glass screen. This pattern is also visible from the other side of the screen. The camera can be focussed since it has an adjustable lens. It picks up the image of the diffraction pattern and is connected to the frame grabber board of the PC. It is stored as an image file using a program to grab the image and save it. Later this image file can be analyzed using the software written for this purpose. Since the camera has a lens, this arrangement must be calibrated.

The machining is carried out on a work piece at the desired spindle RPM, depth of cut and feed, for the desired length of cut. After a fixed number of passes, the milling cutter is withdrawn and positioned in the setup for measurement. The measurements are taken by the driving software and the wear is determined.

The laser light, as it passes through the slit, produces a diffraction pattern on the screen. The sensor uses a CCD camera for grabbing the image and feeding the information into an IBM compatible PC. This image is grabbed by the frame grabber board of the PC and then it is analyzed by various image processing techniques. The tool wear is calculated based on the fringe pattern spacing variation. This technique has high resolution and measurement range. It is also correlated to the commonly used flank wear measurement. This prototype sensor has demonstrated good repeatability and accuracy. It may find industrial applications since it also has high speed, reliability and resolution.

With the advent of optics and computer vision systems, optical sensors are now not only feasible to implement but also economically justifiable. An industrial application must however detect broken tools before a catastrophic failure. They should also be capable of monitoring progressive tool wear. All these must have a high reliability in the shop floor environment to satisfy the industrial requirements. Figure 4-3 shows a typical end-milling process.

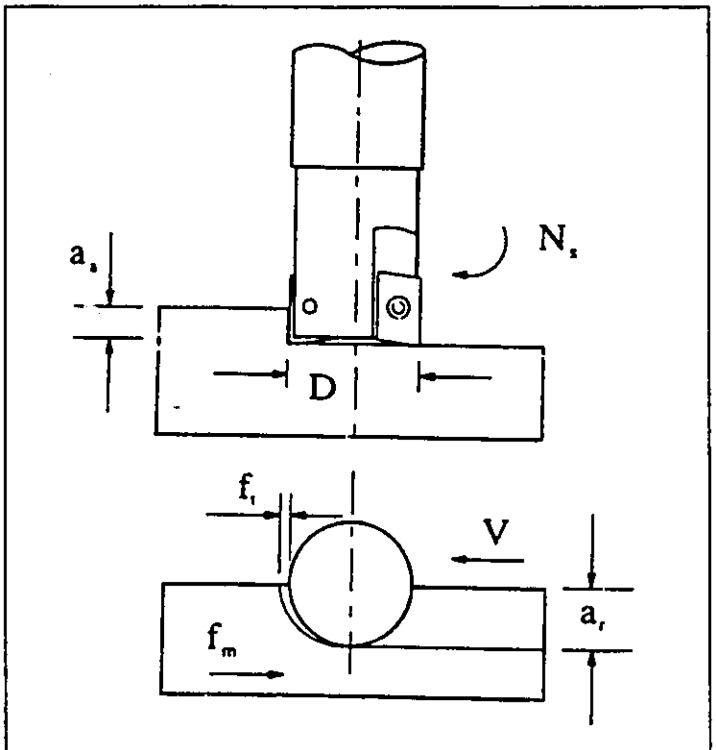


Figure 4-3 : End Milling Process

### 4.4.1 Experimental Procedure

Each time an image is taken, it is necessary to record all possible physical information available. These include all the measurable data like horizontal slide position, vertical slide position, angle of tilt and so on. Other measurements like the distance of the screen and the camera are never altered once fixed and hence can be recorded before and after carrying out the experiments.

The steps followed by the setup can be divided into the following parts. They are:

a) <u>Tool Positioning</u>: Thc tool is held snugly with the V-Block so that the flute touches the stop. The first time this is done, the reference edge must be approximately 0.001 inch away from the edge of the flute and it must be as parallel to it as possible. This will ensure a good diffraction pattern and accuracy.

b) Diffraction Pattern: Once the tool is correctly positioned, the laser is turned on for a brief period and diffraction pattern is obtained. This diffraction pattern is captured by the camera which is controlled by the software.

c) Image Acquisition: The image is acquired from the camera in the frame grabber board. The software then applies image transformation algorithms to process the image and finally the fringe spacing of the diffraction pattern is found The scanning of the scene involves proper lighting and proper placement of the CCD camera with respect to the screen. The CCD camera coupled to the software program has to be calibrated to start with because it has to convert the analogue signals coming from the camera into digital form on a proper scale. After a proper brightness intensity level of illumination is obtained a snapshot of the screen is taken. The image can be displayed on the auxiliary monitor. The camera comes with a preset focus and hence need not be adjusted for focus. The satisfactorily adjusted image is now ready to be stored as a binary raw data file.

The image can be represented by a discrete function f(x,y) such that x and y are the x and y coordinates and f is the grey level function. It is to be noted that x, y and the function are all positive integers. The image is acquired from the camera in the frame grabber board. The software then applies image transformation algorithms to process the image and finally the spacing between the fringes are found.

d) Image Retrieval and Processing: The raw image data file is read in by the computer as a linear array of bytes from the raw data file. It is also displayed on the computer screen which uses a VGA card. This image read in by the computer is ready for subsequent image processing operations. The brightness profile is used to find the fringe widths through elaborate filtering. The entire burden of number crunching is left for the computer to do. Once the minima are located, the difference in the location of these minima give the fringe spacing in pixels in inches.

As the beam passes through the gap between the flute of the end-milling cutter and the adjustable reference edge, the phenomenon of diffraction takes place. This edge is held at the same helical angle as that of the flute. The diffraction pattern is obtained on the screen and this is captured by the CCD camera. The top part of the diffraction pattern refers to the unworn part of the tool. The bottom part corresponds to the worn part of the tool and hence the fringe spacing is smaller.

It will be seen that as the tool gradually wears out, the shape of the pattern changes. It would assume a bell shaped nature when the tool wears or starts to wear out. Now, if the space between two consecutive fringes in the diffraction pattern are taken, the one on the top will have a higher spacing than the one at the bottom.

The analysis can be carried out after obtaining the measured tool wear. The two methods can be compared how the tool wear values obtained by conventional methods match this approach. Once it is established, this work can be further extended to the analysis of tool wear, tool life pattern and other things like how tool wear depends on various machining parameters.

A few other mathematical and statistical operations are carried out. After carrying out all these calculations there will be enough mathematical data on image to start the measurement procedure. The setup for such a sensor is illustrated in Appendix A.

### 4.4.2 Limitations and Control

For the testing of the prototype sensor, there is a need to orient and stop the end milling cutter at the correct angle. This is beyond of the scope of this work but a method for accomplishing this is outlined.

The software developed for the sensor should be capable of issuing commands that the CNC machine would be able to take as input without any manual intervention. This is possible through the use of an output port in PC. The spindle of the milling machine needs a special encoder for finding the orientation of the spindle as it stops. A stepper motor drive is necessary to bring the cutter to the orientation. For this experiment, however, the implementation of this feature may not be feasible and will be left for future work.

## 4.5 Problems

In the preliminary experiments a number of practical problems were encountered. Some of them are relatively easy to solve but some are a bit difficult. These problems can be classified into mechanical problems, optical problems and control problems. A majority of the problems were faced in the image processing. Most of these problems pertain to the actual image processing that needs a more practical approach than a theoretical one. A few of these are discussed below.

Repeatability: This happens due to the finite repeatability error of the machine tool. It cannot be eliminated at the source and needs to be addressed at the image processing stage. However due to the comparative nature of the measurements, this problem is taken care of to some extent. The remaining part of repeatability error can be offset by image processing algorithms to some extent.

Noise spots: These were eliminated partly by filtering the image using a 3 by 3 spatial filter matrix. However, larger noises are hard to segregate and require correction by object selection and highlighting.

Glare: This was due to improper lighting which can be eliminated by adjusting the angles at which the lights are incident on the object. This can also be contained by calibrating the brightness.

Orientation of Cutter: The conceptual method had a problem related to the orientation of the cutter. The other alternative is to use a V-block on a base plate and have the cutter rest upside down such that the shank is snugly in contact with the V-block flat surfaces. This has been incorporated in the prototype tool wear sensor.

Ambient Light: Ambient light can be eliminated by subtracting the image without laser from the image obtained with laser. Alternatively one can carry out the experiments in a dark room. This will ensure that ambient light has no role to play in the measurement.

Noise: The way fringe spacings are measured is using the brightness profile. The brightness profile inherently has noise. This will be quite evident from the graphs shown in the appendix. However there are a few certain properties that all these brightness profiles will have. That is a reasonably well defined minima. The filtering procedures filter out only the prominent minima since there could be faulty or misleading location.

Distance Z: Usually optical diffraction experiments have this of the order of 40 inches. In the prototype, mechanical rigidity was a concern and this was made compact. In future designs, however, the optical length can be suitably increased by the use of mirrors.

After encountering some of these problems, certain modifications in the software were necessary to either reduce, control or eliminate these. The final source code for the program PROFILEX is listed in Appendix B.

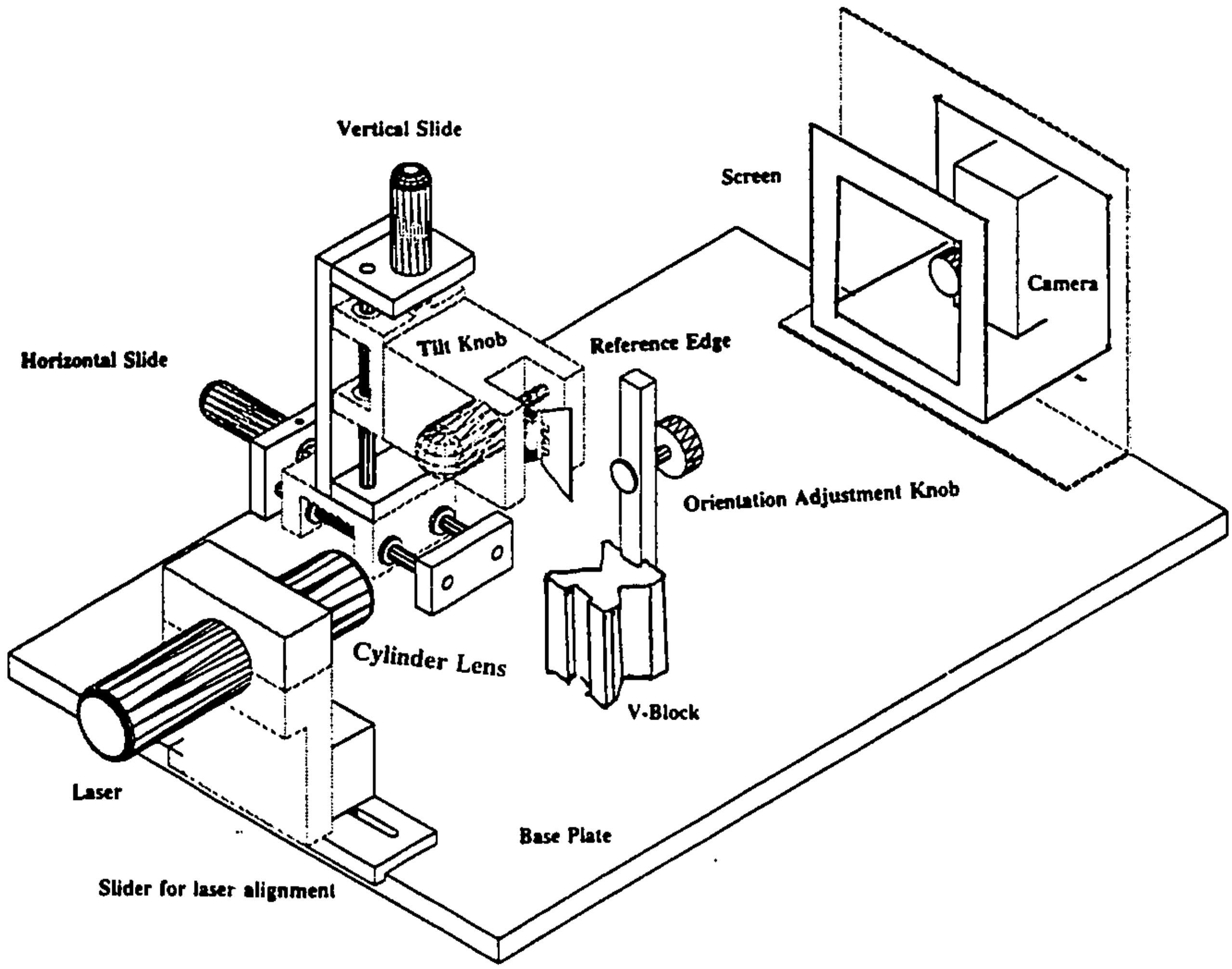


**Figure 4-4** : Perspective View of the Experimental Setup.

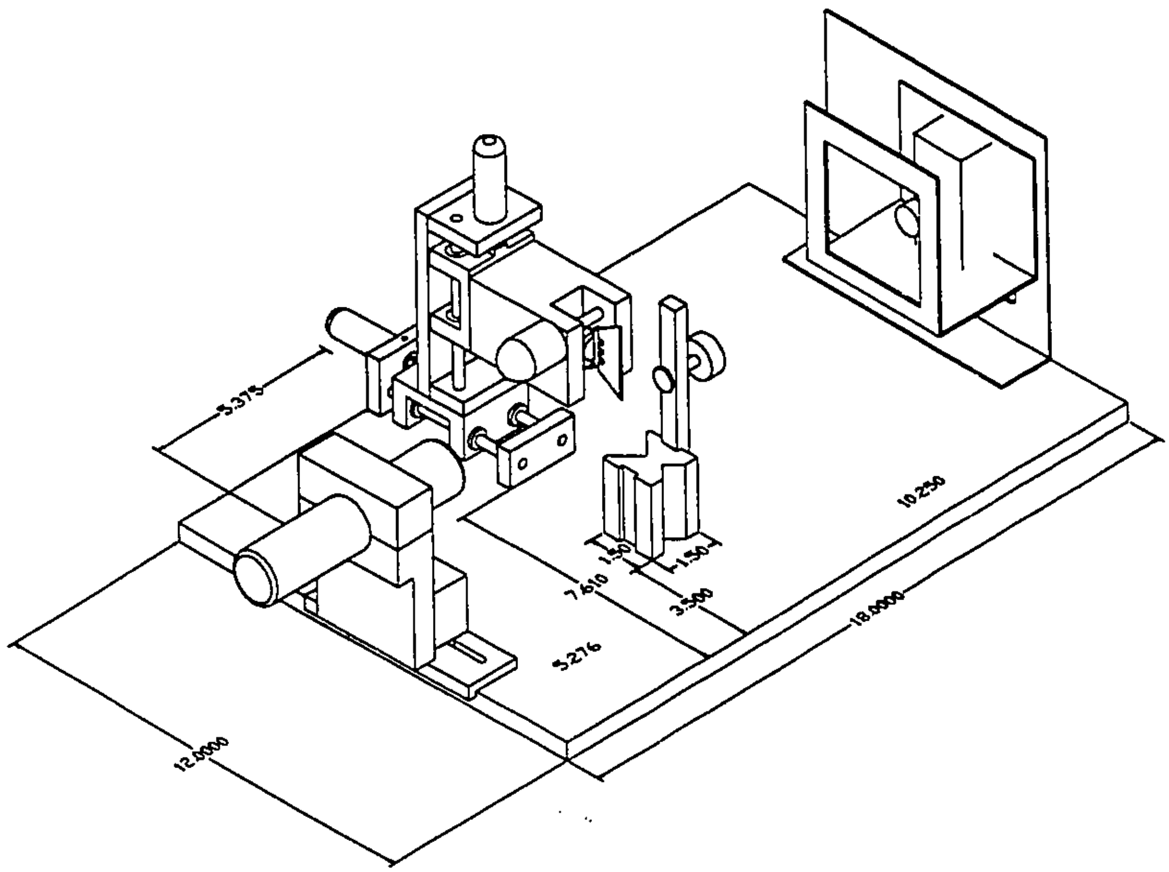


**Figure 4-5 :** Experimental Setup with Important and Critical Dimensions in inches.

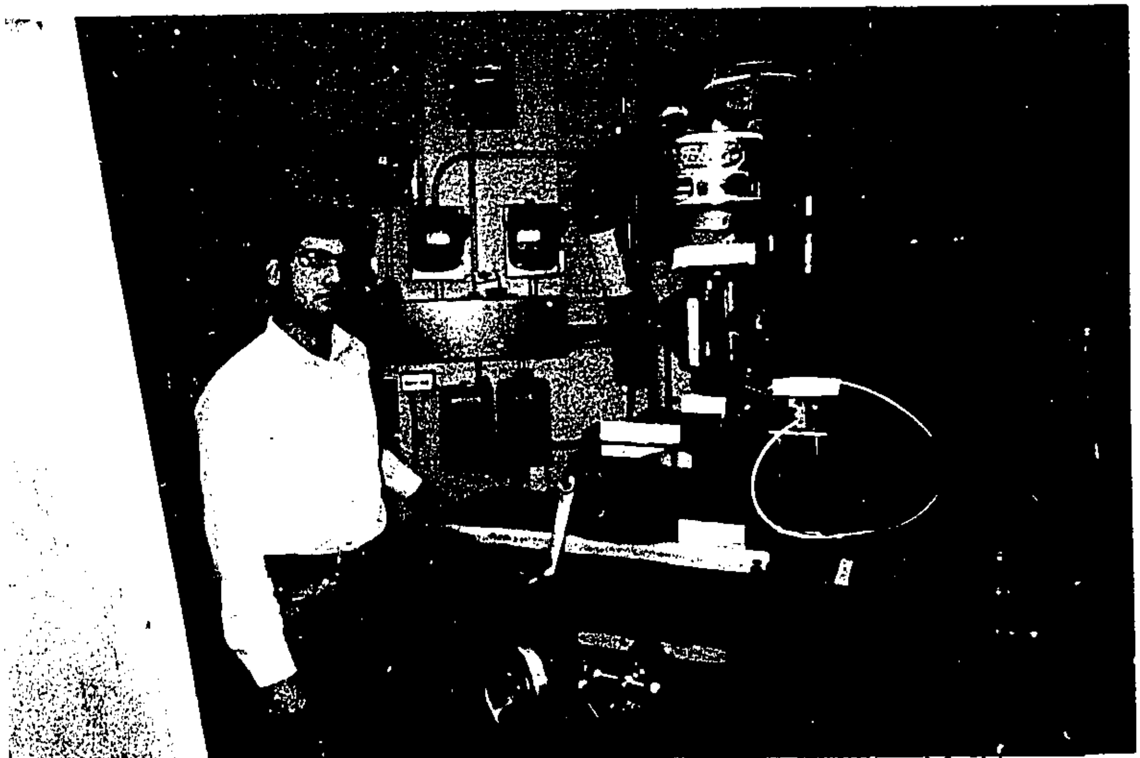

**Figure 4-6** : Conducting experiments on the Bridgeport Milling Machine.

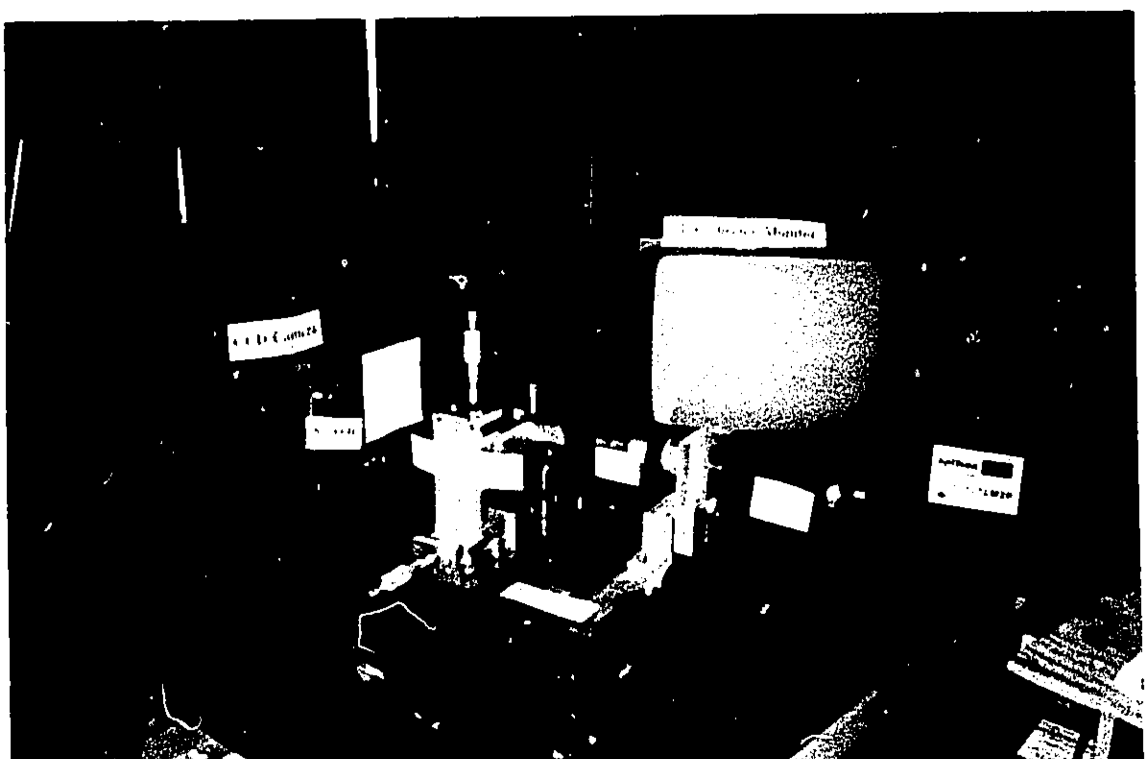

**Figure 4-7** : Picture showing experimental setup.

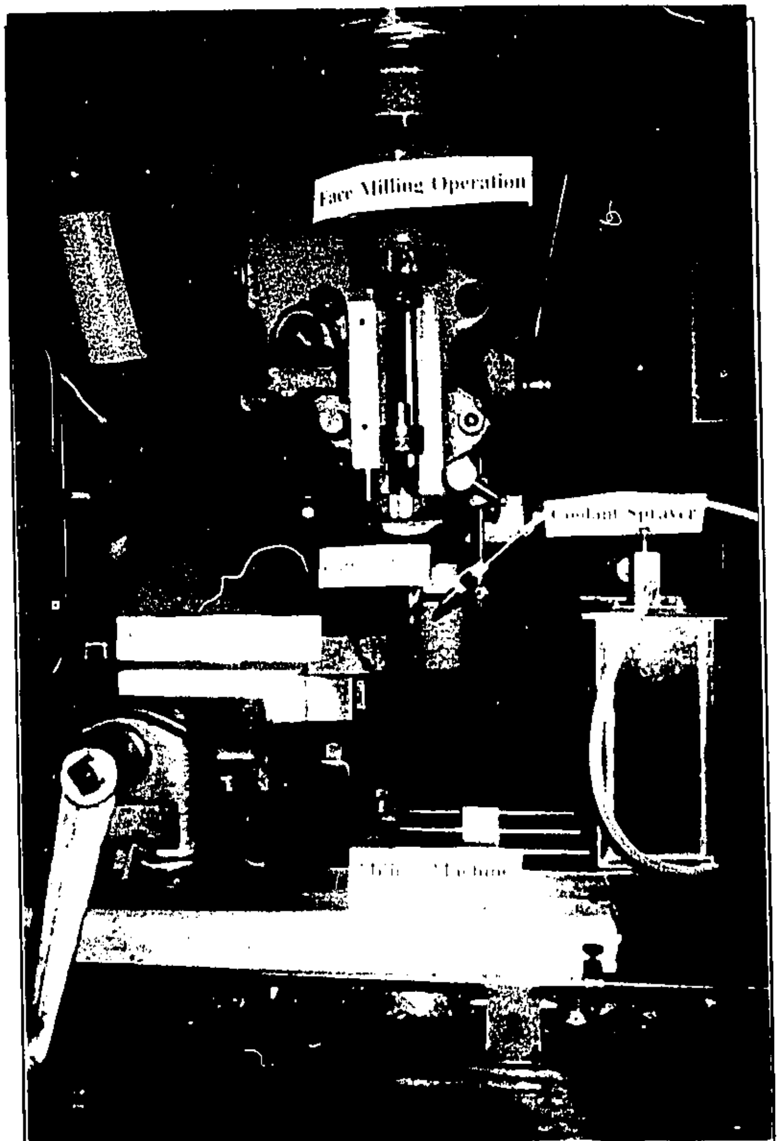


**Figure 4-8** : Closer view of the machining setup while doing experiments.

# CHAPTER 5

## V. EXPERIMENTATION

### 5.1 Design of Experiments

The experiments have to be designed in a way that the number of actual experimental observations is minimized. At the same time it should be possible to vary the maximum number of variables. The variables which play an important role are tool replacement repeatability, use of cylinder lens, horizontal slider position, vertical slider position, tilt angle, tool wear, effect of coolant and effect of the experimenter. These were the most relevant factors concerning the scope of work and the experimental setup.

There are other variables that could have been varied or used but they do not fall within the scope of this research.

### 5.2 Experiments Conducted

There have many experiments conducted which have been documented in Appendix C. The first set of experiments deal with the effect of noise of fringe spacing variation as outlined in Table C-2. This captures the effect of various noise components that are inherent in the system like the CCD, the laser and other hardware. Ambient temperature can also cause some noise into the system. The data files collected are named A01, A02, A03, A04 and A05.

Table C-3 gives the summary of the experiments conducted to assess the effects of different factors on the measurement accuracy. The effects studied are listed in the table and the data sets are numbered from Series 1 to 8.

The eight series of experiments can be briefly described as follows:

Series 1: This deals with the effect of horizontal slider movement on the fringe spacings. The images are taken without the cylinder lens, using a brand new tool, with no tool replacement. The image files collected are named B01 through B13. This series considers the horizontal movement of the reference edge done by rotating the micrometer screw for the horizontal axis. are also present. In addition, the reference edge is moved to see the effect of mechanical movement on the optically measured slit width as performed by the system. This series gives the basis of calibration of the system.

Series 2: This series deals with the replacement of the tool without wear. In this case the repeatability of the tool in the V-Block holder is studied. The factor studied is tool replacement repeatability errors. The files are named C01 through C05.

Series 3: This series deals with checking the effect of introducing the cylinder lens. The files are named D01 through D05.

Series 4: Effect of Vertical Movement of the micrometer is studied in this series.

Series 5: Effect of the tilt angle of the reference edge is studied.

Series 6: Effect of Experimenter on Measurement is studied.

Series 7: Three brand new end-mill cutters are worn out and the tool wear is measured mechanically as well as optically. Coolant is used in all the cases since the work piece material is very hard. Coolant is sprayed on the cutter during machining using a pneumatic mist. Before measurements are taken the cutter flute is wiped off.

Series 8: The effect of coolant not being wiped off is studied in this series. A brand new cutter is worn out to 0.001 inch as well. This time the coolant film remained on the flute. This effect is studied.

In Series 7, three selected image files, namely, IMG1, IMG2 and IMG3 are chosen for different kinds of analysis. The brightness profile of the image itself reveals different kinds of information.

Some of the series have been analyzed to find the calibration curve and other performance parameters. They are present in the form of graphs and tables in the appendix C.

### 5.3 Results Obtained

The results obtained are all presented in the form of tables in Appendix C. The different series have been studied independently and conclusions can be drawn based on these. Figures 5-1 through 5-23 outline different characteristics of the data collected in the form of graphs.

Table C-2 show the effect of noise on the fringe spacing variation. It gives an error of 1.5 %. Hence, the contribution of noise in the system can result an error of 1.5 % which is quite small.

Measurements are done based on line 230. Figure 5-1 shows that there is a drop of the trend on the right side. This is because of non uniform aperture width. This is better illustrated on figure 5-19. Uniform aperture width is very difficult to accomplish and hence the measurements have to be carried out on a particular scan line or its neighbouring lines.

Referring to the variation in the aperture widths, table C-2 shows how the aperture width varies with the horizontal scan line number. A few conclusions can be drawn based on this observation. They are as follows:

(i) It is very difficult to make the slit opening perfectly parallel.

(ii) The average of the aperture width from 5 scan lines have to be used to calculate tool wear.

(iii) There is no guarantee that a new flute will have a straight edge and moreover when the flute is worn, it will not be straight for certain.

Table C-4 deals with the position of the horizontal slider. This is the key data set for calibration of the equipment. Figure 5-4 shows that the mechanical measurement and optical measurement are closely related. The error calculated on Table C-5 are mostly in the range of plus or minus 4% except for the first observation.

Figure 5-7 shows a typical brightness profile. It can be seen that it contains some noise. As the gap is increased the fringes grow in number and come closer to each other as show on Figure 5-9. The fringe spacing is most sensitive to the horizontal position.

Figure 5-10 shows the effect of glare. This is sometimes not avoidable and hence may be a cause of error.

Considering series 2, the tool replacement repeatability is about 6.2 %. This is definitely larger than the noise component as one would expect. In Series 3, adding a cylinder lens causes an error of 3.2 % which is less than the tool replacement repeatability. But taking the fringe spacings into consideration for series 2 and 3, they both have the same order of error.

Effects due to vertical position, tilt and the experimenter are negligible. They are below 1% and of the order of noise in the system.

Figure 5-15 also demonstrates that the aperture width is not uniform and has an interesting pattern in it. This variation in the aperture width is due to the helical nature of the flutes of the cutter. Figures 5-19 to 5-21 show how the diffraction pattern changes with tool wear.

Figure 5-22 contains the most crucial information about the accuracy of the setup. Figure 5-23 show the errors and how they vary. The error in the measurement of the tool wear if between plus and minus 15 %.

The effect of coolant not being wiped resulted in a lower optical reading of the tool wear. This is actually true since the adherence of coolant on the cutter flute causes a liquid film to build on the edge. This shortens the slit width and hence a lower tool wear is reported.

### 5.4 Interpretation

Line 230 happens to be the line containing maximum luminous energy. For all the data processing and fringe spacing calculations, this line is chosen as a reference. From the results in Appendix C, it can be concluded that the accuracy of the setup is good. The accuracy is the lowest when the slit width is small (of the order of 0.001). As the cutter wears out, the distance increases and hence the accuracy improves. From Table C-5 it is clear that for very high values of wear the setup has good accuracy. Referring to table C-14, a 0.0034 inch reduction in cutter diameter is actually 0.31 mm in terms of VB. This amount of wear is easily accommodated in Table C-5 where calibration of the setup has been done.

Experiments have been carried out for the cutters up to 0.001 inch reduction in cutter diameter. However, if it is desired to measure the tool wear till the end of the tool life, one can reset and recalibrate the equipment after every 0.001 inch reduction of cutter diameter. The measurement is most sensitive in the first 0.001 inch reduction.

### 5.5 Analysis and Data Processing

The Software for this sensor is capable of a few things. Firstly it communicates with the frame grabber board which is mounted on the mother board. It captures the image when signalled and takes a snapshot. After acquiring the image, the brightness profile is used for measurements. The fringes are identified and the distance between the selected minima are found. This gives the fringe spacing of the diffraction pattern. An arithmetic mean of the various fringe widths measured give a more accurate value of the fringe spacing.

The software listing is given in Appendix B. The image acquisition program is written in FORTRAN as it uses some FORTRAN libraries supplied with the frame grabber board. The image processing program is written in PASCAL which is interactive and menu driven. The former controls the computer vision card and interfaces it with the mother board of the PC. The latter carries out all the computations. The computer program developed called PROFILEX, reads the image file from the disk drive and performs various operations on the image. It requires a 80486 based PC with a numeric co-processor and a video graphic adapter (VGA) of resolution of 640 by 480 pixels. The program is calculates the fringe widths automatically and can display the tool wear also.

### 5.6 Problems Faced

Some of the data sets as seen in Figure 5-6, are incomplete. Due to noise in the brightness profile, sometimes it is not possible to determine the fringe spacing using the software PROFILEX.

In the experiments a number of practical problems were encountered. Some of them are relatively easy to solve but some are a bit difficult. Theses problems can be classified into mechanical problems, optical problems and control problems. A majority of the problems were faced in the image processing. Most of these problems pertain to the actual image processing that needs a more practical approach than a theoretical one.

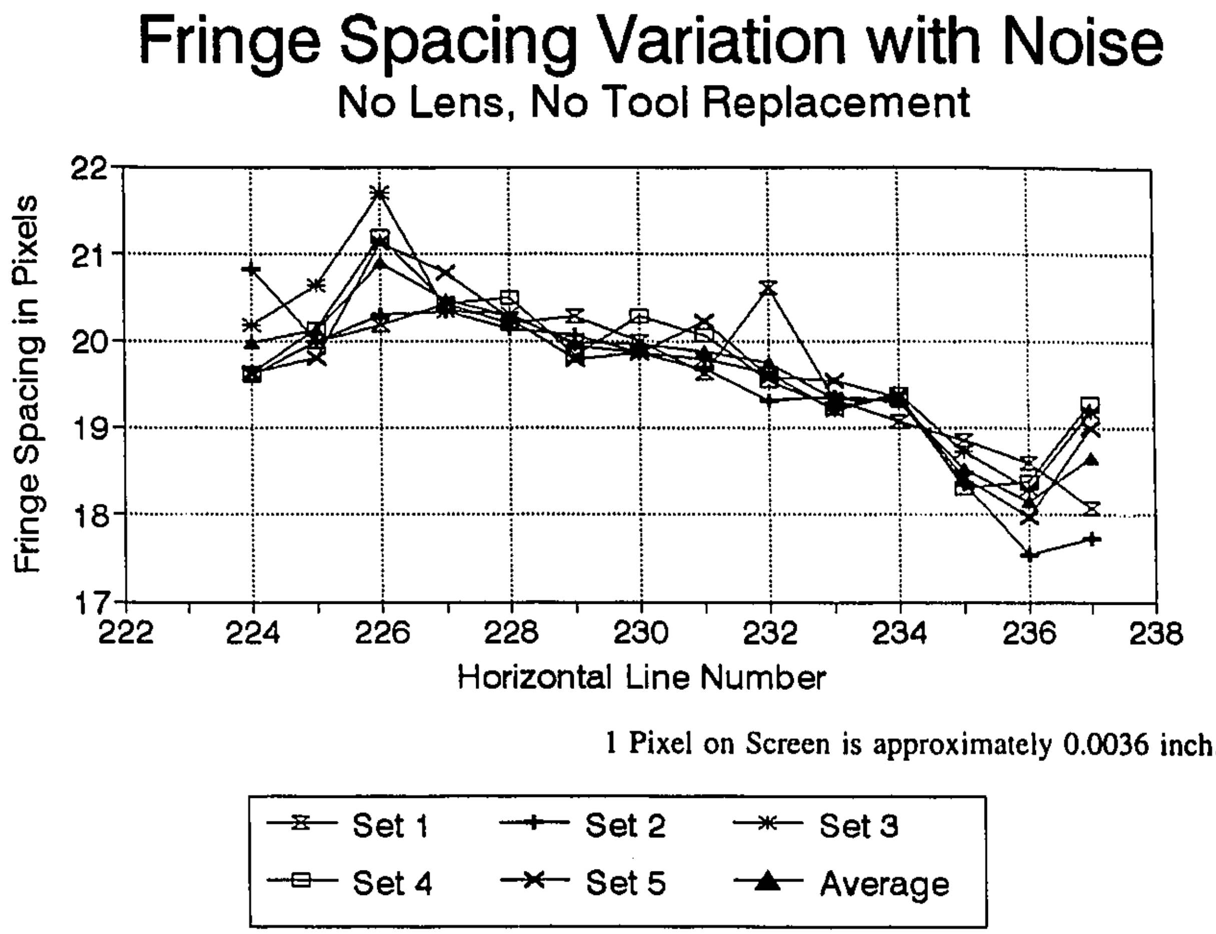


**Figure 5-1** : Fringe Spacing Variation with Noise.

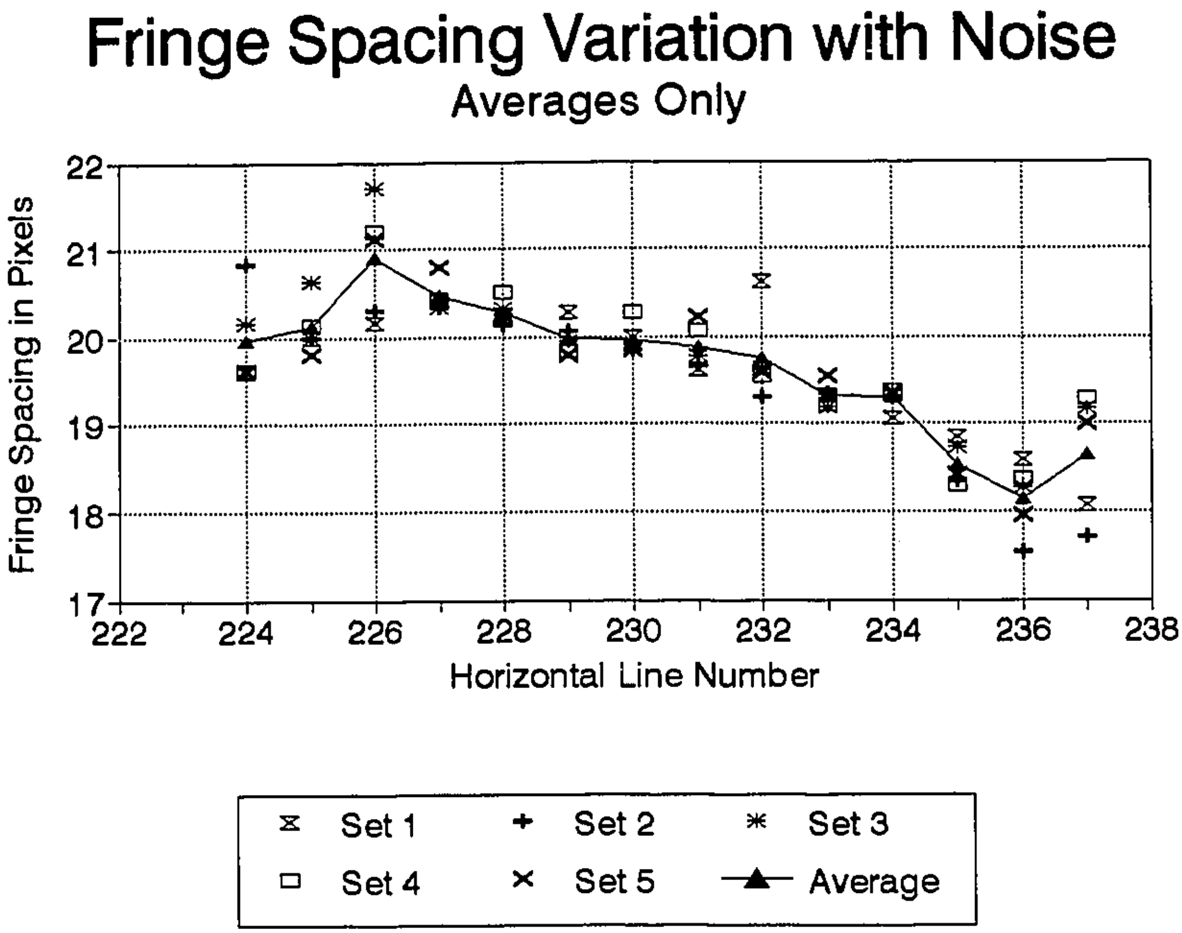


**Figure 5-2 :** Fringe Spacing Variation with Noise (Averages Only).

# Fringes

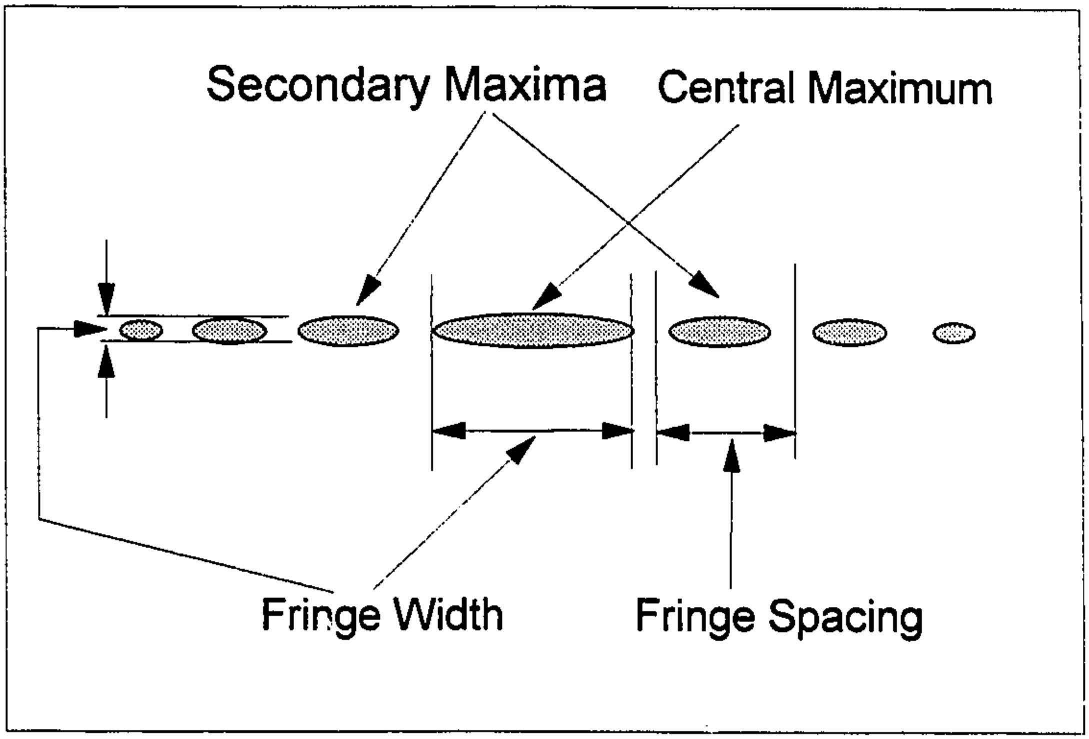


**Figure 5-3 :** Fringe Width and Fringe Spacing.

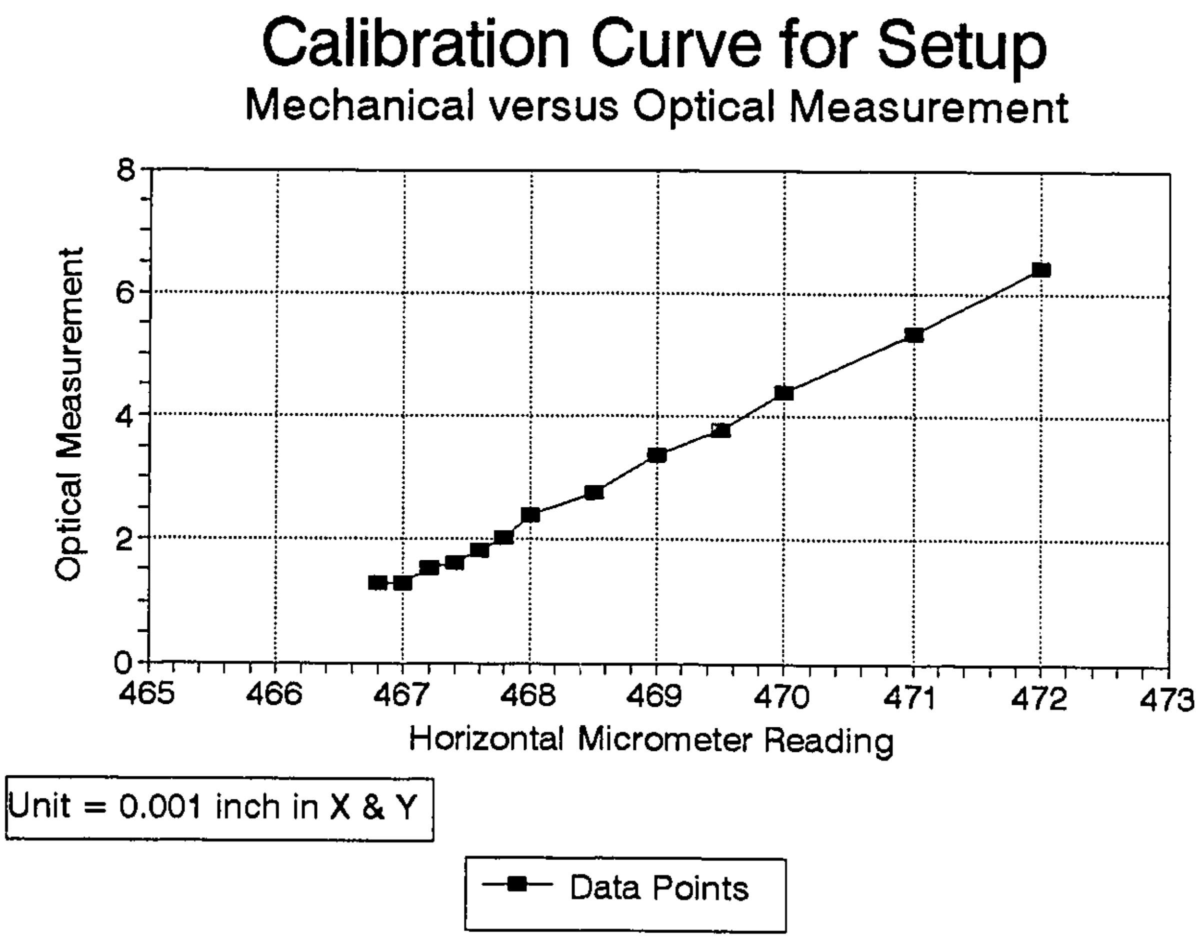


**Figure 5-4** : Calibration Curve for Setup (Mechanical versus Optical Measurement).

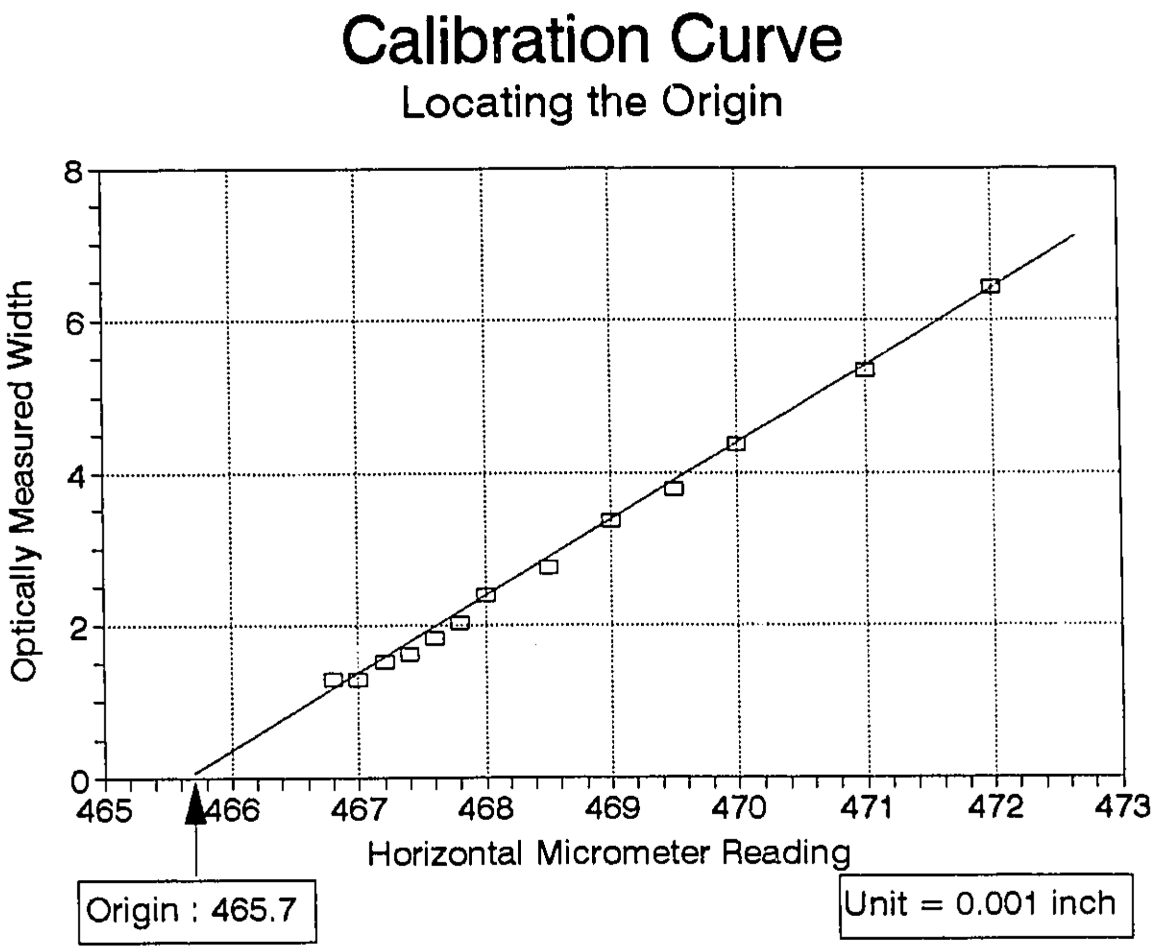


**Figure 5-5 :** Location the Origin using the Calibration Curve.

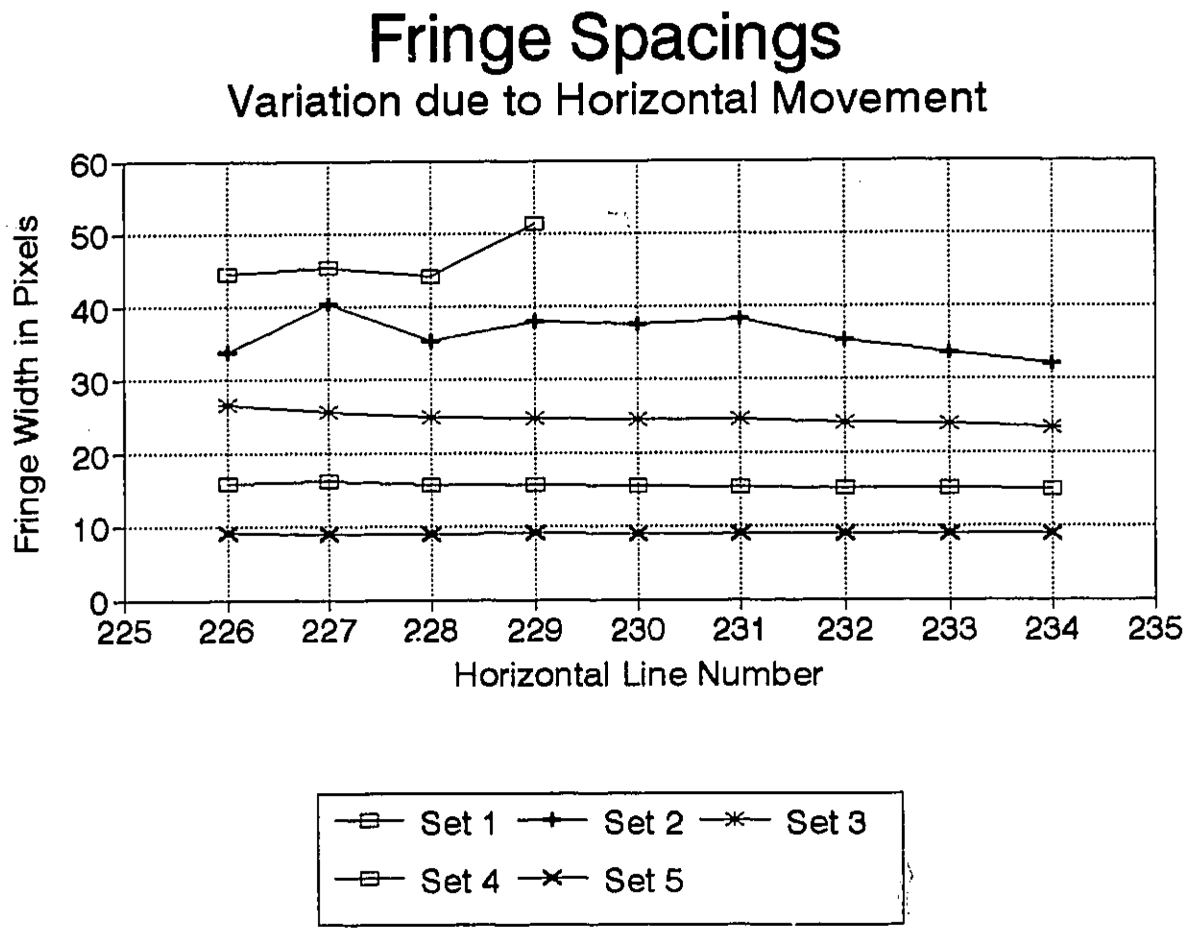


**Figure 5-6 :** Fringe Spacing Variations due to Horizontal Movement.

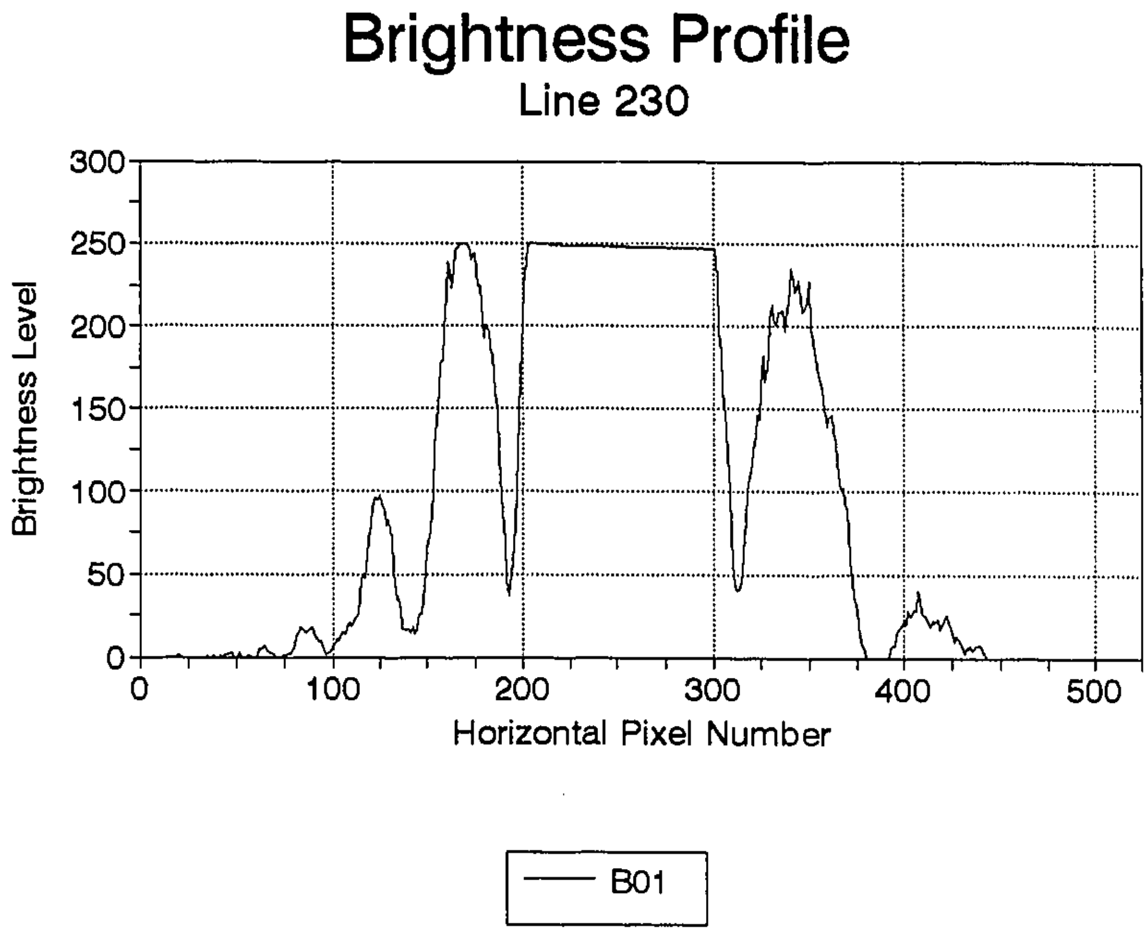


**Figure 5-7** : Brightness Profile of Line 230 of file B01.

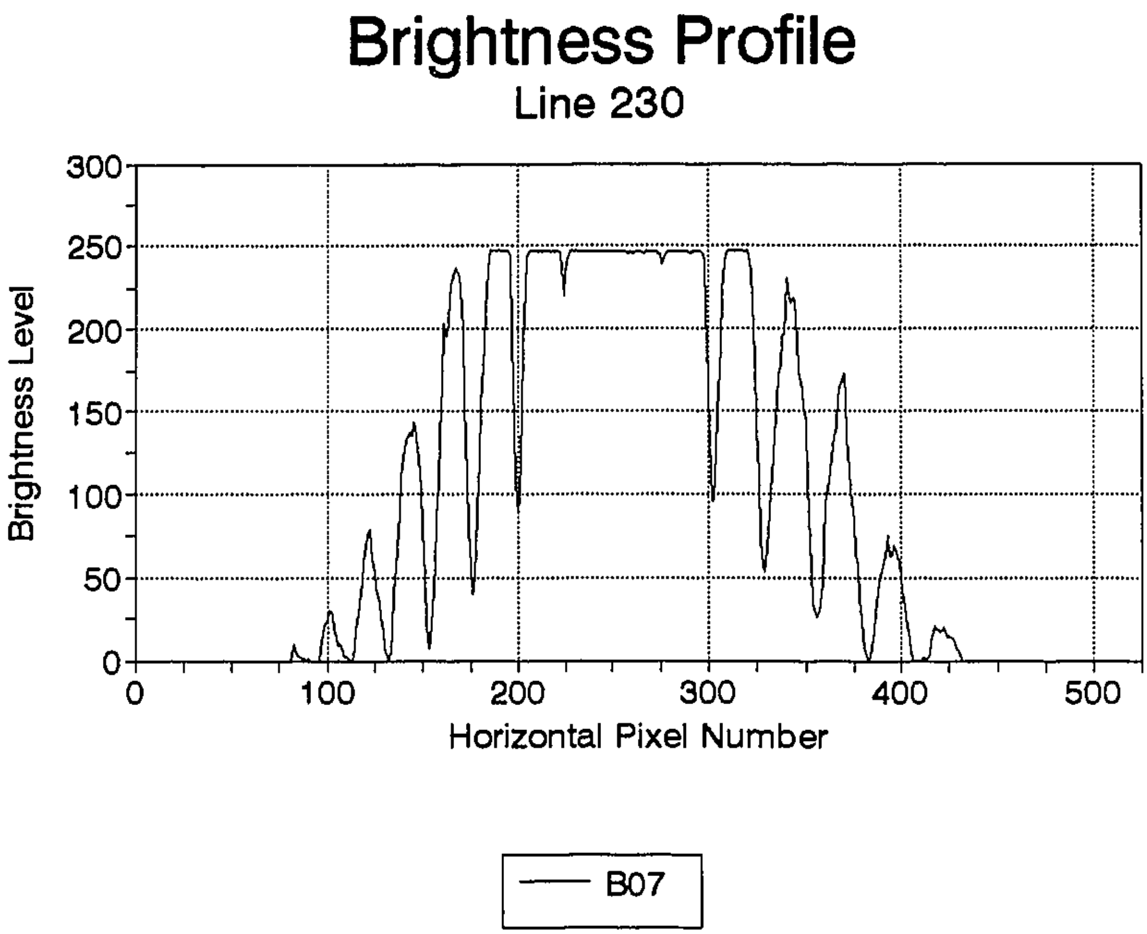


**Figure 5-8** : Brightness Profile of Line 230 of file B07.

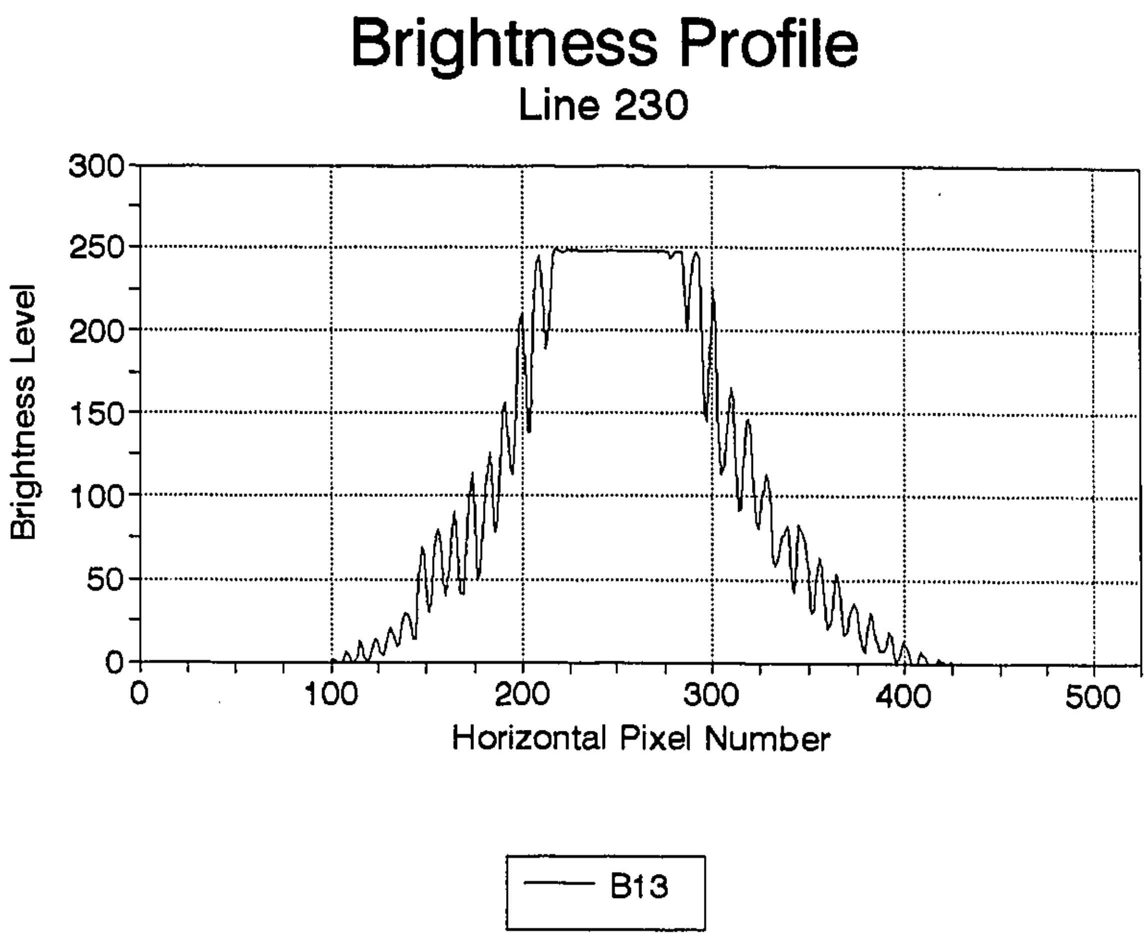


**Figure 5-9 :** Brightness Profile of Line 230 of file B13.

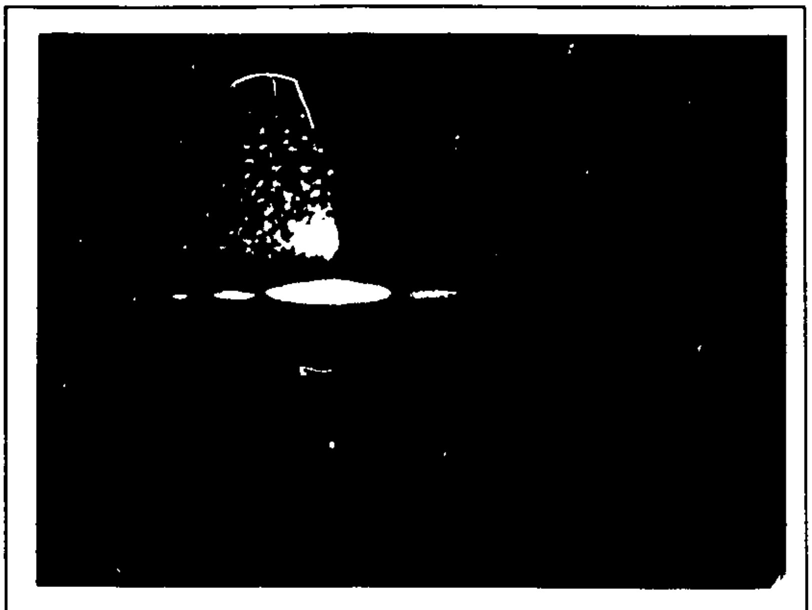

**Figure 5-10** : Image file B01

**Figure 5-11** : Image file B07

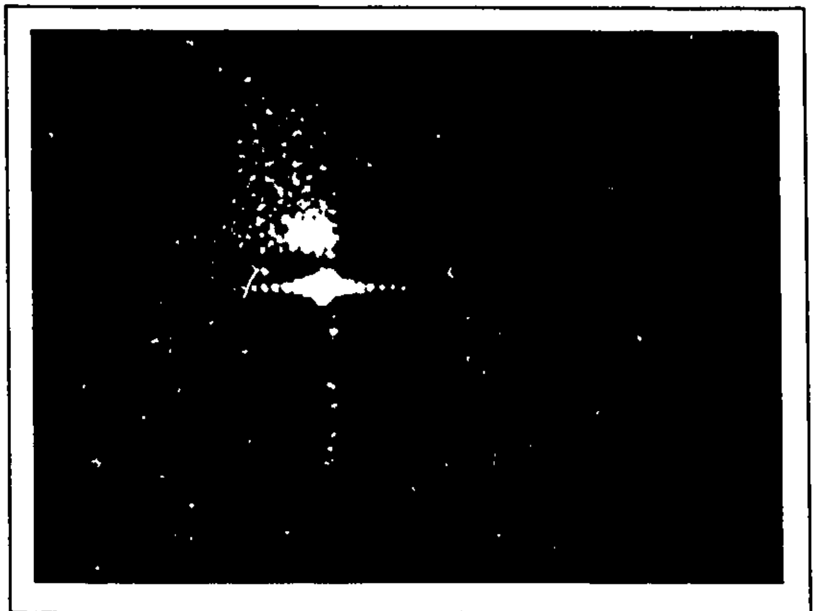

Figure 5-12 : Image file B13

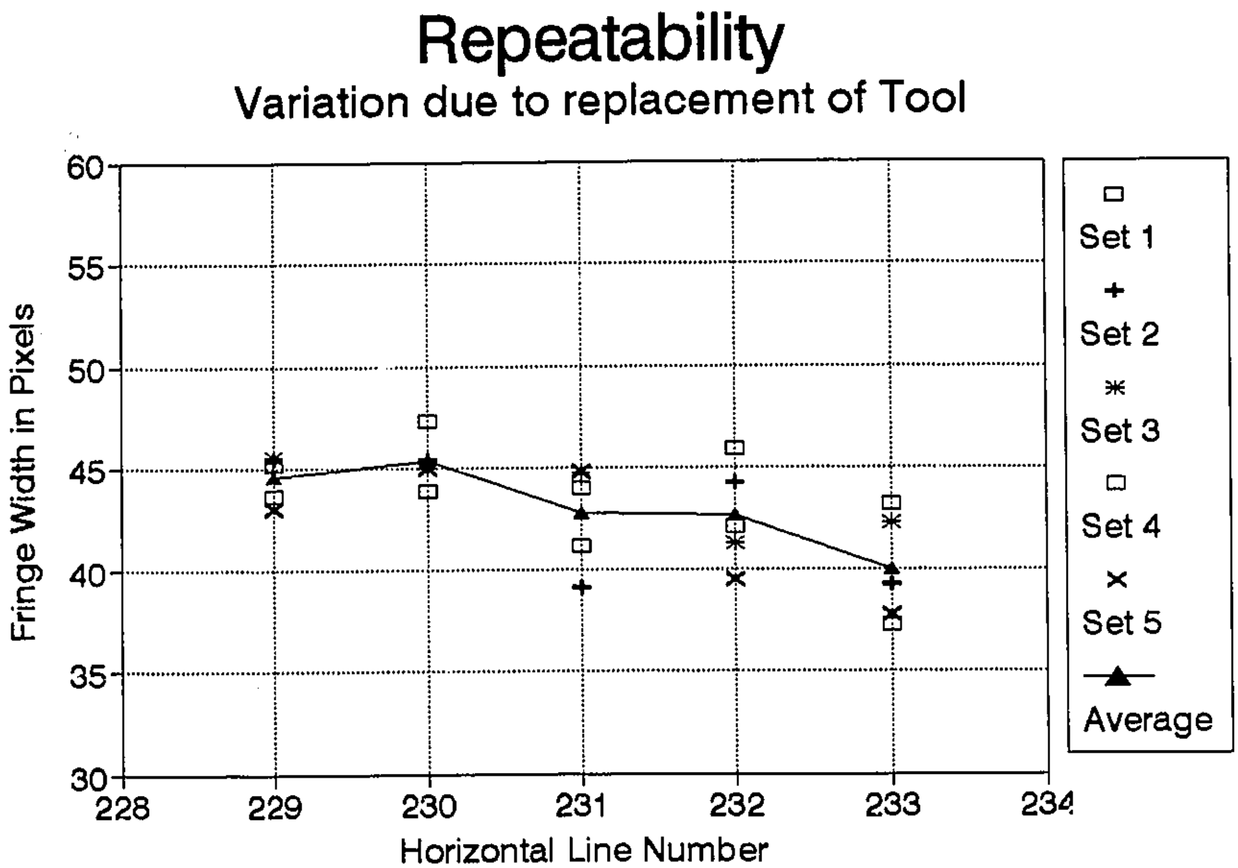


**Figure 5-13 :** Repeatability Effect (Variation due to replacement of cutter).

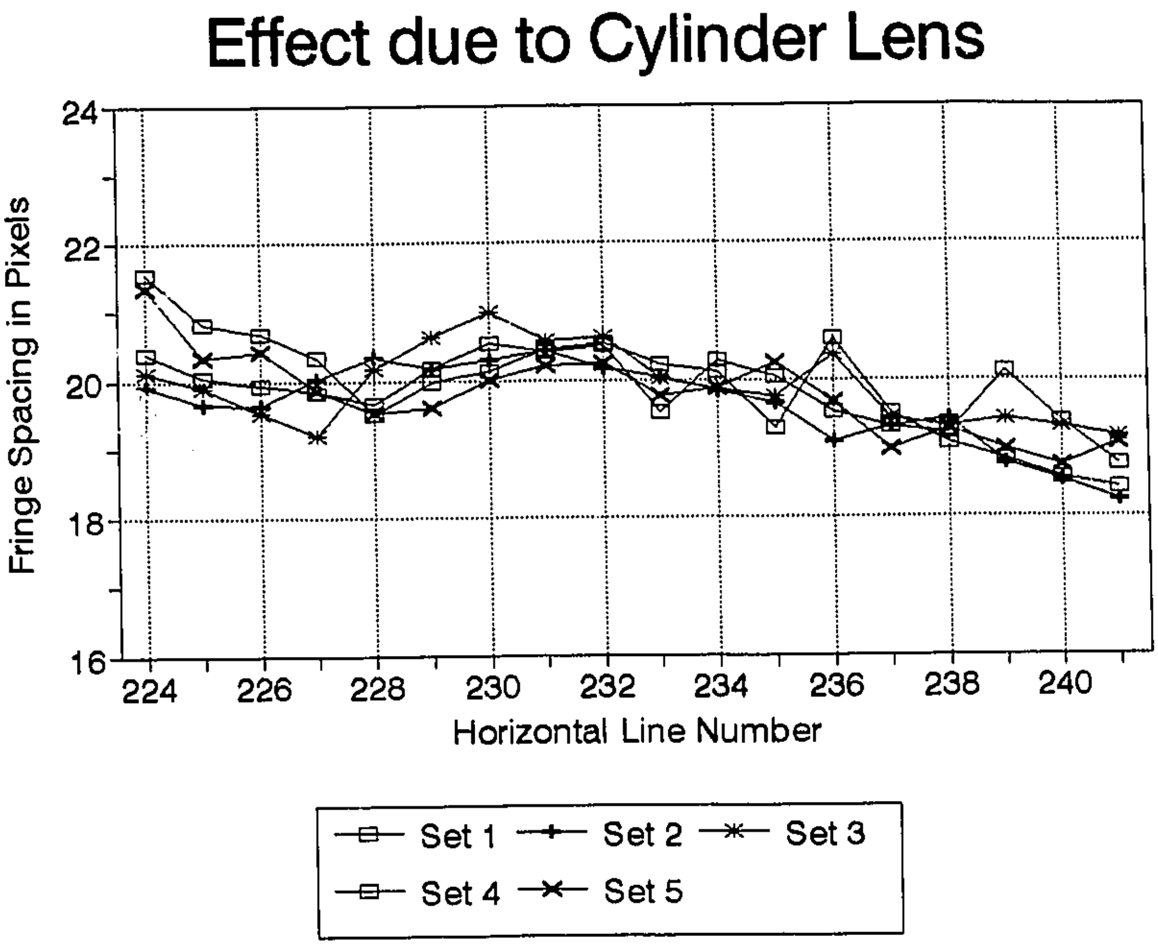


**Figure 5-14 :** Effect due to the addition of a Cylinder Lens.

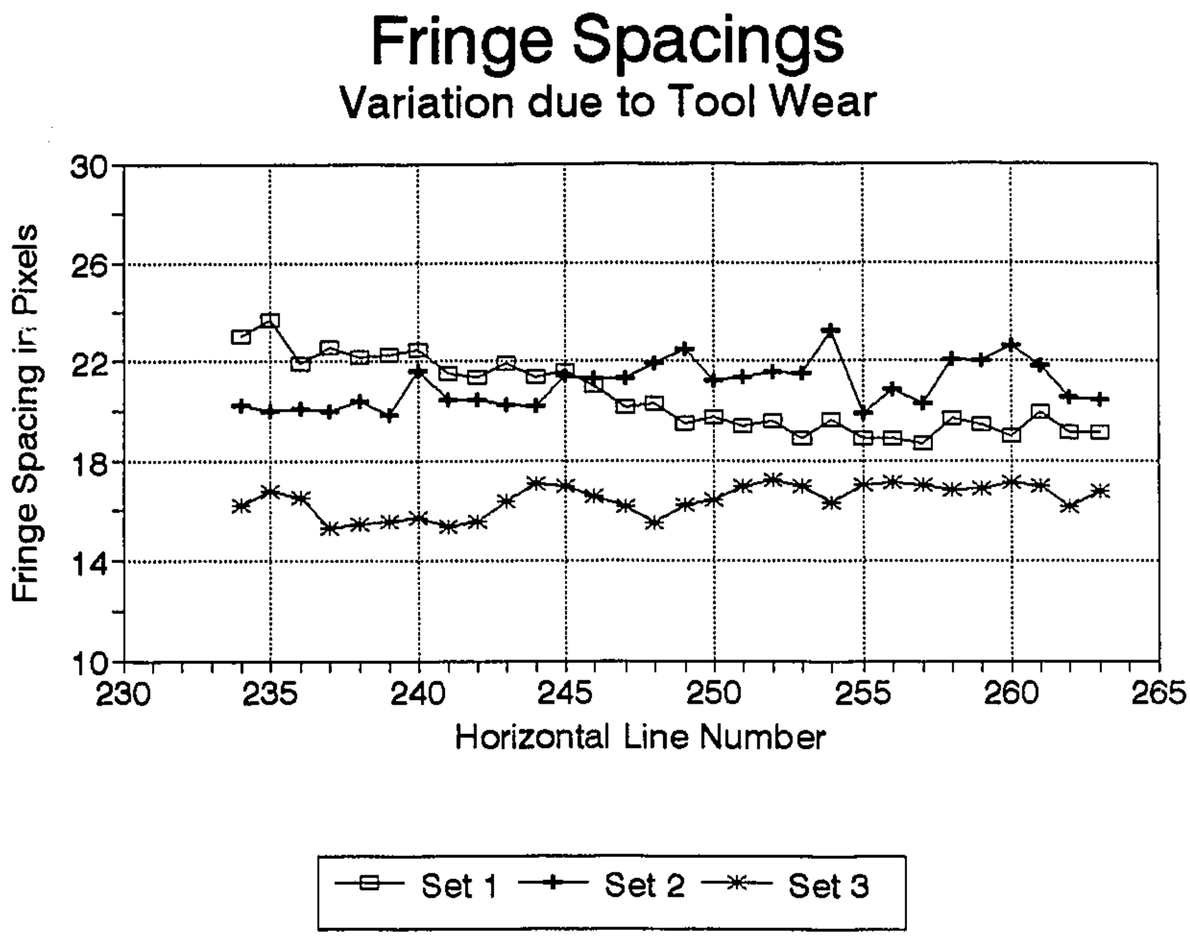


**Figure 5-15 :** Fringe Spacing Variation due to Tool Wear.

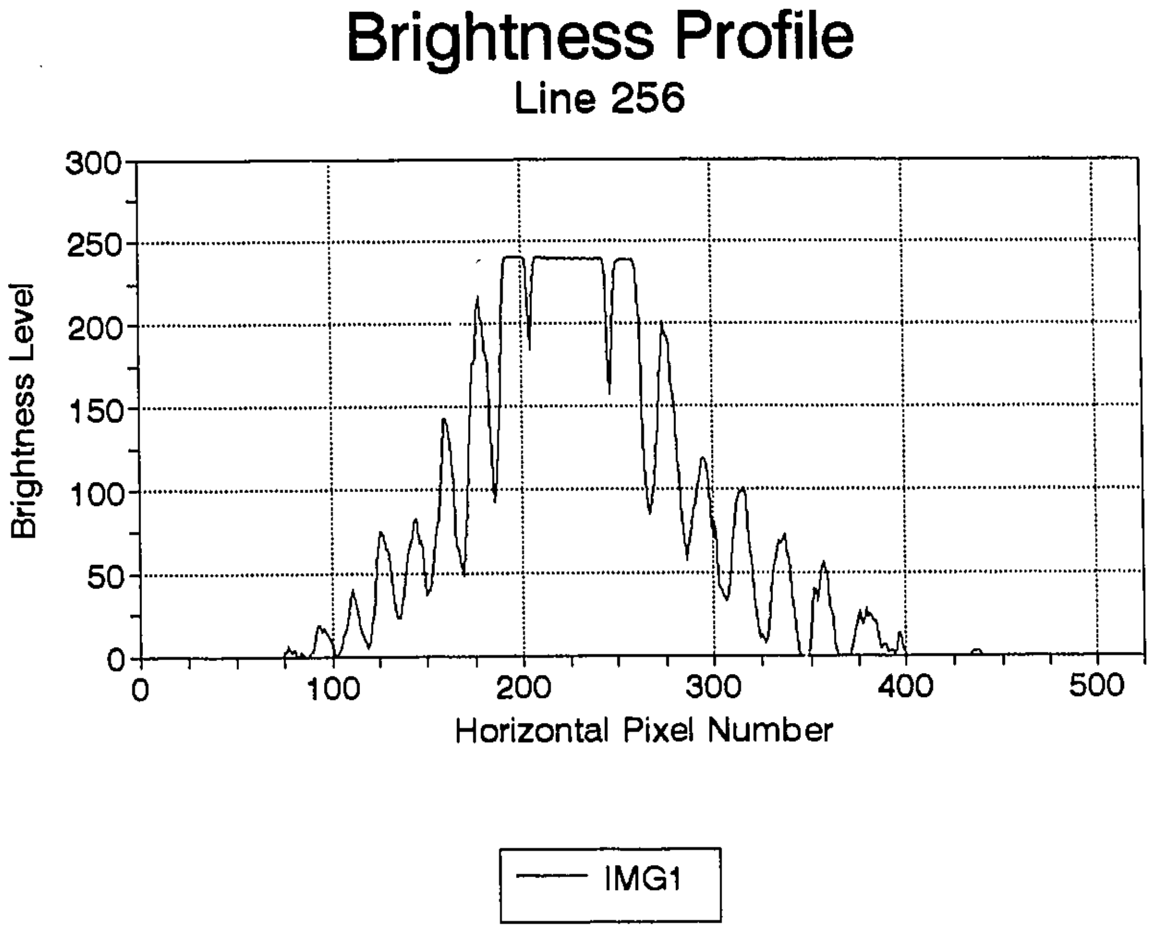


**Figure 5-16 :** Brightness Profile for Line 230 for IMG1.

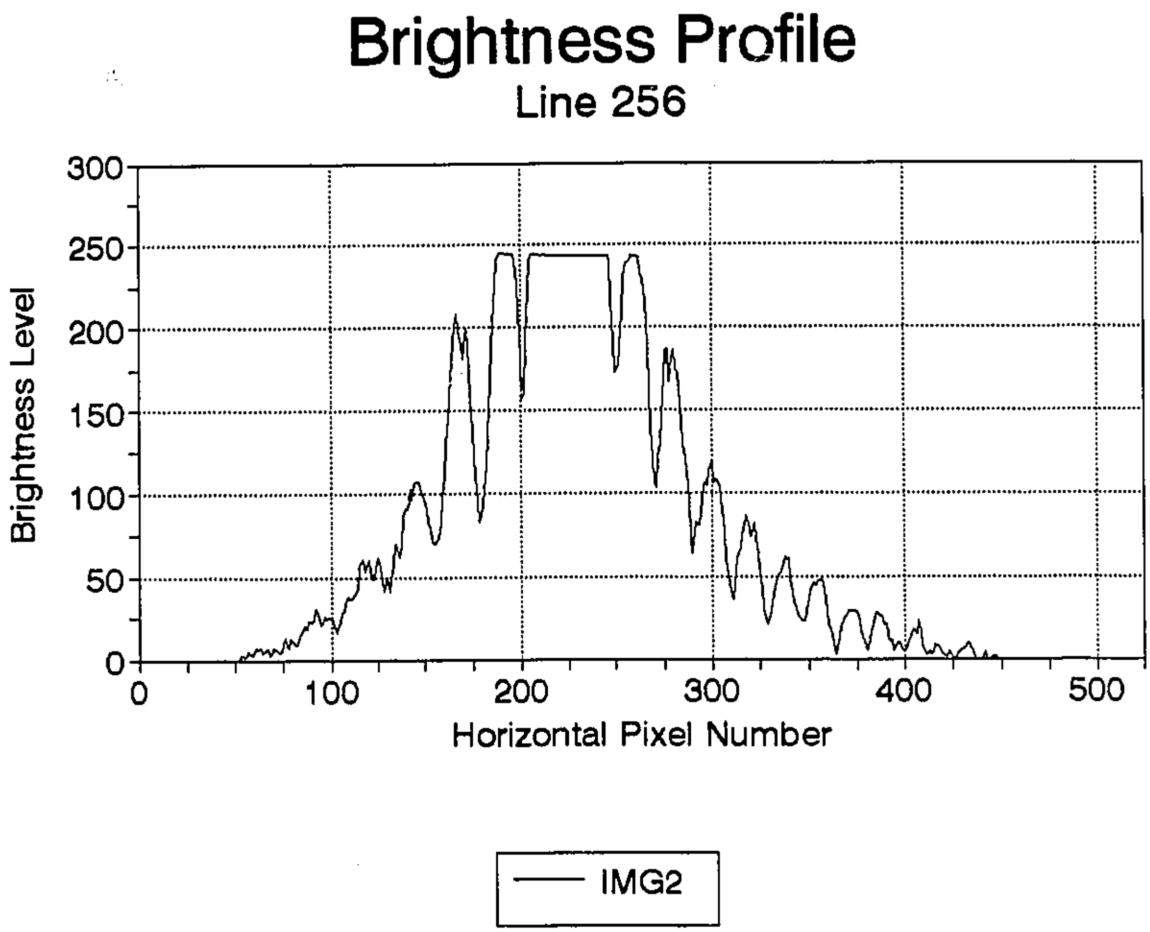


**Figure 5-17 :** Brightness Profile for Line 230 for IMG2.

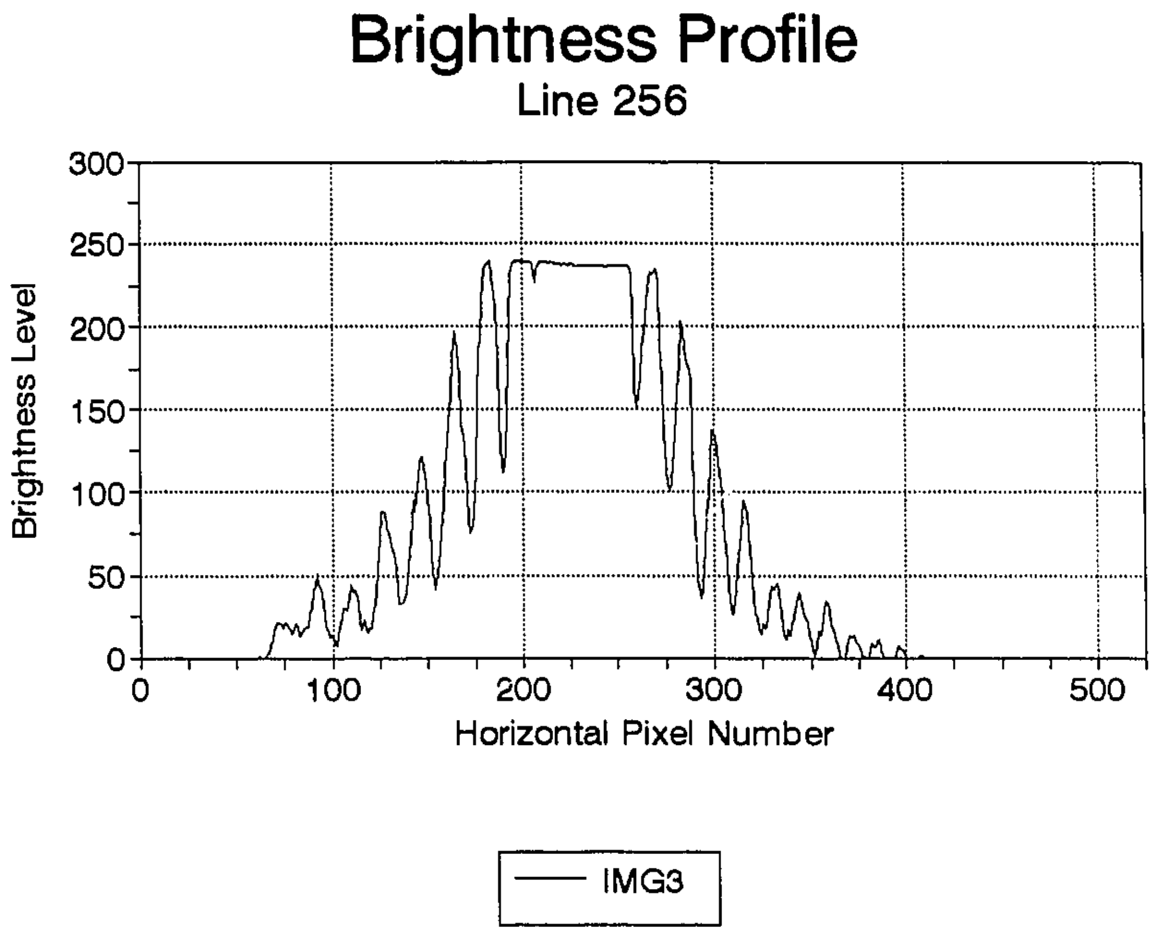


**Figure 5-18 :** Brightness Profile for Line 230 for IMG3.

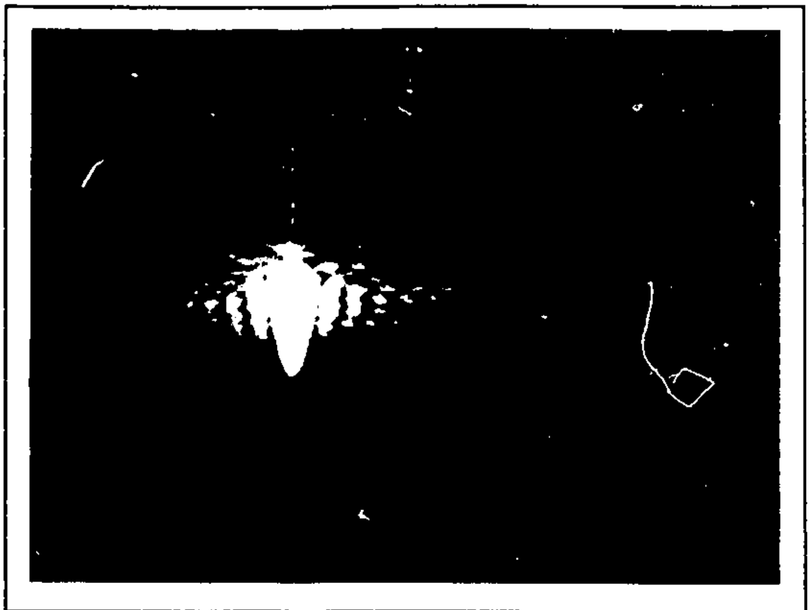

Figure 5-19 : Image file IMG1

Figure 5-20 : Image file IMG2

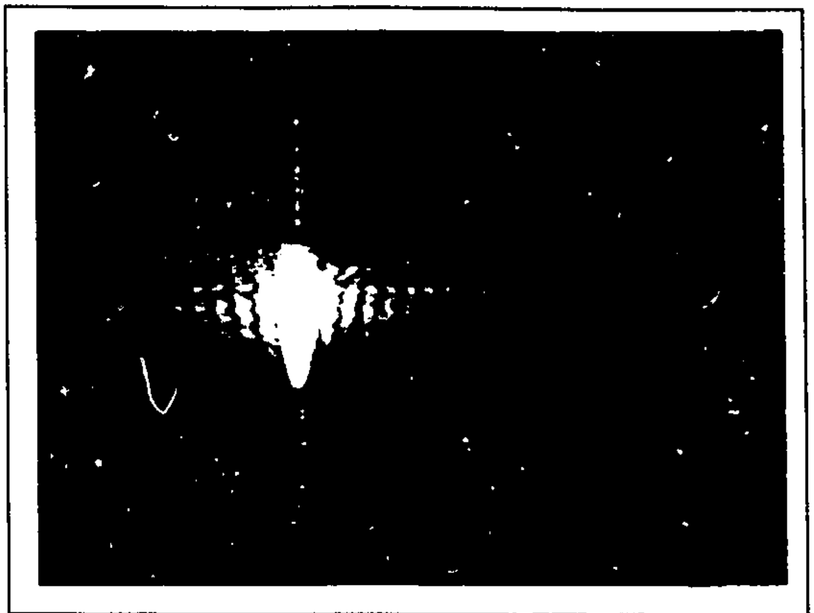

Figure 5-21 : Image file IMG3

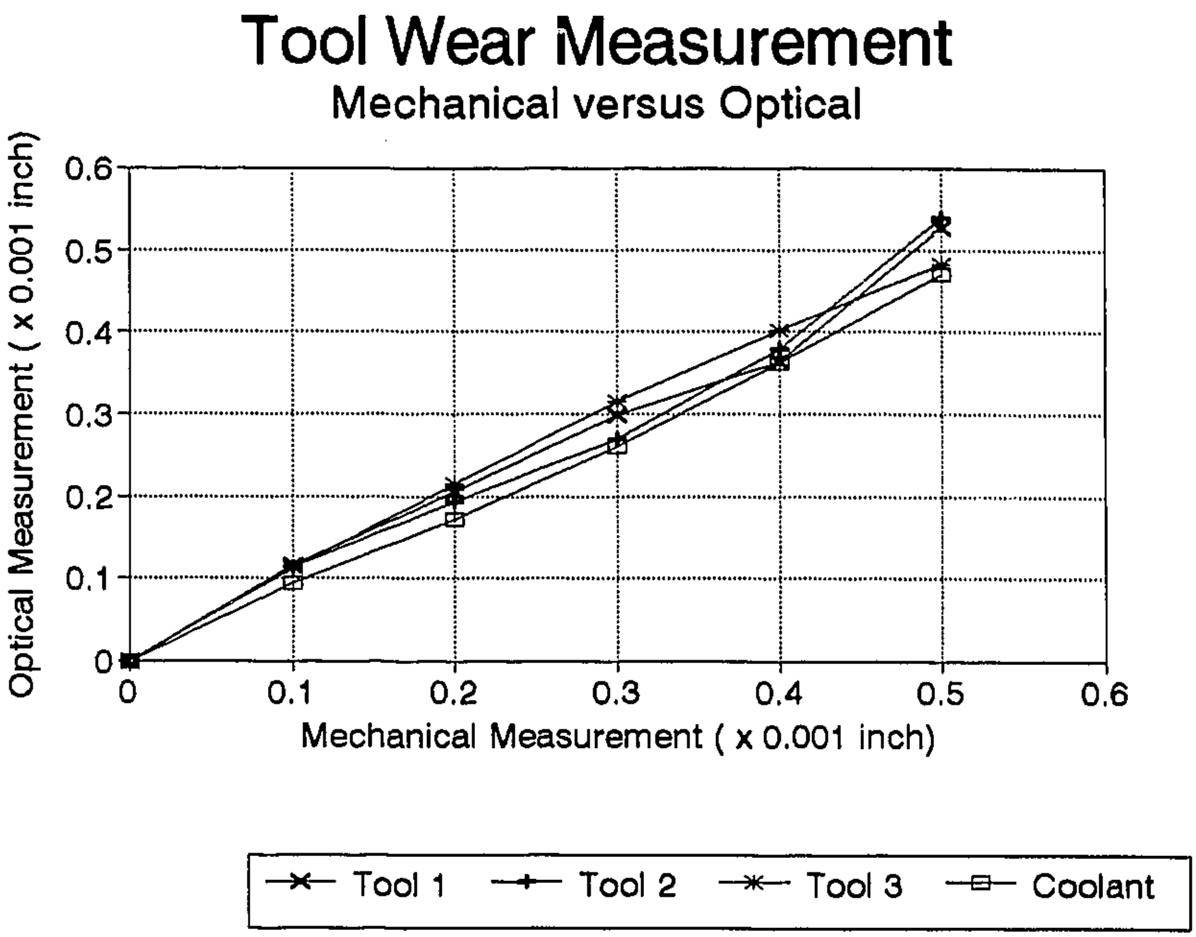


**Figure 5-22 :** Tool Wear Measurement (Mechanical versus Optical).

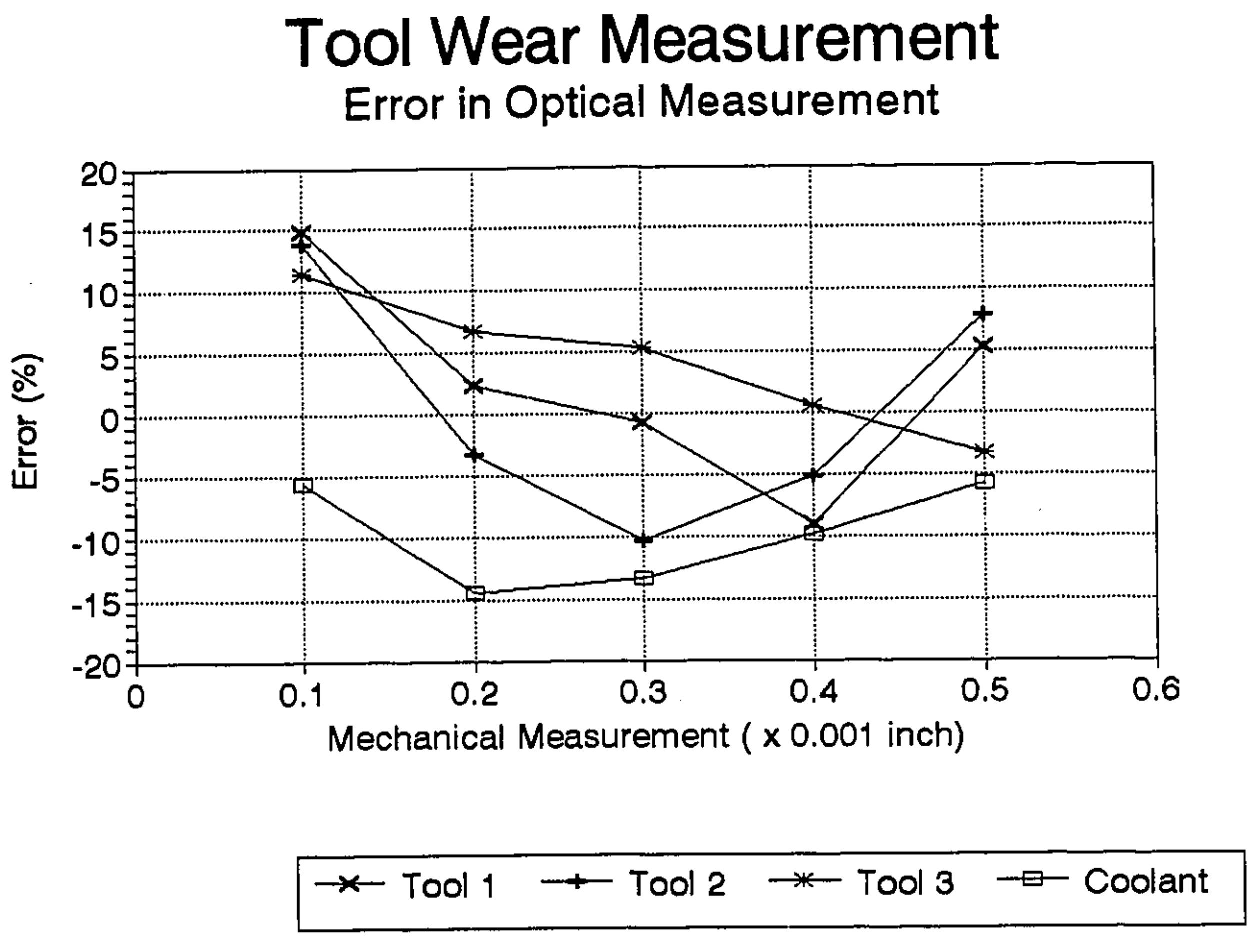


**Figure 5-23 :** Error in Tool Wear Measurement.

# CHAPTER 6

## VI. CONCLUSIONS AND DISCUSSIONS

### 6.1 Conclusions

Based on the study presented in the thesis the following conclusions can be drawn.

(i) A method of tool wear measurement has been developed for monitoring the tool condition of rotating cutters. It has been tested with end-mill cutters and encouraging results have been obtained. Other cutters can be used also with modifications.

(ii) A prototype tool condition monitoring system has been fabricated that include the hardware, software and procedures.

(iii) Different factors have been studied as how they affect the measurement by the system. These include the performance characteristics of the system as discussed below.

1. The system has a signal to noise ratio of 67 which is 1.5 % of the actual value due to the various components of the system and it cannot be eliminated by any means.

2. The accuracy of measurement is found to be 15 % of the actual value starting with a very small gap of 0.001 inch. The larger the gap, the more accurate will be the measurement, because the sensitivity goes down as the gap increases. However, if the gap is too large, there will be no diffraction pattern visible and the brightness will be too low. In addition,

the fringe spacing will be decreased and its measurement is limited by the number of pixels the CCD camera can scan. When the fringe spacing is small, a larger number of fringes are used in the calculations and hence it does not cause accuracy problems.

3. The test range of 0 to 0.001 inch tool wear has been found to be satisfactory.

4. The repeatability error is 6.2 % of the actual value. When a cylinder lens is used in front of the laser and the gap is changed, the repeatability error reduces to 3.2 % of the actual value.

5. Sensitivity can be defined as the ratio of the change in fringe spacing to that of the slit width. Referring to table C-5, this changes from 123 (observation 2 and 3) to 79.4 (observation 6 and 7). This change in sensitivity is around 55%. The error with small values of wear is higher due to the higher sensitivity. This range corresponds to 0 to 0.001 inch tool wear. Measurement beyond that will result in loss of sensitivity and hence it is justified to use this range.

6. Factors like vertical position, tilt angle and experimenter have little contribution to the accuracy. The error introduced is less than one percent of the actual value.

7. The resolution of the setup is 0.0001 inch as defined by the design of the setup. This follows from the movement of the micrometer screws used.

The errors in measurement can be attributed to various factors, some of which are beyond control. They are due to mechanical non-rigidity, noise, temperature variation, repeatability and deviation from the ideal conditions for diffraction. Some of these errors could be reduced by calibrating the setup and fabricating a more rigid setup. As a result, a more reliable measurement can be obtained. The horizontal slide is most sensitive to the diffraction pattern. If the aperture is less than 0.001 inch, the sensitivity is too high and gives rise to errors.

## 6.2 Discussion

In this project, the experimental setup has been fabricated to measure the tool wear and has been found to behave in the way it was designed. The complete commercial version of this system can be made inside a small enclosure. The laser source, the CCD camera and the reference edge plate can be hard-wired inside the enclosure and it can be connected to a PC. The tool wear can be calculated from the captured image.

In the present study, there is an element of error introduced by the experimenter. The cutter had to be unloaded and measured manually. This research shows that the methodology used to measure tool wear is reliable. A real time and on-line tool wear measurement system may be make by taking a snapshot of the diffraction pattern at the correct instant while the spindle shaft is rotating. This will require triggering of the camera by an encoder device mounted onto the shaft. But before this can be done a machine tool has to be built with such a spindle encoder that will make it possible to orient the shaft at any desired orientation.

The alternative way of measurement would be manual alignment of the spindle shaft to the particular orientation. The cutter is positioned so that one cutting edge of the cutter comes very near to the reference edge. The first time this is done, the reference edge is positioned and adjusted using the set screw arrangement. The reference edge must be around 0.001 inch away from the edge of the flute and it must be as parallel to it as possible. This will ensure a good diffraction pattern.

The current work uses the technique for measuring tool wear for end-mill cutters off-line. A method of measurement has been outlined and it can be used for other rotating cutters and principle is the same.

In all the experiments conducted only one particular flute of the 4 flutes was measured. The flutes were color coded and hence could be identified. This can be repeated with all 4 flutes also. This will give insight into factors like radial runout. In the present study, this was not necessary as the cutter is removed from the spindle for measurement.

Different factors have been studied based on experiment design and the performance of the tool condition monitoring system have been studied. This is a major contribution to an area which was not explored before.

### 6.3 Recommendations

The future work can be carried on in the following directions.

a) Future Implementation: It is found that laser diffraction could be used reliably for tool condition monitoring. The measurement is consistent with a maximum error of only 15% of the actual value. This means that a suitable tool replacement signal can be automatically generated by the controlling software and fed into the CNC controller for issuing a tool changer command. Thus automatic tool replacement will be possible for a machining center. The software developed for the sensor should be capable of issuing commands that the CNC machine will be able to take as input without any manual intervention.

A conceptual model of such an implementation will use a spindle encoder to stop the cuttter at a particular orientation for measurements. The CNC milling machine has to be equipped with an optical encoder on the spindle shaft. Due to the non-availability of such a device, manual alignment may be necessary to achieve this at present.

The machine tool in combination with the tool condition monitoring system can be coupled to an intelligent controller that carries a machinability database. This tool condition monitoring system can be integrated with a machine tool. This will be termed as an intelligent machine tool. The use of learning algorithms will help to recognize the same fringes from different angles and orientations. This may cut down on the image processing time.

Since this incorporates modular design, it can be coupled with Computer Aided Design (CAD), Computer Aided Manufacturing (CAM) and Computer Aided Process Planning (CAPP).

b) Study of other cutters: The presented method can be used for rotating cutters of different kinds including cutters that employ carbide inserts. Procedures have to be drawn up for each type of cutter and then they can be tested. Other sensors and sensing techniques can be developed for different type of cutters. The end-milling cutter is the most suitable cutter which can be monitored using this setup. Hence there is virtually unlimited scope for developing sensors for other types of cutters like hobs, broaches, tap drills and so on.

c) Machinability study: There is a wide scope of work remained that can be done. Machinability studies for different materials using different types of rotating cutters can be achieved. The correlation between the various machining parameters and tool life can be established using the system. Also, the correlation between surface finish can be studied.

## Appendix A : Specifications of the Setup

The Tool Condition Monitoring System can be classified into the following subsystems:

A. The Prototype sensor setup.

B. Computer.

C. Monitor.

D. Machine Tool.

A. The prototype sensor setup which is same as the experimental setup has the following parts.

a) The base plate: Measures about 12 inches by 18 inches.

b) The Laser: This is a He-Ne Laser System of make Optikon, model LM2P, Serial Number 427-362519. It has a power supply unit that runs off a 120 volt outlet. The He-Ne tube is encased in a metallic tube and has a narrow aperture on one side through which the light comes out. The wavelength is 670 nanometres.

c) The Slider for laser alignment: The laser holder fixes the tube to the base plate. This allows the laser tube to translate in orthogonal directions horizontally and vertically. The movement in either direction is about 1 inch. This allows the user to set up the position of the laser with respect to the base plate.

d) The V-block: This allows the end-mill cutter to stand upside down and rest its shank against the V-Block. The purpose of this is to provide means for a high degree of repeatability.

e) The orientation adjustment knob stops the flute of the tool so that when placed snugly in the V-block, it is oriented in the same angle every time the tool is to be tested.

f) Lens: There is a cylinder lens of 1.0 dioptre with the axis of the lens horizontal. This is fitted right in front of the laser aperture and helps to form a beam with the cross section of a line.

g) The compound slide mechanism has 2 micrometer screws one each for positioning the reference edge horizontally and vertically. The Tilt Knob adjusts the angle of tilt of the reference edge which is a Black and Decker Jack Knife blade. The horizontal travel and vertical travel of the compound slide is approximately 1 inch and can be controlled to a resolution of 0.0001 inch. The tilt of the blade can be varied 360 degrees and can be measured to 0.5 degrees with the graduations provided.

h) The camera is a CCD camera with a lens of 4.3 mm focal length. It gives composite video output and runs off a 9-Volt adaptor. The width of the CCD camera is 0.23 inch and it is mounted on an adjustable bracket. It can be positioned horizontally and vertically up to 2 inches in each direction.

i) The screen is an ordinary white sheet of paper where the diffraction pattern is formed. It is located 1.5 inches in front of the camera.

## B. Computer

The computer used here is an IBM PC with a PIP 1024 Video Digitizer Board manufactured by Matrox Electronic Systems Limited. This board has a memory of 1 MB. The image grabbing software accesses the frame grabber board memory and saves the image file onto the disk drive. After the image is saved, the fringe spacing measurement is done with the image processing software. It uses PIP EZ software library routine that are supplied with the board, which has serial number 238-A50-01/2..

C. Monitor

The monitor is a Black and White monochrome monitor (Panasonic Video Monitor, Model No. WV 5410, Serial Number 97I00409). It is used to get a live image of the diffraction pattern as obtained on the screen. This helps to verify on-line the picture to be saved. It also helps in focussing, aligning and positioning.

D. Machine Tool

The machine tool used was a Bridgeport Vertical Axis Milling Machine with a digital readout display. It has a traverse of about 30 inches on the X-axis which is required for the experimentation.

A Perspective View of the experimental setup is illustrated in Figure 4-4. In Figure 4-5 some of the important and critical dimensions of the setup are shown. Figures 4-6 to 4-8 are photographs of the experiments conducted.

**Appendix B : Software Listing for Image Capture and Processing**

**Program for capturing image:**

```
$include:'forintf.h'

        implicit integer (a-e)
        implicit real*4 (f)
        implicit integer*2 (g-z)
        real*4 cv,s2
        integer*2 x(20),y(20),prof(1024),prof1(1024)
        character*10 cmx
        character*3 cmax,res
        character*2 ca
        character*13 fname
        character dum,buf1(256),buffer(4096),workbuffer(512),dumy,ask
        ir=init(620)
        if (ir.ne.1) write (*,*)ir
        call chan(2)
        call video (0)
        call sync(0)
        call quadm(1)
        call dquad(0)
        bsize=4096
        cam=1
        call sync (cam)
        call cgrab(1)
        write(*,*)'   HIT <ENTER> TO GRAB PICTURE'
        read(*,'(a1)')ask
        call cgrab(0)
        fname='image.dat'
        iquad=0
        call dquad(iquad)
        iret=itodsk(bsize,iquad,fname,buffer)
        if(iret.eq.1)then
        write(*,*)'TRANSFER COMPLETED'
        else if(iret.eq.0) then
        write(*,*)'COULD NOT OPEN FILE'
        else if(iret.eq.-1) then
        write(*,*)'DISK ERROR'
        end if
        end
```

**Program for processing image:**

```
program brightness_prfofile;
uses dos,crt,graph,bgidriv,bgifont;

var AutoDetect                    : pointer;
   GraphMode,GraphDriver,Drv,
   maxx,maxy                      : integer;
   f                              : file;
   d                              : array [0..511] of byte;
   extl                           : array [0..511] of real;
   extr                           : array [0..511] of integer;
   extp                           : array [0..511] of word;
   fr                             : array [0..40] of real;
   res,h,i,j,k,l,p,q              : word;
   s,fn,gn                        : string;
   flag,done,fff                  : boolean;
   g                              : text;
   op,nf,n                        : byte;
   nop                            : longint;
   sum,avg,old,tmp                : real;

{$F+}
function DetectVGA256 : Integer;
var Vid : Integer;
begin DetectVGA256:=3; end;
{$F-}

procedure initialize;
var a,b    : integer;
begin
a:=RegisterBGIdriver(@CGADriverProc);
a:=RegisterBGIdriver(@EGAVGADriverProc);
a:=RegisterBGIdriver(@HercDriverProc);
a:=RegisterBGIdriver(@ATTDriverProc);
a:=RegisterBGIdriver(@PC3270DriverProc);
b:=RegisterBGIfont(@GothicFontProc);
b:=RegisterBGIfont(@SansSerifFontProc);
b:=RegisterBGIfont(@SmallFontProc);
b:=RegisterBGIfont(@TriplexFontProc);
a:=Detect;
initgraph(a,b,'');
end;
```

```
procedure note(freq,t1,t2:word);
begin
sound(freq);
delay(t1);
nosound;
delay(t2);
end;

procedure beep;
begin
note(512,500,100);
note(660,500,100);
note(572,500,100);
end;

procedure warn;
begin
note(512,200,200);
note(768,200,200);
end;

procedure hold;
var k:char;
begin
k:=readkey;
end;

procedure writeh(s:string);
begin
writeln(s);
writeln;
writeln('Press any key ...');
hold;
end;

procedure warnh(s:string);
begin
warn;
writeh(s);
end;
```

```
procedure prompt(x,y:byte;s:string);
begin
gotoxy(x,y);
write(s);
end;

procedure sline(x1,y1,x2,y2,c:word);
begin
setcolor(c);
line(x1,y1,x2,y2);
end;

procedure link(p1,p2,c:word);
begin
sline(round(extl[p1]+20),400-extr[p1],round(extl[p2]+20),400-extr[p2],c);
end;

procedure readline;
begin
h:=h+1;
blockread(f,d,512,res);
end;

procedure list;
begin
writeln('Pointer List ***');
i:=0;
repeat
  writeln(i:5,extr[i]:5,extl[i]:8:2,extp[i]:6);
  i:=extp[i];
  hold;
until i=0;
end;

function time:string;
var h,m,s,ss:word;
    th,tm:string;
begin
gettime(h,m,s,ss);
str(h:2,th);
str(m:2,tm);
if tm[1]=' ' then tm[1]:='0';
time:=th+':'+tm;
end;
```

```
function date:string;
var d,m,y,w,hh,mm,ss,s100:word;
    td,tm,ty,thh,tmm,tss:string;
begin
gettime(hh,mm,ss,s100);
getdate(y,m,d,w);
str(hh:2,thh);
str(mm:2,tmm);
str(ss:2,tss);
str(y:4,ty);
str(m:2,tm);
str(d:2,td);
if tm[1]=' ' then tm[1]:='0';
if td[1]=' ' then td[1]:='0';
if thh[1]=' ' then thh[1]:='0';
if tmm[1]=' ' then tmm[1]:='0';
if tss[1]=' ' then tss[1]:='0';
date:=ty+'-'+tm+'-'+td+' '+thh+':'+tmm+':'+tss;
end;

function lz3(x:word):string;
var s:string;
    i:byte;
begin
str(x:3,s);
for i:=1 to 3 do
  if s[i]=' ' then s[i]:='0';
lz3:=s;
end;


procedure showfile1;
begin
reset(f,1);
AutoDetect:=@DetectVGA256;
GraphDriver:=InstallUserDriver('SVGA256',AutoDetect);
GraphDriver:=Detect;
InitGraph(GraphDriver,GraphMode,'');
if graphresult=0 then
  begin
  for i:=0 to 63 do setrgbpalette(i,i,i,i);
  setrgbpalette(64,63,0,0);
  setrgbpalette(65,0,0,63);
  setrgbpalette(66,20,20,0);
```

```
setrgbpalette(67,30,30,35);
h:=0;
repeat
  readline;
  for i:=0 to 511 do putpixel(i,h,d[i] div 4);
until h>=480;
hold;
setcolor(67);
rectangle(0,0,511,479);
setcolor(66);
for i:=1 to 19 do line(0,25*i,511,25*i);
for i:=1 to 20 do line(25*i,0,25*i,479);
hold;
reset(f,1);
h:=0;
repeat
  readline;
  for i:=1 to 510 do
    begin
    if (d[i-1]>(d[i]+3)) and ((d[i]+3)<d[i+1]) then putpixel(i,h,64);
    if (d[i-1]<(d[i]-3)) and ((d[i]-3)>d[i+1]) then putpixel(i,h,65);
    end;
until h>=480;
hold;
for i:=0 to 63 do setrgbpalette(i,0,0,0);
beep;
hold;
closegraph;
writeh('That''s the picture!');
end
else writeh('Could not open graphic driver in SVGA mode');
end;


procedure showfile2;
var sk:char;
begin
initialize;
if graphresult=0 then
  begin
  setgraphmode(2); {herc 0}
  maxx:=getmaxx;
  maxy:=getmaxy;
  reset(f,1);
```

```
  setcolor(15);
  rectangle(0,0,maxx,maxy);
  setcolor(12);
  rectangle(19,401,532,144);
  h:=0;
  repeat
    readline;
    setcolor(11);
    rectangle(maxx-150,10,maxx-10,70);
    setfillstyle(1,1);
    floodfill(maxx-70,40,11);
    str(h:3,s);
    setcolor(14);
    settextstyle(1,0,4);
    settextjustify(1,1);
    outtextxy(maxx-70,40,s);
    setcolor(7);
    for i:=1 to 20 do line(20+25*i,400,20+25*i,145);
    for i:=1 to 10 do line(20,400-25*i,531,400-25*i);
    if res=512 then
      begin
      for i:=0 to 510 do sline(i+20,400-d[i],i+21,400-d[i+1],14);
      sk:=readkey;
      for i:=0 to 510 do sline(i+20,400-d[i],i+21,400-d[i+1],0);
      case ord(upcase(sk)) of
        ord('S') : for i:=1 to 19 do readline;
        ord('Q') : h:=480;
        end;
      end;
  until h>=480;
  closegraph;
  writeh('That''s the profile');
  end
else writeh('BGI graphics - cannot initialize!!');
end;


procedure grid;
begin
setcolor(7);
for i:=1 to 20 do line(20+25*i,400,20+25*i,145);
for i:=1 to 10 do line(20,400-25*i,531,400-25*i);
end;
```

```
procedure fringefile;
var ll:word;
begin
clrscr;
repeat
  writeln('Enter Line number of interest');
  readln(ll);
until ((ll>0) and (ll<=480));
initialize;
if graphresult=0 then
  begin
  reset(f,1);
  h:=0;
  repeat readline until h=ll;
  setgraphmode(2); { For herc use 0}
  maxx:=getmaxx;
  maxy:=getmaxy;
  setcolor(15);
  rectangle(0,0,maxx,maxy);
  setcolor(12);
  rectangle(19,401,532,144);
  setcolor(11);
  rectangle(maxx-150,10,maxx-10,70);
  setfillstyle(1,1);
  floodfill(maxx-70,40,11);
  str(h:3,s);
  setcolor(14);
  settextstyle(1,0,4);
  settextjustify(1,1);
  outtextxy(maxx-70,40,s);
  grid;
  for i:=0 to 511 do
    begin extp[i]:=i+1; extl[i]:=i; extr[i]:=d[i]; end;
  extp[511]:=0;
  i:=0;
  repeat
    j:=extp[i];
    link(i,j,1);
    i:=j;
  until i=0;
  beep;
  hold;
  nop:=0;
  i:=0;
```

```
repeat
  op:=0; nop:=nop+1;
  j:=extp[i];    k:=extp[j];    l:=extp[k];
  link(i,j,11);  link(j,k,12);  link(k,l,13);
  {hold;}
  link(i,j,1);   link(j,k,1);   link(k,l,1);
  if (abs(extr[j]-extr[i])<=2) and (abs(extr[j]-extr[i])>0)
     and (op=0) then op:=1;
  if (extr[i]<>extr[j]) and (extr[j]=extr[k]) and (op=0) then op:=2;
  if (extr[i]<extr[j]) and (extr[j]<extr[k]) and (op=0) then op:=3;
  if (extr[i]>extr[j]) and (extr[j]>extr[k]) and (op=0) then op:=3;
  if (extr[i]>extr[k]) and (extr[k]>extr[j]) and (extr[j]>extr[l]) and
     (op=0) and (extr[j]+20>extr[k]) then op:=4;
  if (extr[i]<extr[k]) and (extr[k]<extr[j]) and (extr[j]<extr[l]) and
     (op=0) and (extr[j]-20<extr[k]) then op:=4;
  if ((i>j) or (j>k) or (k>l)) then op:=0;
  if (600*op>nop) then op:=0;
  case op of
    0 : i:=extp[i];
    1 : begin
        link(i,j,0); link(j,k,0);
        extr[j]:=extr[i];
        link(i,j,1); link(j,k,1);
        i:=extp[i];
        end;
    2 : begin
        link(i,j,0); link(j,k,0); link(k,l,0);
        extp[j]:=l;
        extl[j]:=extl[j]+0.5;
        link(i,j,1); link(j,l,1);
        end;
    3 : begin
        link(i,j,0); link(j,k,0);
        extp[i]:=k;
        link(i,k,1);
        end;
    4 : begin
        link(i,j,0); link(j,k,0); link(k,l,0);
        extp[i]:=l;
        link(i,l,1);
        end;
    end;
until nop>3000;
beep;
```

```
hold;
n:=0;
nf:=0;
fr[0]:=0;
i:=0;
repeat
  i:=extp[i];
  j:=extp[i];
  k:=extp[j];
  link(i,j,14);
  link(j,k,14);
  if (extr[i]+30<extr[j]) and (extr[j]>extr[k]+30) and (i<j) and (j<k) then
    begin
    nf:=nf+1;
    fr[nf]:=extl[k]-extl[i];
    floodfill(maxx-70,40,11);
    str(fr[nf]:6:2,s);
    setcolor(14);
    outtextxy(maxx-70,40,s);
    hold;
    end;
   link(i,j,1);
   link(j,k,1);
 until i>j;
 closegraph;
 clrscr;
 gn:=fn+'-fr.'+lz3(ll);
 assign(g,gn);
 rewrite(g);
 writeln(g,fn);
 writeln(g,date);
 writeln(g,ll:4);
 if (nf>=4) then
   begin
   sum:=0.0;
   for i:=1 to nf do
     begin
     writeln(g,i:4,fr[i]:8:2);
     writeln(i:4,fr[i]:8:2);
     sum:=sum+fr[i];
     end;
   avg:=sum/nf;
   writeln(avg:12:3);
   hold;
```

```
 for p:=1 to nf-1 do
  for q:=p+1 to nf do
   if fr[p]>fr[q] then
    begin
    tmp:=fr[p];
    fr[p]:=fr[q];
    fr[q]:=tmp;
    end;
 avg:=(fr[(nf+1) div 2]+fr[(nf+2) div 2])/2;
 repeat
  old:=avg;
  sum:=0;
  n:=0;
  for i:=1 to nf do
   begin
   write(i:4,fr[i]:8:2);
   if (abs(ln(fr[i]/avg))<0.25) then
    begin
    write(' taken');
    sum:=sum+fr[i];
    n:=n+1;
    end;
   writeln;
   end;
  if (n>0) then
   begin
   avg:=sum/n;
   writeln(avg:8:3);
   hold;
   end;
 until old=avg;
 end;
writeln('Line Number  : ',ll:12);
write('Fringe Spacing : ');
if (n>=2) then
 begin
 writeln(avg:12:3);
 writeln(g,'Fringe Spacing = ',avg:12:3);
 end
else
 begin
 writeln('Not resolved');
 writeln(g,'Fringe Spacing = ',avg:12:3);
 end;
```

```
  beep;
  close(g);
  hold;
  end
else writeh('BGI graphics - cannot initialize!!');
end;


procedure fringegraph;
var ll:word;
begin
clrscr;
gn:=fn+'-fr.gph';
assign(g,gn);
rewrite(g);
writeln(g,fn);
writeln(g,date);
for ll:=1 to 480 do
  begin
  reset(f,1);
  h:=0;
  repeat readline until h=ll;
  for i:=0 to 511 do
    begin extp[i]:=i+1; extl[i]:=i; extr[i]:=d[i]; end;
  extp[511]:=0;
  nop:=0;
  i:=0;
  repeat
    op:=0; nop:=nop+1;
    j:=extp[i];   k:=extp[j];   l:=extp[k];
    if (abs(extr[j]-extr[i])<=2) and (abs(extr[j]-extr[i])>0)
       and (op=0) then op:=1;
    if (extr[i]<>extr[j]) and (extr[j]=extr[k]) and (op=0) then op:=2;
    if (extr[i]<extr[j]) and (extr[j]<extr[k]) and (op=0) then op:=3;
    if (extr[i]>extr[j]) and (extr[j]>extr[k]) and (op=0) then op:=3;
    if (extr[i]>extr[k]) and (extr[k]>extr[j]) and (extr[j]>extr[l]) and
       (op=0) and (extr[j]+20>extr[k]) then op:=4;
    if (extr[i]<extr[k]) and (extr[k]<extr[j]) and (extr[j]<extr[l]) and
       (op=0) and (extr[j]-20<extr[k]) then op:=4;
    if ((i>j) or (j>k) or (k>l)) then op:=0;
    if (600*op>nop) then op:=0;
    case op of
      0 : i:=extp[i];
      1 : begin extr[j]:=extr[i]; i:=extp[i]; end;
```

```
    2 : begin extp[j]:=l; extl[j]:=extl[j]+0.5; end;
    3 : extp[i]:=k;
    4 : extp[i]:=l;
    end;
until nop>3000;

n:=0;
nf:=0;
fr[0]:=0;
i:=0;
repeat
  i:=extp[i]; j:=extp[i]; k:=extp[j];
  if (extr[i]+30<extr[j]) and (extr[j]>extr[k]+30) and (i<j) and (j<k) then
    begin
    nf:=nf+1;
    fr[nf]:=extl[k]-extl[i];
    end;
until i>j;


if (nf>=4) then
  begin
  for p:=1 to nf-1 do
    for q:=p+1 to nf do
      if fr[p]>fr[q] then
        begin
        tmp:=fr[p];
        fr[p]:=fr[q];
        fr[q]:=tmp;
        end;
  avg:=(fr[(nf+1) div 2]+fr[(nf+2) div 2])/2;
  repeat
    old:=avg;
    sum:=0;
    n:=0;
    for i:=1 to nf do
      if (abs(ln(fr[i]/avg))<0.25) then
        begin sum:=sum+fr[i]; n:=n+1; end;
    if (n>0) then avg:=sum/n;
  until old=avg;
  end;
if (n>=2) then
  begin
  writeln(ll:6,avg:12:3,n:5);
```

```
    writeln(g,ll:4,avg:12:3,n:5);
    end;
  end;
close(g);
beep;
hold;
end;

procedure writefile;
var l:word;
begin
clrscr;
writeln('Enter Line number (1 to 480) to output');
readln(l);
reset(f,1);
gn:=fn+'-bp.'+lz3(l);
assign(g,gn);
rewrite(g);
writeln(g,fn);
writeln(g,date);
writeln(g,l:4);
h:=0;
repeat readline until h=l;
for i:=0 to 511 do writeln(g,i:4,d[i]:4);
close(g);
end;


procedure menu;
var choice,yesno:char;
begin
clrscr;
prompt(20,5,'***  MAIN MENU OF PROFILEX  ***');
prompt(10,11,'F : Enter File name');
prompt(10,12,'V : View the file as a picture');
prompt(10,13,'P : View the brightness profile');
prompt(10,14,'W : Write output file for profile');
prompt(10,15,'M : Fringe Measurements');
prompt(10,16,'G : Fringe Graph');
prompt(10,17,'Q : Quit from Profilex');
prompt(20,20,'Press option key');
note(256,200,200);
choice:=readkey;
clrscr;
```

```
case ord(upcase(choice)) of
  ord('V') :
    if fff then showfile1
    else warnh('No file loaded!');
  ord('P') :
    if fff then showfile2
    else warnh('No file loaded!');
  ord('W') :
    if fff then writefile
    else warnh('No file loaded!');
  ord('M') :
    if fff then fringefile
    else warnh('No file loaded!');
  ord('G') :
    if fff then fringegraph
    else warnh('No file loaded!');
  ord('Q') :
    begin
    writeln('Are you sure (Y/N) ?');
    yesno:=readkey;
    done:=(upcase(yesno)='Y');
    end;
  ord('F') :
    begin
    writeln('Enter file name');
    readln(fn);
    assign(f,fn);
    {$i-}
    reset(f,1);
    {$i+}
    fff:=(ioresult=0);
    if fff then
      begin
      if (filesize(f)<>262144) then
        begin
        warnh('Incorrect file size');
        fff:=false;
        end
      else writeh('O.K. File found');
      end
    else warnh('Sorry! File not found');
    end;
  end;
end;
```

```
begin
checkbreak:=false;
done:=false;
fff:=false;
repeat menu until done;
writeh('Thank you for using profilex');
end.
```

## Appendix C : Data Collected and Performance

The experiments were carried out using an end-mill cutter of the following specifications:

| | |
|---|---|
| Cutter Type | : CT20-F (32WP) |
| Cutter diameter | : 1 inch |
| Shank diameter | : 3/4 inch |
| Material | : HSS-NAS |

The work piece used was hardened Tool Steel.

Cutting Conditions: 210 RPM

Feed Rate: 0.6 inch/minute

Depth of Cut: 0.15 inch

Coolant: Pneumatic mister

Mode: Alternate conventional-milling and climb-milling.

| Cutter | VB(mm) | Tool Edge Wear (mm) |
|---|---|---|
| A | 0.0 | 0.000 |
| B | 0.2 | 0.015 |
| C | 0.31 | 0.023 |
| D | 0.4 | 0.034 |
| E | 0.5 | 0.046 |
| F | Broken | ------ |

**Table C-1** : Experimental Results for the Rotating Tool Sensor

| Characteristics: | Micrometer Readings | | Tilt Angle | |
|---|---|---|---|---|
| No Lens | Horizontal | 0.4683 | 28.0 | Degrees |
| No Tool Replacement | Vertical | 0.5627 | | |

| Horizontal Line Number | Fringe Spacing in Number of Pixels | | | | | | |
|---|---|---|---|---|---|---|---|
| | Set 1 | Set 2 | Set 3 | Set 4 | Set 5 | Average | SD |
| 224 | 19.600 | 20.833 | 20.167 | 19.625 | 19.625 | 19.970 | 0.481 |
| 225 | 20.000 | 20.000 | 20.625 | 20.125 | 19.800 | 20.110 | 0.278 |
| 226 | 20.167 | 20.300 | 21.700 | 21.200 | 21.125 | 20.898 | 0.579 |
| 227 | 20.417 | 20.333 | 20.333 | 20.417 | 20.786 | 20.457 | 0.169 |
| 228 | 20.187 | 20.125 | 20.313 | 20.500 | 20.250 | 20.275 | 0.129 |
| 229 | 20.278 | 20.050 | 19.950 | 19.833 | 19.778 | 19.978 | 0.177 |
| 230 | 20.000 | 19.850 | 19.850 | 20.278 | 19.850 | 19.966 | 0.167 |
| 231 | 19.625 | 19.667 | 19.773 | 20.050 | 20.227 | 19.868 | 0.233 |
| 232 | 20.611 | 19.308 | 19.636 | 19.542 | 19.583 | 19.736 | 0.452 |
| 233 | 19.321 | 19.357 | 19.192 | 19.214 | 19.538 | 19.324 | 0.124 |
| 234 | 19.071 | 19.308 | 19.385 | 19.385 | 19.346 | 19.299 | 0.118 |
| 235 | 18.846 | 18.346 | 18.727 | 18.292 | 18.417 | 18.526 | 0.220 |
| 236 | 18.583 | 17.545 | 18.273 | 18.375 | 17.958 | 18.147 | 0.362 |
| 237 | 18.071 | 17.714 | 19.167 | 19.286 | 19.000 | 18.648 | 0.633 |

| | | |
|---|---|---|
| Mean of Averages | 19.66 | |
| Standard Deviation | 0.29 | |
| Percentage Error | 1.50 | % due to Noise |

SD = Standard Deviation

Table C-2 : Effect of Noise on Fringe Spacing Variation.

# Experimental Design

| Summary of Experiments | | | | | | | | |
|---|---|---|---|---|---|---|---|---|
| | Series | | | | | | | |
| Effects Studied | 1 | 2 | 3 | 4 | 5 | 6 | 7 | 8 |
| Horizontal Position | Y | N | N | N | N | N | N | N |
| Repeatibility | N | Y | Y | N | N | N | Y | Y |
| Adding Cylinder Lens | N | N | Y | N | N | N | Y | Y |
| Vertical Position | N | N | N | Y | N | N | N | N |
| Tilt of Blade | N | N | N | N | Y | N | N | N |
| Experimenter | N | N | N | N | N | Y | N | N |
| Tool Wear | N | N | N | N | N | N | Y | Y |
| Coolant | N | N | N | N | N | N | N | Y |
| Number of Experiments | 13 | 5 | 5 | 5 | 5 | 5 | 18 | 6 |

Y = Yes
N = No

Table C-3 : Summary of Experiments performed.

| Characteristics of Series 1 | | | | | |
|---|---|---|---|---|---|
| No Lens. | Factors | Micrometer Reading | | Tilt Angle | |
| No Replacement. | Horizontal Movement | Vertical | 0.5627 | 28 | Degrees |

| Series B | Set 1 | Set 2 | Set 3 | Set 4 | Set 5 | Set 6 | Set 7 | Set 8 | Set 9 | Set 10 | Set 11 | Set 12 | Set 13 |
|---|---|---|---|---|---|---|---|---|---|---|---|---|---|
| Micrometer Horz. (in) | 0.4668 | 0.4670 | 0.4672 | 0.4674 | 0.4676 | 0.4678 | 0.4680 | 0.4685 | 0.4690 | 0.4695 | 0.4700 | 0.4710 | 0.4720 |
| Horz. Line No. | | | | | | | | | | | | | |
| 223 | | | | | | | | | | | 13.900 | | |
| 224 | | | | | | 29.000 | | 21.833 | 18.125 | 15.625 | 13.571 | 11.167 | |
| 225 | | | | 48.333 | 31.000 | 28.875 | 25.375 | 21.600 | 17.667 | 16.000 | 13.500 | 11.100 | |
| 226 | | | 34.500 | 33.833 | 33.250 | 28.000 | 26.600 | 22.300 | 17.929 | 15.750 | 13.429 | 11.187 | 9.167 |
| 227 | | | 38.250 | 40.250 | 32.375 | 29.700 | 25.417 | 22.100 | 17.375 | 16.111 | 13.500 | 11.050 | 8.938 |
| 228 | | | 43.125 | 35.333 | 31.583 | 30.125 | 25.000 | 21.071 | 17.400 | 15.600 | 13.250 | 10.846 | 8.955 |
| 229 | | 46.500 | 42.000 | 38.000 | 31.000 | 28.500 | 24.714 | 21.437 | 17.045 | 15.636 | 13.308 | 10.962 | 9.038 |
| 230 | | 45.833 | 40.500 | 37.500 | 32.643 | 28.000 | 24.562 | 21.150 | 17.136 | 15.333 | 13.200 | 10.867 | 8.857 |
| 231 | 44.500 | 49.375 | 40.200 | 38.333 | 31.500 | 28.250 | 24.562 | 20.900 | 17.033 | 15.179 | 13.033 | 10.667 | 8.875 |
| 232 | 45.333 | 45.200 | 38.500 | 35.417 | 31.500 | 28.250 | 24.143 | 21.542 | 16.714 | 15.063 | 13.000 | 10.250 | 8.875 |
| 233 | 44.000 | 47.667 | 38.333 | 33.583 | 31.889 | 28.900 | 23.800 | 20.464 | 16.588 | 15.031 | 12.800 | 10.500 | 8.917 |
| 234 | 51.250 | 44.833 | 36.917 | 32.143 | 30.500 | 28.100 | 23.417 | 20.167 | 16.833 | 14.800 | 12.765 | 10.667 | 9.000 |
| 235 | 43.833 | 42.700 | 34.688 | 29.100 | 32.071 | 26.333 | 22.731 | 19.000 | 16.269 | 14.529 | 12.529 | 10.929 | |
| 236 | 44.000 | 41.583 | 30.071 | 29.100 | 28.357 | | 22.667 | 19.500 | 16.250 | 14.571 | 12.467 | 10.333 | |
| 237 | 41.250 | 38.167 | 37.625 | 30.417 | | | 21.071 | 19.643 | 17.400 | 15.250 | 13.625 | | |
| 238 | | | | | | | | 22.667 | 17.333 | | | | |
| Average | 44.881 | 44.651 | 37.892 | 35.488 | 31.472 | 28.503 | 24.158 | 21.025 | 17.140 | 15.320 | 13.192 | 10.810 | 8.958 |

Table C-4 : Characteristics of Series 1

| Data used for Calibration | | | | |
|---|---|---|---|---|
| Width of CCD (mm) | 5.84 | 1 pxl = | 0.4491 | mil |
| No. of pixels | 512 | = | 3.6552 | mil on screen |
| Focal Length (mm) | 4.3 | | | |
| Screen Dist (mm) | 35 | | | |
| Wavelength (nm) | 670 | lambda = | 0.0264 | mil |
| Dist R (mm) | 203 | R = | 7992.11 | mil |
| | | Lambda R | 210.82 | square mil |

1 mil = 0.001 inch

| Calibration Chart for Laser Sensor Setup | | | | | | | | |
|---|---|---|---|---|---|---|---|---|
| Sl No. | Micrometer Reading Horzizontal | | Average Fringe Spacing | | Slit Width Optical | Comparison with Mechanical 465.7 | Difference | Error |
| | inch | x 0.001 in | Pixel | x 0.001 in | x 0.001 in | x 0.001 in | x 0.001 in | % |
| 1 | 0.4668 | 466.8 | 44.881 | 164.05 | 1.285 | 1.1 | 0.185 | 16.83 |
| 2 | 0.4670 | 467.0 | 44.651 | 163.21 | 1.292 | 1.3 | -0.008 | -0.64 |
| 3 | 0.4672 | 467.2 | 37.892 | 138.50 | 1.522 | 1.5 | 0.022 | 1.47 |
| 4 | 0.4674 | 467.4 | 35.488 | 129.71 | 1.625 | 1.7 | -0.075 | -4.40 |
| 5 | 0.4676 | 467.6 | 31.472 | 115.04 | 1.833 | 1.9 | -0.067 | -3.55 |
| 6 | 0.4678 | 467.8 | 28.503 | 104.18 | 2.024 | 2.1 | -0.076 | -3.64 |
| 7 | 0.4680 | 468.0 | 24.158 | 88.30 | 2.387 | 2.3 | 0.087 | 3.80 |
| 8 | 0.4685 | 468.5 | 21.025 | 76.85 | 2.743 | 2.8 | -0.057 | -2.03 |
| 9 | 0.4690 | 469.0 | 17.140 | 62.65 | 3.365 | 3.3 | 0.065 | 1.97 |
| 10 | 0.4695 | 469.5 | 15.320 | 56.00 | 3.765 | 3.8 | -0.035 | -0.93 |
| 11 | 0.4700 | 470.0 | 13.192 | 48.22 | 4.372 | 4.3 | 0.072 | 1.68 |
| 12 | 0.4710 | 471.0 | 10.810 | 39.51 | 5.336 | 5.3 | 0.036 | 0.67 |
| 13 | 0.4720 | 472.0 | 8.958 | 32.74 | 6.438 | 6.3 | 0.138 | 2.20 |

Table C-5 : Calibration Chart for Laser Sensor Setup

| Fringe Spacings - Series 1 | | | | | |
|---|---|---|---|---|---|
| Horizontal | Pixels | | | | |
| Line No. | Set 1 | Set 4 | Set 7 | Set 10 | Set 13 |
| 226 | | 33.833 | 26.600 | 15.750 | 9.167 |
| 227 | | 40.250 | 25.417 | 16.111 | 8.938 |
| 228 | | 35.333 | 25.000 | 15.600 | 8.955 |
| 229 | | 38.000 | 24.714 | 15.636 | 9.038 |
| 230 | | 37.500 | 24.562 | 15.333 | 8.857 |
| 231 | 44.500 | 38.333 | 24.562 | 15.179 | 8.875 |
| 232 | 45.333 | 35.417 | 24.143 | 15.063 | 8.875 |
| 233 | 44.000 | 33.583 | 23.800 | 15.031 | 8.917 |
| 234 | 51.250 | 32.143 | 23.417 | 14.800 | 9.000 |

Table C-5 (contd) : Calibration Chart for Laser Sensor Setup

| Characteristics of Series 2 | | Micrometer Readings | | Angle in |
|---|---|---|---|---|
| No Lens. | Factors | Horz. | 0.4668 | Degrees |
| Tool Replacement. | Repeatability | Vert. | 0.5627 | 28 |

| | Fringe Width in Number of Pixels | | | | | | |
|---|---|---|---|---|---|---|---|
| Horz. Line No. | Set 1 | Set 2 | Set 3 | Set 4 | Set 5 | Average | SD |
| 226 | | 55.000 | 42.750 | 43.750 | 43.250 | | |
| 227 | | 60.167 | 57.500 | | | | |
| 228 | | 45.625 | 60.000 | | 58.250 | | |
| 229 | 43.667 | 45.375 | 45.500 | 45.125 | 43.000 | 44.533 | 1.009 |
| 230 | 43.833 | 45.375 | 45.000 | 47.333 | 45.000 | 45.308 | 1.138 |
| 231 | 44.000 | 39.125 | 44.750 | 41.167 | 44.800 | 42.768 | 2.254 |
| 232 | 45.900 | 44.250 | 41.250 | 42.125 | 39.500 | 42.605 | 2.248 |
| 233 | 43.167 | 39.250 | 42.300 | 37.333 | 37.750 | 39.960 | 2.369 |
| 234 | | 38.500 | 41.250 | 39.400 | 41.750 | | |
| 235 | | 46.667 | 37.333 | 38.375 | 42.250 | | |

| | |
|---|---|
| Mean of Averages | 43.04 |
| Standard Deviation | 2.65 |
| Percentage Error | 6.16 % |

Table C-6 : Effect of Tool Replacement Repeatibility

| Characteristics of Series 3 | | Micrometer Readings | | Angle in |
|---|---|---|---|---|
| With Cylinder Lens | Factors Lens | Horz. | 0.4685 | Degrees |
| Tool Replacement Repeatibility | Repeatability | Vert. | 0.5610 | 28.0 |

| Horizontal Line Number | Fringe Width in Number of Pixels | | | | |
|---|---|---|---|---|---|
| | Set 1 | Set 2 | Set 3 | Set 4 | Set 5 |
| 224 | 21.56 | 19.92 | 20.10 | 20.40 | 21.35 |
| 225 | 20.83 | 19.67 | 19.89 | 20.05 | 20.34 |
| 226 | 20.67 | 19.64 | 19.54 | 19.94 | 20.43 |
| 227 | 20.33 | 20.02 | 19.20 | 19.83 | 19.86 |
| 228 | 19.52 | 20.33 | 20.17 | 19.66 | 19.54 |
| 229 | 19.98 | 20.17 | 20.63 | 20.17 | 19.60 |
| 230 | 20.12 | 20.30 | 20.98 | 20.53 | 20.01 |
| 231 | 20.45 | 20.43 | 20.56 | 20.41 | 20.20 |
| 232 | 20.53 | 20.17 | 20.62 | 20.48 | 20.23 |
| 233 | 20.22 | 20.04 | 20.03 | 19.53 | 19.77 |
| 234 | 20.10 | 19.84 | 19.85 | 20.27 | 19.88 |
| 235 | 19.30 | 19.67 | 19.74 | 20.04 | 20.23 |
| 236 | 20.59 | 19.09 | 20.35 | 19.53 | 19.69 |
| 237 | 19.52 | 19.32 | 19.43 | 19.32 | 18.98 |
| 238 | 19.07 | 19.41 | 19.32 | 19.23 | 19.28 |
| 239 | 18.85 | 18.78 | 19.42 | 20.10 | 18.98 |
| 240 | 18.57 | 18.53 | 19.32 | 19.37 | 18.74 |
| 241 | 18.43 | 18.23 | 19.17 | 18.77 | 19.07 |
| Average | 19.92 | 19.64 | 19.91 | 19.87 | 19.79 |

| | | |
|---|---|---|
| Mean of Averages | 19.83 | |
| Standard Deviation | 0.64 | |
| Percentage Error | 3.22 | % |

Table C-7 : Effect of Adding a Cylinder Lens

| Characteristics of Series 4 | | |
|---|---|---|
| Effect of Vertical Movement | | |
| Micrometer Readings | | Angle in |
| Horizontal | 0.4675 | Degrees |
| Vertical | 0.5627 | 28.0 |
| Serial Number | Fringe Spacing | Slit Width |
| | Pixel | x 0.001 in |
| 1 | 34.881 | 1.654 |
| 2 | 34.651 | 1.664 |
| 3 | 35.253 | 1.636 |
| 4 | 34.937 | 1.651 |
| 5 | 34.840 | 1.655 |
| Average | | 1.65 |
| Standard Deviation | | 0.01 |
| Error (%) | | 0.56 |

Table C-8 : Effect of Vertical Position

| Characteristics of Series 5 | | |
|---|---|---|
| Effect of Tilt Angle | | |
| Micrometer Readings | | Angle in |
| Horizontal | 0.4675 | Degrees |
| Vertical | 0.5627 | 28.0 |
| Serial Number | Fringe Spacing | Slit Width |
| | Pixel | x 0.001 in |
| 1 | 36.874 | 1.564 |
| 2 | 36.387 | 1.585 |
| 3 | 36.305 | 1.589 |
| 4 | 36.498 | 1.580 |
| 5 | 37.195 | 1.551 |
| Average | | 1.57 |
| Standard Deviation | | 0.01 |
| Error (%) | | 0.91 |

Table C-9 : Effect of Tilt Angle

| Characteristics of Series 6 | | |
|---|---|---|
| Effect of Experimenter | | |
| Micrometer Readings | | Angle in |
| Horizontal | 0.4675 | Degrees |
| Vertical | 0.5627 | 28.0 |
| Serial Number | Fringe Spacing | Slit Width |
| | Pixel | x 0.001 in |
| 1 | 36.348 | 1.587 |
| 2 | 35.987 | 1.603 |
| 3 | 35.993 | 1.602 |
| 4 | 36.289 | 1.589 |
| 5 | 35.393 | 1.630 |
| Average | | 1.60 |
| Standard Deviation | | 0.02 |
| Error (%) | | 0.95 |

1 thou = 0.001 inch

Table C-10 : Effect of Experimenter on Measurement

Note : Tables C-8, C-9 and C-10 show effects of various factors.

| Characteristics of Series 7 | | | | | |
|---|---|---|---|---|---|
| With Cylinder Lens | Factors | | Micrometer Readings | | Angle |
| Repeatibility | Wear | Lens | Horz. | 0.4675 | 28 |
| Tool Wear | Position | | Vert. | 0.5610 | Degrees |

| Horz. Line No. | Set 1 | Set 2 | Set 3 |
|---|---|---|---|
| 224 | | | 17.30 |
| 225 | | | 18.10 |
| 226 | | | 15.90 |
| 227 | | | 16.30 |
| 228 | | | 18.06 |
| 229 | | 23.67 | 18.42 |
| 230 | | 24.14 | 16.56 |
| 231 | | 23.00 | 16.78 |
| 232 | | 18.50 | 16.55 |
| 233 | | 21.19 | 16.77 |
| 234 | 23.05 | 20.28 | 16.25 |
| 235 | 23.71 | 20.00 | 16.75 |
| 236 | 21.89 | 20.13 | 16.56 |
| 237 | 22.61 | 20.00 | 15.35 |
| 238 | 22.17 | 20.44 | 15.50 |
| 239 | 22.28 | 19.83 | 15.58 |
| 240 | 22.50 | 21.63 | 15.68 |
| 241 | 21.56 | 20.50 | 15.39 |
| 242 | 21.39 | 20.50 | 15.57 |
| 243 | 21.93 | 20.25 | 16.41 |
| 244 | 21.38 | 20.20 | 17.09 |
| 245 | 21.67 | 21.44 | 17.00 |
| 246 | 21.00 | 21.33 | 16.58 |
| 247 | 20.17 | 21.33 | 16.15 |
| 248 | 20.32 | 21.90 | 15.54 |
| 249 | 19.55 | 22.50 | 16.23 |

| Horz. Line No. | Set 1 | Set 2 | Set 3 |
|---|---|---|---|
| 250 | 19.78 | 21.20 | 16.46 |
| 251 | 19.41 | 21.40 | 16.96 |
| 252 | 19.65 | 21.58 | 17.22 |
| 253 | 18.88 | 21.55 | 16.96 |
| 254 | 19.70 | 23.25 | 16.35 |
| 255 | 18.91 | 19.90 | 17.05 |
| 256 | 18.91 | 20.88 | 17.11 |
| 257 | 18.71 | 20.33 | 17.05 |
| 258 | 19.73 | 22.07 | 16.79 |
| 259 | 19.45 | 22.00 | 16.86 |
| 260 | 19.00 | 22.67 | 17.11 |
| 261 | 19.95 | 21.88 | 17.00 |
| 262 | 19.17 | 20.60 | 16.20 |
| 263 | 19.17 | 20.50 | 16.75 |
| 264 | 20.50 | | 17.80 |
| 265 | 19.00 | | 13.75 |
| 266 | 20.75 | | 16.90 |
| 267 | 19.20 | | 16.83 |
| 268 | 17.83 | | 17.50 |
| 269 | | | |
| 270 | | | |
| 271 | | | 16.33 |
| 272 | | | 16.00 |
| 273 | | | 17.33 |
| 274 | | | 16.17 |
| | | | |

Table C-11 : Effect on Fringe Spacing due to Tool Wear.

| Characteristics of Series 7 (continued) | | | | |
|---|---|---|---|---|
| Factors: | | Micrometer Readings | | Angle in |
| Repeatibility | Wear | Horizontal | 0.4668 | Degrees |
| Cylinder Lens | | Vertical | 0.5627 | 28.0 |

| Tool 1 | Tool Tip | Fringe | Slit Width | Tool Wear | | Difference | Error |
|---|---|---|---|---|---|---|---|
| Observation | Diameter | Spacing | | By Calliper | By Sensor | | |
| Number | inch | pixel | x 0.001 in | x 0.001 in | x 0.001 in | x 0.001 in | (%) |
| 1 | 1.0000 | 45.673 | 1.263 | 0.00 | 0.000 | 0.000 | ---- |
| 2 | 0.9998 | 41.867 | 1.378 | 0.10 | 0.115 | 0.015 | 14.80 |
| 3 | 0.9996 | 39.302 | 1.468 | 0.20 | 0.205 | 0.005 | 2.35 |
| 4 | 0.9994 | 36.954 | 1.561 | 0.30 | 0.298 | -0.002 | -0.68 |
| 5 | 0.9992 | 35.452 | 1.627 | 0.40 | 0.364 | -0.036 | -8.98 |
| 6 | 0.9990 | 32.238 | 1.789 | 0.50 | 0.526 | 0.026 | 5.25 |

| Tool 2 | Tool Tip | Fringe | Slit Width | Tool Wear | | Difference | Error |
|---|---|---|---|---|---|---|---|
| Observation | Diameter | Spacing | | By Calliper | By Sensor | | |
| Number | inch | pixel | x 0.001 in | x 0.001 in | x 0.001 in | x 0.001 in | (%) |
| 1 | 1.0000 | 46.021 | 1.253 | 0.00 | 0.000 | 0.000 | ---- |
| 2 | 0.9998 | 42.187 | 1.367 | 0.10 | 0.114 | 0.014 | 13.90 |
| 3 | 0.9996 | 39.868 | 1.447 | 0.20 | 0.193 | -0.007 | -3.29 |
| 4 | 0.9994 | 37.891 | 1.522 | 0.30 | 0.269 | -0.031 | -10.37 |
| 5 | 0.9992 | 35.323 | 1.633 | 0.40 | 0.380 | -0.020 | -5.11 |
| 6 | 0.9990 | 32.174 | 1.793 | 0.50 | 0.539 | 0.039 | 7.87 |

| Tool 3 | Tool Tip | Fringe | Slit Width | Tool Wear | | Difference | Error |
|---|---|---|---|---|---|---|---|
| Observation | Diameter | Spacing | | By Calliper | By Sensor | | |
| Number | inch | pixel | x 0.001 in | x 0.001 in | x 0.001 in | x 0.001 in | (%) |
| 1 | 1.0000 | 45.582 | 1.265 | 0.00 | 0.000 | 0.000 | ---- |
| 2 | 0.9998 | 41.893 | 1.377 | 0.10 | 0.111 | 0.011 | 11.42 |
| 3 | 0.9996 | 39.002 | 1.479 | 0.20 | 0.213 | 0.013 | 6.74 |
| 4 | 0.9994 | 36.476 | 1.581 | 0.30 | 0.316 | 0.016 | 5.29 |
| 5 | 0.9992 | 34.587 | 1.668 | 0.40 | 0.402 | 0.002 | 0.56 |
| 6 | 0.9990 | 32.973 | 1.749 | 0.50 | 0.484 | -0.016 | -3.23 |

Table C-12 : Effect of Tool Wear on Fringe Spacing and its Measurement.

| Characteristics of Series 8 | | | | |
|---|---|---|---|---|
| Factors: | | Micrometer Readings | | Angle in |
| Repeatibility | Wear | Horzontal | 0.4668 | Degrees |
| Cylinder Lens | Coolant | Vertical | 0.5627 | 28.0 |

| | Tool Tip | Fringe | Slit Width | Tool Wear | | Difference | Error |
|---|---|---|---|---|---|---|---|
| Observation | Diameter | Spacing | | By Calliper | By Setup | | |
| Number | inch | pixel | x 0.001 in | x 0.001 in | x 0.001 in | x 0.001 in | (%) |
| 1 | 1.0000 | 44.563 | 1.294 | 0.00 | 0.000 | 0.000 | ---- |
| 2 | 0.9998 | 41.533 | 1.389 | 0.10 | 0.094 | -0.006 | -5.58 |
| 3 | 0.9996 | 39.364 | 1.465 | 0.20 | 0.171 | -0.029 | -14.53 |
| 4 | 0.9994 | 37.109 | 1.554 | 0.30 | 0.260 | -0.040 | -13.34 |
| 5 | 0.9992 | 34.843 | 1.655 | 0.40 | 0.361 | -0.039 | -9.74 |
| 6 | 0.9990 | 32.663 | 1.766 | 0.50 | 0.472 | -0.028 | -5.69 |

Table C-13 : Effect of Coolant on Optical Measurement

| Sl No. | Reduction in Tool Diameter ( x 0.001 in) | Tool Wear VB (mm) |
|---|---|---|
| 1 | 0.2 | 0.02 |
| 2 | 0.4 | 0.04 |
| 3 | 0.6 | 0.05 |
| 4 | 0.8 | 0.07 |
| 5 | 1.0 | 0.09 |
| 6 | 1.2 | 0.11 |
| 7 | 1.4 | 0.13 |
| 8 | 1.6 | 0.15 |
| 9 | 1.8 | 0.16 |
| 10 | 2.0 | 0.18 |
| 11 | 2.2 | 0.20 |
| 12 | 2.4 | 0.22 |
| 13 | 2.6 | 0.24 |
| 14 | 2.8 | 0.26 |
| 15 | 3.0 | 0.27 |
| 16 | 3.2 | 0.29 |
| 17 | 3.4 | 0.31 |
| 18 | 3.6 | 0.33 |
| 19 | 3.8 | 0.35 |
| 20 | 4.0 | 0.37 |

Table C-14 : Comparison of Reduction of Tool Tip Diameter and Flank Wear (VB).

# REFERENCES

**Alauddin, M., El-Baradie and Hashmi, M. J. H.,** "Surface Roughness Model for End Milling Metal Matrix Composite (Al/SiC)", *Proceedings of 30th International Machine Tool Design and Research Conference,* pp 135-142, 1993.

**Arsovski, S. M.,** "Wear Sensors in the Adaptive Control Systems of Machine Tools", *International Journal of Production Research,* Vol. 21, No. 3, pp 347-356, 1983.

**Balakrishnan, P. and DeVries, M. F.,** "Sequential Estimation of Machinability Parameters for Adaptive Optimization of Machinability Data Base Systems", *ASME Journal of Engineering for Industry,* Series B, Vol. 127, pp 159-166, 1985.

**Barkman, W. E., Babelay, E. F., Demint, P. D., Hebble, T. L., Igou, R. E., Klages, E. J. and Williams, R. R.,** "Monitoring Tool Condition With an Optical Tool Inspection System", Y/DX-1131, Dec 1990.

**Brandon, J. and Binglin, Z.,** "Data Acquisition, Signal Processing and Mathematical Modelling Strategies for in Process Condition Monitoring", *Proceedings of the 29th International Machine Tool Design and Research Conference,* Manchester, pp 501-505, April 1992.

**Chen, W.,** "A New Rapid Wear Test of Cutting Tools", *Proceedings of the 27th International Machine Tool Design and Research Conference,* Manchester, 1988, pp 261-265.

**Cloud, G.,** *Optical Methods of Engineering Analysis,* Cambridge University Press 1995.

**Cook, N. H.,** "Tool Wear Sensors", *Wear,* Vol. 62, pp 49-57, 1980.

**Cook, N. H.,** "Tool Wear and Tool Life", *ASME Journal of Engineering for Industry,* Vol. 95, pp 931-937, 1973.

**Cuthbert, L and Huynh, V. M.,** "Statistical Analysis of Optical Fourier Transform Patterns for Surface Texture Assessment", *Measurement Science and Technology,* Vol. 3, No. 8, pp 740-745, 1992.

**Cuppini, D., D'Errico, G. and Rutelli G.,** "Tool Image Processing with Applications to Unmanned Metal-cutting. A Computer Vision System for Wear Sensing and Failure Detection", *SPIE,* Vol. 701, pp 416-422, ECOOSA, 1986.

**Dan, L. and Mathew, J.,** "Tool Wear and Failure Monitoring Techniques for Turning -

A Review", *International Journal of Machine Tools Manufacture,* Vol. 30, No. 4, pp 579-598, 1990.

**Danai, K. and Ulsoy, A. G.,** "A Dynamic State Model for On-Line Tool Wear Estimation in Turning", *ASME Journal of Engineering for Industry,* Vol. 109, Nov 1987, pp 396-399.

**Daneshmand, L. K., and Pak, H. A.,** "Performance Monitoring of a Computer Numerically Controlled (CNC) Lathe Using Pattern Recognition Techniques", *The 3rd International Conference on Robot Vision and Sensory Control,* Cambridge, 1983, pp 589-599.

**Daschenko, A. I., and Redin, V. N.,** "Control of Cutting Tool Replacement by Durability Distributions", *The International Journal of Advanced Manufacturing Technology,* Vol. 3, No. 5, pp 39-60, 1988.

**Dornfeld, D. A.,** "Neural Network Sensor Fusion for Tool Condition Monitoring", *Annals of the CIRP,* Vol. 39, No. 1, pp 101-105, 1990.

**Du, R., Zhang, B., Hungerford, W., Pryor, T.,** "Tool Condition Monitoring and Compensation in Finish Turning Using Optical Sensor", *Proceedings of the 1993 ASME Winter Annual Meeting,* New Orleans, pp 245-250, 1993.

**Du, R., Elbestawi, M. A. and Li, S.,** "Tool Condition Monitoring in Turning Using Fuzzy Set Theory", *International Journal of Machine Tool Manufacture,* Vol. 32, No. 6, pp 781-796, 1992.

**Elbestawi, M. A., Papazafiriou, T. A. and Du, R. X.,** "In-Process Monitoring of Tool Wear in Milling Using Cutting Force Signature", *International Journal of Machine Tools Manufacture,* Vol. 31, No. 1, pp 55-77, 1991.

**El-Gomayel, J. I. and Bregger, K. D.,** "On-Line Tool Wear Sensing for Turning Operations", *Transactions of ASME Journal of Engineering for Industry,* Vol. 108, pp 44-47, February 1986.

**El-Wardany, T. I., El-Bestawi, M. A., Attia, M. H. and Mohamed, E. H.,** "Surface finish characteristic in turning of harden steel", *University of McMaster,* 1991.

**Fan, K. C., Liao, Y. S., Chang, T. S. and Huang, J. J.,** "Development of a Simple, Low Cost, and Portable Compensator for CNC Controllers", *Proceedings of the 27th International Conference,* pp 217-221, 1988.

**Fan, Y. and Du, R.,** "Monitoring Rotating Tools Using Laser Diffraction", *Proceedings of the International Symposium on Manufacturing Science and Technology for the 21st*

*Century,* pp 274-278, Beijing 1994.

**Fei, J. and Jawahir, I. S.,** "A Fuzzy Knowledge-Based System for Predicting Surface Roughness in Finish Turning", *IEEE International Conference on Fuzzy System,* San Diego, USA, pp 899-906, 1992.

**Giardini, C., Bugini, A. and Pacagnella, R.,** "The Optimal Cutting Conditions as a Function of Probability Distribution Function of Tool Life and Experimental Test Numbers", *International Journal of Machine Tools Manufacturc,* Vol. 28, No. 4, pp 453-459, 1988.

**Giusti, F. Santochi, M. and Tantussi, G.,** "On-Line Sensing of Flank and Crater Wear of Cutting Tools", *Annals of the CIRP,* Vol. 36, No. 1, pp 41-44, 1987.

**Harding, K. G.,** "Sensors for the '90s", *Manufacturing Engineering,* Vol. 106, No. 4, pp 57-61, 1991.

**Hardwick, B. R.,** "Improving the Accuracy of CNC Machine Tools Using Software Compensation for Thermally Induced Errors", *Proceedings of the 29th International Machine Tool Design and Research Conference,* pp 269-276, Manchester, April 92.

**Hasegawa, M., Seirag, A. and Lindberg, R. A.,** "Surface Roughness Model for Turning", *Tribology International,* pp285-289, Dec, 1976.

**Hines, W. W. and Montgomery, D. C.,** *Probability and Statistics in Engineering and Management Science,* John Wiley & Sons, Inc., 1980.

**Hingle, H, T. and Rakels, J. H.,** "The Practical Application of Diffraction Techniques to Assess Surface Finish of Diamond Turned Parts", *Annals of the CIRP,* Vol. 32, No. 1, pp499-501, 1983.

**Huynh, V. M., Kurada, S. and North, W.,** "Texture Analysis of Rough Surfaces Using Optical Fourier Transform", *Measurement Science and Technology,* Vol. 2, No. 9, pp 831-837, 1991.

**Jacobs, H. J. and Hentschel, B.,** "On-Line Forecast and Detection of Cutting Tool Failure in the Operating Range of Manufacturing Cell - A Challenge to Integrated Development of the System of Machine Tool Tool-Sensor for Unmanned Factories", *International Conference of Production Research,* Hungary, 1984.

**Jacobs, H. J., Hentschel, B. and Stange, B.,** "Intelligent Tool Monitoring for Machining", *Presented at 9th International Conference of Production Research,* Cincinnati, USA, 1987.

**Jalali, S. A., and Kolarik, W. J.**, "Tool Life and Machinability Models for Drilling Steels", *International Journal of Machine Tools Manufacture*, Vol. 31, No. 3, pp 273-282, 1991.

**Jang, D. Y. and Seireg, A.**, "Machining Parameter Optimization for Specified Surface Conditions", *Transactions of ASME Journal of Engineering for Industry*, Vol. 114, pp 254-257, May 1992.

**Jang, D. Y. and Seireg, A.**, "A Model for Predicting Residual Stress in Metal Cutting", *Proceedings of the Japan International Tribology Conference*, pp 439-444, Nagoya, 1990.

**Jang, D. Y. and Seireg, A.**, "Dynamic Simulation for Predicting Surface Roughness in Turning", *12th Biennial Conference on Mechanical Vibration and Noise*, pp 31-36, Montreal, Canada, 1989.

**Jeon, J. U. and Kim, S. W.**, "Optical Flank Wear Monitoring of Cutting Tools by Image Processing", *Wear*, Vol. 127, pp 207-217, 1988.

**Kendall, L. A. and Bayoumi, A.**, "Automated Tool-Wear Monitoring and Tool Changing Using Intelligent Supervisory Control", *International Journal of Production Research*, Vol. 26, No. 10, pp 1619-1628, 1988.

**Konishi, Y., Hasegawa, M. and Sugimoto, I.**, "Development of EDM Monitoring System Using Neural Networks", *Proceedings of the 29th International Machine Tool Design and Research Conference*, Manchester, pp 481-485, April 1992.

**Kopac, J., Zalar, D. and Kuzman, K.**, "Fine and/or Finish Machining of Cold Worked Steel in Near-Net-Shape Manufacturing Processes", *Proceedings of the 29th International Machine Tool Design and Research Conference*, Manchester, pp 519-523, April 1992.

**Krar, S. F. and Oswald, J. W.**, T*echnology of Machine Tools*, Fourth Edition, Mc Graw Hill 1994.

**Lee, K. S., Teo, S. C. and Lee, L. C.**, "A PC-Based In-Process Tool Wear Monitoring System", *Proceedings of the 29th International Machine Tool Design and Research Conference*, Manchester, pp 487-491, April 1992.

**Lee, L. C., Lee, K. S. and Gan, C. S.**, "On the Correlation between Dynamic Cutting Force and Tool Wear", *International Journal of Machine Tools Manufacture*, Vol. 29, No. 3, pp 295-303, 1989.

**Lee, Y. H., Bandyopadhyay, P. and Kaminski, B.**, "Cutting Tool Wear Measurement Using Computer Vision", *Society of Manufacturing Engineers Technical Paper No. MR86-934*, 1986.

**Leskovar, L. and Peklenik, J.**, "Influences Affecting Surface Integrity in the Cutting Process", *Annals of the CIRP,* Vol. 31, No. 1, pp 447-450, 1982.

**Lister, P. M. and Barrow, G.**, "Tool Condition Monitoring Systems", *Proceedings of the 26th International Machine Tool Design and Research Conference,* pp 271-288, 1986.

**Luggen, W. W.**, *Flexible Manufacturing Cells and Systems,* Prentice-Hall Inc., 1991.

**Maeda, Y., Uchida, H. and Yamamoto, A.**, "Estimation of Wear Land Width of Cutting Tool Flank with the Aid of Digital Image Processing Technique", *Bulletin of Japanese Society of Precision Engineering,* Vol. 21, No. 3, pp 211-213, 1987.

**Mielink, E. M.**, "Design of a Metal-Cutting Drilling Experiment: A Discrete Two-Variable Problem", *Quality Engineering,* Vol. 6, No. 1, pp 71-98, 1993-94.

**Montgomery, D. C.**, *Design and Analysis of Experiments,* John Wiley & Sons, Inc., 1991.

**Mulvaney, D. J., Newland, D. F. and Gill, K. F.**, "A Comparison of Orthogonal Transforms in their Application to Surface Texture Analysis", *Proceedings of Institution of Mechanical Engineerings,* Vol. 200, No. C6, pp 407-414, 1986.

**Nair, R. Danai, K. and Kalkin, S.**, "Turning Process Identification Through Force Transients", *Transactions of ASME Journal of Engineering for Industry,* Vol. 114, pp 1-6, February 1992.

**Nigm, M. M., Sadek, M. M. and Tobias, S. A.**, "Dimensional Analysis of the Steady State Orthogonal Cutting Process", *International Journal of Machine Tool Design and Research,* Vol. 17, pp 1-18, 1977.

**Park, J. and Ulsoy, A, G.**, "On-Line Flank Wear Estimation Using an Adaptive Observer and Computer Vision, Part 1: Theory", *Transactions of ASME Journal of Engineering for Industry,* Vol. 115, pp 30-36, February 1993.

**Park, J. and Ulsoy, A, G.**, "On-Line Flank Wear Estimation Using an Adaptive Observer and Computer Vision, Part 2: Experiment", *Transactions of ASME Journal of Engineering for Industry,* Vol. 115, pp 37-43, February 1993.

**Pedersen, K. B.**, "Wear Measurement of Cutting Tools By Computer Vision", *International Journal of Machine Tools Manufacture,* Vol. 30, No. 1, pp 131-139, 1990.

**Petropoulos, P. G.**, "Optimal Selection of Machining Rate Variables by Geometric Programming", *International Journal of Production Research,* Vol. 11, No. 4, pp 305-314, 1973.

**Ravindra, H. V., Raghunandan, M., Srinivasa, Y. G. and Krishnamurthy, R.,** "Tool Wear Estimation by Group Method of Data Handling in Turning", *International Journal of Production Research,* Vol. 32, No. 6, pp 1295-1312, 1994.

**Ryabukho, V. P., Avetisyan, Y. A., Grinevich, A. E., Zimnyakov, D. A., Feduleev, B. V. and Khomutov, V. L.,** "Surface Quality Inspection Using a Laser Beam with a Regular Dynamic Interference Pattern", *SPIE Vol. 2066, Industrial Optical Sensing and Metrology,* pp 168-179, 1993.

**Shalaby, M. A. and Riad, M. S. M.,** "A Linear Optimisation Model for Single-Pass Turning Operations", *Proceedings of the 27th International Machine Tool Design and Research Conference,* pp 231-235, Manchester, 1988.

**Shaw, M. C. and Crowell, J. A.,** "Finish Machining", *Annals of the CIRP,* Vol. 13,pp 5-22, 1965.

**Shinno, H., Mustafizur, R. and Inaba, C.,** "In-Process Monitoring System for Machining Environment Based on Heat Flux Sensing", *JSME International Journal,* Series 3, Vol. 35, No. 2, pp 307-312, 1992.

**Solaja, V.,** "Wear of Carbide Tools and Surface Finish Generated in Finish Turning of Steel", *Wear,* Vol. 2, pp 40-58, 1958/59.

**Sukvittayawong, S. and Inasaki, I.,** "Optimization of Turning Process by Cutting Force Measurement", *JSME? International Journal,* Series3, Vol. 31, No. 1, pp 546-552, 1991.

**Sukvittayawong, S. and Inasaki, I.,** "Identification of Chip Form in Turning Process", *JSME International Journal,* Series3, Vol. 31, No. 1, pp 553-560, 1991.

**Tansel, I. N. and McLaughlin, C.,** "On-line Monitoring of Tool Breakage with Unsupervised Neural Networks", *Transactions of NAMRI/SME,* pp 364-370, 1991.

**Tansel, I. N.,** "Neural Network Approach for Represention and Simulation of 3D-Cutting Dynamics", *Transactions of North American Metal Research Institute,* pp 193-200, 1990.

**Tonshoff, H. K.,** "Fast Sensor Systems for the Diagnosis of Grinding Wheel and Workpiece", *Society of Manufacturing Engineers Technical Paper MR93-369,* 1993.

**Tonshoff, H. K., Wulfsberg, J. P., Kals, H. J. J., Konig, W., Van Luttervelt, C. A.,** "Developments and Trends in Monitoring and Control of Machining Processes", *Annals of CIRP,* Vol. 37, pp 611-622, 1988.

**Torras, C.,** *Computer Vision: Theory and Industrial Applications,* Springer-Verlag, 1992.

**Usui, E. and Shirakashi, T.**, "Analytical Prediction of Cutting Tool Wear", *Wear,* Vol. 100, pp 129-151, 1984.

**Whitehall, B. L., Lu, S. C. Y. and Stepp, R. E.,** "CAQ: A Machine Learning Tool for Engineering", *Artificial Intelligence in Engineering,* Vol. 5, No. 4, 1990.

**Wolff, R.,** "The Influence of Surface Roughness and Surface Texture on Scuffing in Sliding Contact", *Proceedings of the Japan International Tribology Conference,* pp 1277-1282, Nagoya, 1990.

**Wu, S. M.,** "Tool-Life Testing by Response Surface Methodology - Part 1", *Transactions of ASME Journal of Engineering for Industry,* pp 105-110, May 1964.

**Wu, S. M. and Eman, K. F.,** "CAM-Another Viewpoint", *Proceedings of the 24th International Machine Tool Design and Research Conference,* pp 391-397, 1984.

**Young, M.,** *Optics and Lasers,* Second Revised Edition, Springer-Verlag Inc., 1984.

# VITA AUCTORIS

| | |
|---|---|
| Name: | Koushik Ray |
| Place of Birth: | Ottawa, Ontario |
| Year of Birth: | 1970 |
| Education: | South Point High School,<br>Calcutta, India<br>1983 - 1989 |
| | Indian Institute of Technology,<br>Kharagpur, India<br>1989 - 1993 B. Tech. (Hons) in<br>Mechanical Engineering. |